

Cold Jupiters and small planets: friends, foes, or indifferent?

A search for correlations with the largest exoplanet samples

A. S. Bonomo¹, L. Naponiello¹, E. Pezzetta², A. Sozzetti¹, D. Gandolfi², R. Wittenmyer³, and M. Pinamonti¹

¹ INAF - Osservatorio Astrofisico di Torino, via Osservatorio 20, 10025 Pino Torinese, Italy

² Dipartimento di Fisica, Università degli Studi di Torino, via Pietro Giuria 1, 10125 Torino, Italy

³ University of Southern Queensland, Centre for Astrophysics, West Street, Toowoomba, QLD 4350, Australia

Received 7 October 2024 / Accepted 20 May 2025

ABSTRACT

Finding out whether there is any correlation between the presence of short-period small planets (SPs) with $P \lesssim 100$ d ($a \lesssim 0.4$ AU) and $1 < M_p < 20 M_\oplus$ and that of outer cold Jupiters (CJs) with $a = 1 - 10$ AU and $M_p = 0.5 - 20 M_{\text{Jup}}$ around solar-type stars may provide crucial constraints on the models of formation and/or migration of SPs. However, somehow discrepant results about the occurrence rates of CJs in SP systems have been reported in the literature, with a few recent works claiming a strong SP-CJ correlation but only at super-solar metallicity and/or mass of the host stars. Here we homogeneously recomputed the occurrence rates of CJs at average, sub-solar ($[\text{Fe}/\text{H}] < -0.1$), solar ($-0.1 \leq [\text{Fe}/\text{H}] \leq 0.1$), and super-solar ($[\text{Fe}/\text{H}] > 0.1$) metallicity as well as at average and sub-intervals of stellar mass, namely $0.6 - 0.8$, $0.8 - 1.0$, and $1.0 - 1.2 M_\odot$, with (i) a carefully-selected sample of 217 SP systems detected through transits or radial velocity, and (ii) a large comparison sample of 1167 solar-type stars, regardless of the possible presence of SPs. We determined the integrated occurrence rate of CJs in SP systems to be $f_{\text{CJ|SP}} = 11.1^{+2.5}_{-1.8}\%$ at average metallicity $[\text{Fe}/\text{H}] = -0.011 \pm 0.005$ and mass $\overline{M_\star} = 0.916 \pm 0.012 M_\odot$; this is consistent with the estimated frequencies of CJs in both the comparison sample ($f_{\text{CJ}} = 9.8^{+0.9}_{-0.8}\%$ at $[\text{Fe}/\text{H}] = -0.072 \pm 0.009$ and $\overline{M_\star} = 0.994 \pm 0.004 M_\odot$) and the HARPS-N survey of transiting SP systems. We found a possible correlation ($f_{\text{CJ|SP}} > f_{\text{CJ}}$) only at super-solar mass and metallicity, namely $1.0 \leq M_\star < 1.2 M_\odot$ and $[\text{Fe}/\text{H}] > 0.1$, though with a statistical confidence less than 3σ . To test some theoretical predictions, we also searched for possible SP-CJ relations as a function of SP and CJ multiplicity as well as SP composition, albeit with the inevitably limited current sample, and found none. We show that the architectures of SP systems are not indifferent to the presence of CJs as the multiplicity of SPs strongly depends on the CJ eccentricity, as expected from planetary dynamics. A more comprehensive understanding of the relation between SPs and CJs requires larger samples of SP systems. The increasing number of well-characterized systems and the anticipated discoveries from both the Gaia and PLATO missions will enable a definitive assessment of the impact of CJs on the formation of SPs.

Key words. Planetary systems – Planets and satellites: formation – Stars: statistics – Stars: solar-type – Methods: statistical – Techniques: radial velocities.

1. Introduction

Whether the presence of short-period small planets (SPs) with $P \lesssim 100$ d (corresponding to semi-major axis of $a \lesssim 0.4$ AU) and $1 < M_p < 20 M_\oplus$ around solar-type stars is somehow correlated with that of cold Jupiters (CJs), that is gaseous giant planets with $a \simeq 1 - 10$ AU and mass $0.5 \leq M_p \leq 20 M_{\text{Jup}}$ (or $0.3 \leq M_p \leq 13 M_{\text{Jup}}$, depending on the definition), is becoming a very intriguing question in exoplanetary science because it could potentially reveal crucial features of planet formation and evolution. However, there are strong discrepancies about this possible correlation in the literature from both theoretical and observational perspectives.

As for the theory, an anti-correlation between SPs and CJs would be expected if CJs could either (i) act as a dynamical barrier to the inward migration of icy SPs from beyond the water snowline at $\sim 1 - 3$ AU (Izidoro et al. 2015) and/or (ii) reduce considerably the inward flux of pebbles to the inner regions of the protoplanetary disk, which is required to form dry SPs within the water snowline (Lambrechts et al. 2019). From the Generation 3 Bern simulations of planet formation and evolution,

Schlecker et al. (2021) instead found no or a weak SP-CJ correlation, and predicted a strong architecture-composition link, with more icy (rocky) SPs in the absence (presence) of one or more CJs, due to the same above-mentioned effect of dynamical barrier by the CJ (Izidoro et al. 2015). Furthermore, Schlecker et al. (2021) predicted a scarcity of SPs at high stellar metallicity due to the disruption of inner planetary systems by more dynamically active CJs (see their Fig. 19). A recent work by Bitsch & Izidoro (2023) shows that it would also be possible to obtain a correlation between the presence of SPs and that of CJs, depending on the gas contraction rate for the formation of CJs: for slow gas contraction rates, the cores that form in the proximity of the water snowline are too small to effectively accrete large envelopes and can migrate inward thus becoming SPs, while cores at greater distances can grow into cold gas giants.

As for the observations, occurrence rates of CJs in SP systems ($f_{\text{CJ|SP}}$ ¹) as high as $\sim 40\%$ reported by both Zhu & Wu (2018) and Bryan et al. (2019) seem to disagree with a more recent estimate of $f_{\text{CJ|SP}} = 8.7^{+7.3}_{-2.7}\%$ for $M_p = 0.5 - 20 M_{\text{Jup}}$ (or $f_{\text{CJ|SP}} = 9.3^{+7.7}_{-2.9}\%$ for $M_p = 0.3 - 13 M_{\text{Jup}}$) by Bonomo et al.

¹ $f_{\text{CJ|SP}}$ is defined as the fraction of FGK dwarfs with at least one SP, which also host one or more CJs.

(2023) (hereafter B23). In order to reconcile those estimates, both Zhu (2024) and Bryan & Lee (2024) (hereafter BL24) explored the SP-CJ relation as a function of stellar metallicity and claimed a correlation at super-solar metallicity ($[Fe/H] > 0$). In particular, BL24 analyzed a large sample of 184 SP systems detected by either transit or radial velocity (RV) surveys, and compared their derived $f_{CJ|SP}$ with the frequency of CJs (f_{CJ})² from the California Legacy Survey (CLS, Rosenthal et al. 2021). For that purpose, they considered the confirmed CJs, and homogeneously computed the sensitivity to CJs for both their sample and the CLS survey. They found no correlation at $[Fe/H] \leq 0$ and a SP-CJ correlation at $[Fe/H] > 0$ with a 2.7σ significance level ($f_{CJ|SP} = 28.0^{+4.9}_{-4.6}\%$ vs $f_{CJ} = 14.3^{+2.0}_{-1.8}\%$). After submission of this Letter, Bryan & Lee (2025) (hereafter BL25) reported a positive correlation with a significance level greater than 2σ in metal-rich stars with mass $M_\star > 0.8 M_\odot$. This was interpreted by BL24 as evidence of the critical role of stellar metallicity and/or mass (regarded as a proxy for the disk solid and gas budget, respectively) to nucleate both inner low-mass and outer large-mass planets.

The works by Zhu (2024) and BL24 were partly motivated by the fact that those authors noticed that several stars in the *Kepler* and K2 sample by B23 are metal poor, which might have biased the B23 estimate of $f_{CJ|SP}$ towards lower values for the well-known relation between giant planets and stellar metallicity (e.g., Fischer & Valenti 2005; Johnson et al. 2010; Sousa et al. 2011; Mortier et al. 2013). However, the average metallicity of the B23 sample ($[Fe/H] = -0.066 \pm 0.014$) and that of the Anglo Australian Telescope (AAT) RV survey ($[Fe/H] = -0.045 \pm 0.018$) (Wittenmyer et al. 2020), which was used as a comparison sample by B23, are consistent within 1σ and are both lower than the peak of the metallicity at about -0.1 dex in a volume-limited sample of the solar neighborhood (e.g., Sousa et al. 2011).

Building upon the work of BL24, in the present article we recompute (i) $f_{CJ|SP}$ with a larger and more carefully selected sample of SP systems, and (ii) f_{CJ} using three different blind RV campaigns, namely the AAT, CLS, and HARPS (Mayor et al. 2011; Trifonov et al. 2020) surveys, and merging the stars of these three surveys into a unique large sample. We then compare $f_{CJ|SP}$ and f_{CJ} to search for possible SP-CJ correlations as a function of stellar metallicity and/or mass as well as planet properties, and draw our conclusions about their possible existence.

2. Samples and radial velocity data

2.1. Small planet transit and radial velocity sample

The sample of SP systems to compute $f_{CJ|SP}$ was built through queries to the NASA Exoplanet Archive³ on 2 December 2024 following the same criteria as BL24: the systems must have (1) at least one confirmed SP with $1 < M_p < 20 M_\oplus$ ⁴ for transiting planets and $1 < M_p \sin i < 20 M_\oplus$ for planets discovered by RV surveys; (2) a solar-type (i.e., FGK dwarf or sub-giant) star as host, which thus excludes M dwarfs with $M_\star \leq 0.6 M_\odot$, and (3) at least one publicly available RV dataset with more than 20 measurements and baseline $\Delta T \geq 1$ yr. However, unlike BL24, we initially discarded “mixed systems” with both SP

² f_{CJ} is defined as the fraction of FGK dwarfs hosting at least one CJ, regardless of the presence or absence of SPs.

³ <https://exoplanetarchive.ipac.caltech.edu/>.

⁴ Unlike BL24, we did not consider the criterion on the radius to be $R_p \leq 4 R_\oplus$ as this information is not available for the RV planets.

and short-period ($P < 100$ d) planets with $M_p \geq 20 M_\oplus$, such as the WASP-47 system which also hosts a hot Jupiter (WASP-47b) in between the two SPs WASP-47e and d (e.g., Vanderburg et al. 2017; Nascimbene et al. 2023); indeed, it is unclear whether the theoretical predictions mentioned in Sect. 1 apply to such systems in which giant planets, especially the hot Jupiters, may have undergone a substantial migration process (e.g., Dawson & Johnson 2018). Nonetheless, we computed the occurrence rates by also taking the mixed systems into account, and noted no significant differences (see Sect. 3). We cleaned the BL24 sample from a couple of outliers like TOI-1853b, which has $M_p = 73 \pm 3 > 20 M_\oplus$ (Naponiello et al. 2023), or Kepler-22b, whose orbital period is $P = 290 > 100$ d (Borucki et al. 2012).

Our SP sample results in 217 systems, of which 134 were detected by transit surveys and 83 with RVs. It is therefore considerably larger than that of BL24 (184 mixed systems), and contains 148 systems in common (see Table A.1). The inclusion of the mixed systems leads to 242 systems, 151 and 91 of which were found with transits and RVs, respectively (Tables A.1 and A.2). As in BL24, for each system we selected the available RV dataset with the best sensitivity to the detection of CJs (see Sect. 3).

2.2. Radial velocity comparison samples

As comparison samples to estimate f_{CJ} , we considered the three largest RV surveys with high-precision RVs to our knowledge, namely the AAT, CLS, and HARPS surveys, after applying the same criteria (2) and (3) as above for consistency. This led to 196, 402, and 782 solar-type stars for the AAT, CLS, and HARPS campaigns. The number of solar-type stars from the CLS survey (402) is lower than that considered by BL24 (562), likely due to the fact that BL24 made use of the third selection criterion only for their SP sample and not for the CLS one. Using the third criterion (Sect. 2.1) for the CLS survey thus reduced the number of solar-type stars by 160, while excluding only one system out of 52 with CJs, showing that a baseline $\Delta T \geq 1$ yr and an amount of RVs more than 20 for the best dataset of a given target are key to discover CJs. The reduced number of the CLS stars resulted in a slightly higher estimate of f_{CJ} (see Table H.1), which gets more consistent with the f_{CJ} determinations from the other two AAT and HARPS surveys (see Table H.2).

The mass, metallicity and uncertainty on the metallicity of the selected solar-type stars from the three surveys were all taken from the Hypatia catalog⁵ (Hinkel et al. 2014) and are given in Table B.1.

We also merged the three aforementioned RV surveys to create a large comparison sample with 1167 stars, 213 of which are in common between two or even all three surveys (Table B.1). In this way, we could compute a more precise and accurate f_{CJ} (see Tables F.1 and H.2).

2.3. Comparison of the small planet and the RV merged samples

The distributions of the stars of both the SP and RV merged samples with stellar metallicity and mass are compared in Figs. C.1 and C.2, respectively.

The Kolmogorov-Smirnov (K-S) test between the two empirical cumulative distribution functions (eCDF) of metallicity gives a relatively low p-value of 0.021 as the SP sample has a

⁵ <https://www.hypatiacatalog.com/>.

lower fraction of metal-poor stars at $[\text{Fe}/\text{H}] \lesssim -0.2$ than the comparison sample (see Fig. C.1).

The same K-S test for the stellar mass cumulative distributions returns a p-value of 3e-09 indicating that the two distributions are highly incompatible. This is due to an excess of stars of the SP sample at lower masses (see Fig. C.2), given that SPs are more easily detected around smaller stars with both the transit and RV methods.

In Fig. C.3 we show the stellar metallicity distributions and eCDFs of both the SP and RV merged samples at the three intervals of stellar mass considered in Sect. 3, namely $0.6 - 0.8$, $0.8 - 1.0$, and $1.0 - 1.2 M_{\odot}$. While the eCDFs of metallicity are compatible in the $0.6 - 0.8 M_{\odot}$ and $0.8 - 1.0 M_{\odot}$ intervals with p-values of 99% and 27%, respectively, they considerably differ at super-solar mass (p-value < 1%) because of the considerably larger number of metal-poor stars in the RV merged sample (right panels of Fig. C.3).

3. Statistical analyses

We determined $f_{\text{CJ|SP}}$ from the SP sample (Sect. 2.1), and f_{CJ} from both the individual RV surveys and the comparison sample (Sect. 2.2), first at the average metallicity of the different samples, and then by considering three intervals in stellar metallicity, i.e. sub-solar ($[\text{Fe}/\text{H}] < -0.1$), solar ($-0.1 \leq [\text{Fe}/\text{H}] \leq 0.1$), and super-solar ($[\text{Fe}/\text{H}] > 0.1$) metallicity. Similarly to BL24, we also split the samples in two broad intervals, namely $[\text{Fe}/\text{H}] \leq 0$ and $[\text{Fe}/\text{H}] > 0$, even though, in our view, given the typical uncertainties of $\sim 0.04 - 0.07$ dex on $[\text{Fe}/\text{H}]$, a star with $0.0 < [\text{Fe}/\text{H}] < 0.1$ ($-0.1 < [\text{Fe}/\text{H}] < 0.0$) should not be classified as metal rich (poor), but rather as solar in metallicity.

Given the different distributions of stellar mass in the SP and comparison samples (Sect. 2.3), we further considered three different intervals in stellar mass, namely $0.6 \leq M_{\star} < 0.8 M_{\odot}$, $0.8 \leq M_{\star} < 1.0 M_{\odot}$, and $1.0 \leq M_{\star} < 1.2 M_{\odot}$ ⁶. This is of interest because the frequency of giant planets also depends on stellar mass, though to a lesser extent than metallicity (e.g., Johnson et al. 2010; Fulton et al. 2021).

For each sample and its relative sub-samples in metallicity we used the binomial statistics

$$b(d|N_{\star,\text{eff}}, f_{\text{CJ|SP}}) = \frac{N_{\star,\text{eff}}!}{d!(N_{\star,\text{eff}} - d)!} f_{\text{CJ|SP}}^d (1 - f_{\text{CJ|SP}})^{N_{\star,\text{eff}} - d}, \quad (1)$$

where d is the number of systems with at least one confirmed CJ, and $N_{\star,\text{eff}}$ is the “effective” number of stars given by the product of the number of stars of the survey, N_{\star} , and the average survey sensitivity (or completeness) to CJs, C , i.e. $N_{\star,\text{eff}} = N_{\star} \cdot C$.

The completeness of each individual star, C_i , was computed in the same way as B23 and BL24 (see their Sect. 3), that is through experiments of injection and recovery of CJ RV signals in a logarithmic grid of $30 \times 30 \Delta M_p \cdot \Delta a$ cells covering the ranges $0.3 - 20 M_{\text{Jup}}$ and $1 - 10$ AU, respectively. Specifically, for each cell, we simulated 200 RV signals of CJs at the epochs of the RV dataset by randomly varying (i) M_p and a within the cell bounds, (ii) T_c within the range of P corresponding to a and the stellar mass M_{\star} (Tables A.1, A.2 and B.1) from Kepler’s third law; (iii) $\cos i$ from 0 to 1, where i is the orbital inclination; and iv) the argument of periastron ω from 0 to 2π , while drawing the orbital eccentricity e from a β distribution (Kipping 2013). We then shifted every RV point at time t following a Gaussian distribution

⁶ BL25 also considered similar intervals of stellar mass to investigate the SP-CJ relation as a function of stellar metallicity and mass.

with mean and standard deviations equal to the RV value and its uncertainty, respectively. C_i was estimated as the recovery rate of the simulated signals (Keplerian orbits or linear and quadratic trends if ΔT was considerably shorter than the simulated CJ orbital period) across the whole grid using the ΔBIC criterion (see B23 and BL24). The average completeness C of each sample (or sub-sample) was then simply obtained by the mean of the completenesses of the stars in that sample: $C = (1/N_{\star}) \sum_{i=1}^{N_{\star}} C_i$. The average completenesses of all the samples described in Sect. 2 are displayed in Fig. D.1. We note a very good agreement when comparing our average completenesses of the SP RV and transit samples (upper panels in Fig. D.1) with those shown in Fig. A.1 of BL24 (for $a = 1 - 10$ AU).

We considered two ranges of CJ mass⁷, namely $M_p = 0.5 - 20 M_{\text{Jup}}$ and $M_p = 0.3 - 13 M_{\text{Jup}}$ (for comparison with B23), but we mainly rely on the former because the latter suffers from incompleteness issues between 0.3 and $0.5 M_{\text{Jup}}$ (Fig. D.1). For each CJ mass range and the aforementioned bins of stellar metallicity and/or mass we give the number of solar-type stars (N_{\star}), the number of stars with confirmed CJs (d), the average completenesses (C), and CJ occurrence rates from (i) the SP and the large comparison samples in Tables F.1 and F.2, (ii) the SP transit, RV, and transit+RV samples as well as the SP and mixed transit, RV, and transit+RV samples in Table G.1, and (iii) the AAT, CLS, and HARPS surveys in Table H.2. Tables E.1, E.2, and E.3 list the known CJs and their properties in the SP, SP and mixed, and comparison samples. Fig. E.4 shows on the left (right) the architectures of the 27 (23) systems with CJs with $M_p = 0.3 - 13 M_{\text{Jup}}$ ($0.5 - 20 M_{\text{Jup}}$) in the SP sample, respectively.

4. Results

4.1. Frequency of CJs at average stellar metallicity and mass

At the average stellar metallicity ($\overline{[\text{Fe}/\text{H}]} = -0.011 \pm 0.005$) and mass ($\overline{M_{\star}} = 0.916 \pm 0.012 M_{\odot}$) of the SP (transit+RV) stars we determined $f_{\text{CJ|SP}} = 11.1_{-1.8}^{+2.5}\%$ for the CJ mass range $M_p = 0.5 - 20 M_{\text{Jup}}$. Adding the 25 mixed systems yielded $f_{\text{CJ|SP+Mixed}} = 12.5_{-1.8}^{+2.5}\%$. Going back to the original sample of BL24 with $\overline{[\text{Fe}/\text{H}]} = -0.001 \pm 0.005$ and $\overline{M_{\star}} = 0.923 \pm 0.014 M_{\odot}$, which includes the “mixed systems”, and accounting for its average completeness⁸, we found a fully compatible result: $15.2_{-2.3}^{+3.1}\%$. It is interesting to note that both occurrence rates well agree within 1σ with the estimate of $f_{\text{CJ|SP}} = 8.7_{-2.7}^{+7.3}\%$ by B23, whose smaller sample is on average slightly poorer in metals by ~ 0.06 dex, and are lower than previous claims of $f_{\text{CJ|SP}} \sim 40\%$ (Sect. 1).

As for the comparison sample, at its average metallicity ($\overline{[\text{Fe}/\text{H}]} = -0.072 \pm 0.009$) and mass ($\overline{M_{\star}} = 0.994 \pm 0.004 M_{\odot}$), we found $f_{\text{CJ}} = 9.8_{-0.8}^{+0.9}\%$, which is fully compatible with $f_{\text{CJ|SP}}$ ⁹.

From our occurrence rates $f_{\text{CJ|SP}}$ and f_{CJ} , and the frequency of SPs $f_{\text{SP}} = 28.1_{-5.1}^{+6.6}\%$ from Rosenthal et al. (2022) (see also Zhu et al. 2018), we can derive the conditional probability that a solar-type star with a CJ also hosts a SP (Zhu & Wu 2018), namely $f_{\text{SP|CJ}} = f_{\text{SP}} \times f_{\text{CJ|SP}} / f_{\text{CJ}} = 32 \pm 11\%$. This agrees within

⁷ Note that only minimum masses, $M_p \sin i$, are known for the majority of CJs as their orbital inclination i cannot be determined from RVs alone.

⁸ This was extracted from Fig. A.1 in BL24.

⁹ The possible, though not significant, hint for a SP-CJ anti-correlation reported by B23 can be ruled out as our f_{CJ} recomputed from the AAT survey is approximately half that derived from Wittenmyer et al. (2020).

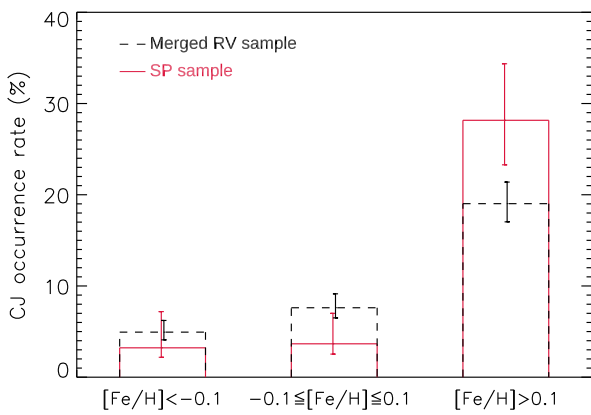


Fig. 1. Occurrence rates of cold Jupiters with $M_p = 0.5 - 20 M_{\text{Jup}}$ in the small planet sample (red solid line) and the merged RV comparison sample (black dashed line) at sub-solar ($[\text{Fe}/\text{H}] < -0.1$), solar ($-0.1 \leq [\text{Fe}/\text{H}] \leq 0.1$), and super-solar ($[\text{Fe}/\text{H}] > 0.1$) metallicity. See also Table F.1.

1σ with the $f_{\text{SP|CJ}}$ computed from a sample of 115 solar-type stars known to host a CJ (Ruggieri, A., et al. in prep.), and is substantially lower than the estimate of $f_{\text{SP|CJ}} \sim 100\%$ in Bryan et al. (2019).

4.2. Frequency of CJs as a function of stellar metallicity

We report $f_{\text{CJ|SP}}$ and f_{CJ} for the three sub-intervals of stellar metallicity (Sect. 3) in Table F.1, and display them in Fig. 1 (see also Fig. E.2 for $M_p = 0.3 - 13 M_{\text{Jup}}$). For the same metallicity bins, we also give the estimates of f_{CJ} from the AAT, CLS, and HARPS surveys separately in Table H.2, which are fully consistent with each other (see Fig. E.1).

By comparing $f_{\text{CJ|SP}}$ and f_{CJ} in Table F.1, we found that (i) at sub-solar and solar metallicities, they are fully compatible within 1σ , and (ii) at super-solar metallicity, the value of $f_{\text{CJ|SP}}$ is higher than f_{CJ} by approximately 3/2 ($\sim 30\%$ vs $\sim 20\%$; Fig. 1), but the significance of this difference is low, that is 1.7σ (compared to 2.7σ in BL24 for $[\text{Fe}/\text{H}] > 0$).

4.3. Frequency of CJs as a function of stellar metallicity and mass

We report $f_{\text{CJ|SP}}$ and f_{CJ} for the same bins of stellar metallicity as above, and for the three ranges of stellar mass discussed in Sect. 3, in Table F.2. We show them in Fig. 2 (see also Fig. E.3 for $M_p = 0.3 - 13 M_{\text{Jup}}$).

We found an excess of CJs in SP systems at 2.5σ significance level only at super-solar mass and metallicity, namely $M_{\star} \geq 1.0 M_{\odot}$ and $[\text{Fe}/\text{H}] > 0$ (see the right plot in Fig. 2, and Table F.2), in agreement with the recent findings of BL25. This is the origin of the higher $f_{\text{CJ|SP}}$ compared to f_{CJ} at super-solar metallicity and integrated stellar masses (Sect. 4.2 and Fig. 1).

4.4. SP-CJ relations as a function of SP and CJ multiplicity

We explored possible SP-CJ trends as a function of SP multiplicity, for which purpose we chose the $0.3 - 13 M_{\text{Jup}}$ mass range (instead of $0.5 - 20 M_{\text{Jup}}$), given the higher number of systems with both CJs and SPs (27 compared to 23). Indeed, if the presence of CJs really hindered the formation/migration of SPs, a lower

degree of SP multiplicity would be expected in the presence of CJs, for instance because low-mass “jumpers” overtaking the CJ towards inner orbits most likely form a single SP system (see Fig. 3 in Izidoro et al. 2015). By comparing the frequency of multiple systems with a number of SPs $n_p \geq 2$ in the SP subsamples with and without CJs, we found $f_{n_p \geq 2, \text{w/CJ}} = 37^{+10}_{-8}\%$ (10 out of 27 systems) and $f_{n_p \geq 2, \text{w/o CJ}} = 43^{+4}_{-3}\%$ (81 out of 190 systems), respectively; these rates are statistically consistent within the uncertainties.

We also searched for possible (anti)correlations as a function of CJ multiplicity to investigate whether two (or more) CJs may hinder the formation of SPs more than a single CJ system (Sect. 1). To this end, we compared the frequency of single SPs in systems with one CJ to that in systems with two (or more) CJs; indeed, the latter should be higher if two (or more) CJs had a more deleterious effect than a single CJ on the formation of multiple SP systems. We did not find any evidence for that: the rates of single SP systems with one CJ and two CJs are compatible, namely $63^{+9}_{-12}\%$ (12 out of 19 systems) and $62^{+13}_{-18}\%$ (5 out of 8 systems), respectively (see Fig. E.4).

4.5. SP-CJ relation as a function of SP composition

We investigated the possible presence of an architecture-composition link by determining the frequency of rocky SPs¹⁰ in CJ systems. This is intended to test whether the formation of rocky planets may be favored in the presence of CJs in the event CJs block the migration of icy sub-Neptunes from beyond the water snowline (Schlecker et al. 2021). We derived $f_{\text{rocky,w/CJ}} = 33^{+13}_{-9}\%$ from 5 transiting systems with rocky planets (HD219134, Kepler-139, Kepler-407, K2-312, K2-364) out of 15 in total (including 3 RV systems that were later found transiting). This shows that systems with both rocky planets and CJs do not represent the majority of the SP-CJ transiting systems.

4.6. SP multiplicity as a function of CJ eccentricity

When ordering the SP systems with CJs as a function of the CJ eccentricity (Fig. 3), only single or, more rarely, two SPs are found with eccentric ($e \gtrsim 0.4$) CJs, the most extreme case being K2-312/HD 80653 (B23). On the contrary, higher multiplicity (up to $n_p = 4$ for HD 219134) SP systems are seen in the company of CJs in quasi-circular orbits. This is in line with the expectation of stronger dynamical perturbations at inner orbital separations by eccentric CJs (e.g., Huang et al. 2017).

5. Discussion and conclusions

5.1. Cold Jupiters and small planets are friends, foes, or indifferent?

In the present work we first investigated the possible SP-CJ relation as a function of stellar metallicity and mass, and did not reveal any correlation or anticorrelation (i.e., SPs and CJs are neither friends nor foes) in eight of the nine mass and metallicity bins, that is at sub-solar mass for any metallicity as well as at super-solar mass for solar and sub-solar metallicity. We instead found an enhancement of CJs in SP systems (i.e., SPs and CJs could be friends) at super-solar mass and metallicity, though at less than 3σ , in general agreement with BL25.

¹⁰ We define a rocky planet as a planet that is located between the 100% iron and 100% silicate compositions in the mass-radius diagram of small planets (e.g., Zeng & Sasselov 2013).

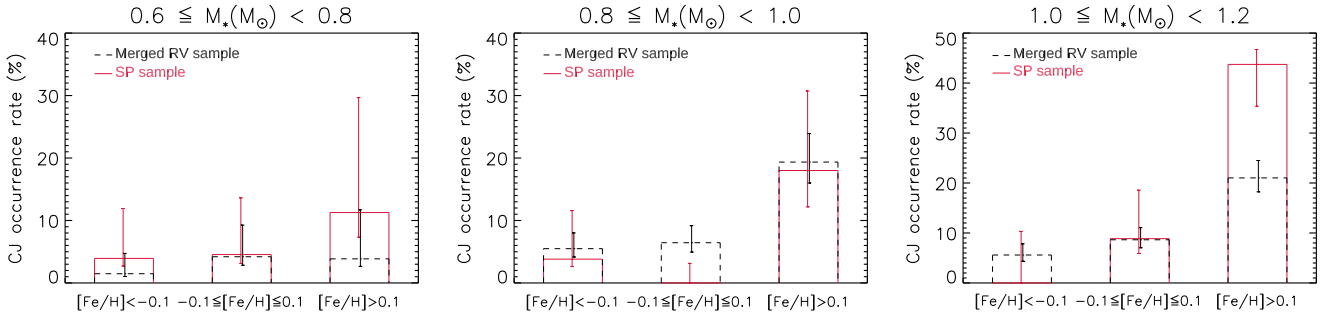


Fig. 2. Same as Fig. 1 for three different bins of stellar mass, namely $0.6 - 0.8 M_{\odot}$ (left), $0.8 - 1.0 M_{\odot}$ (center), and $1.0 - 1.2 M_{\odot}$ (right); see Table F.2.

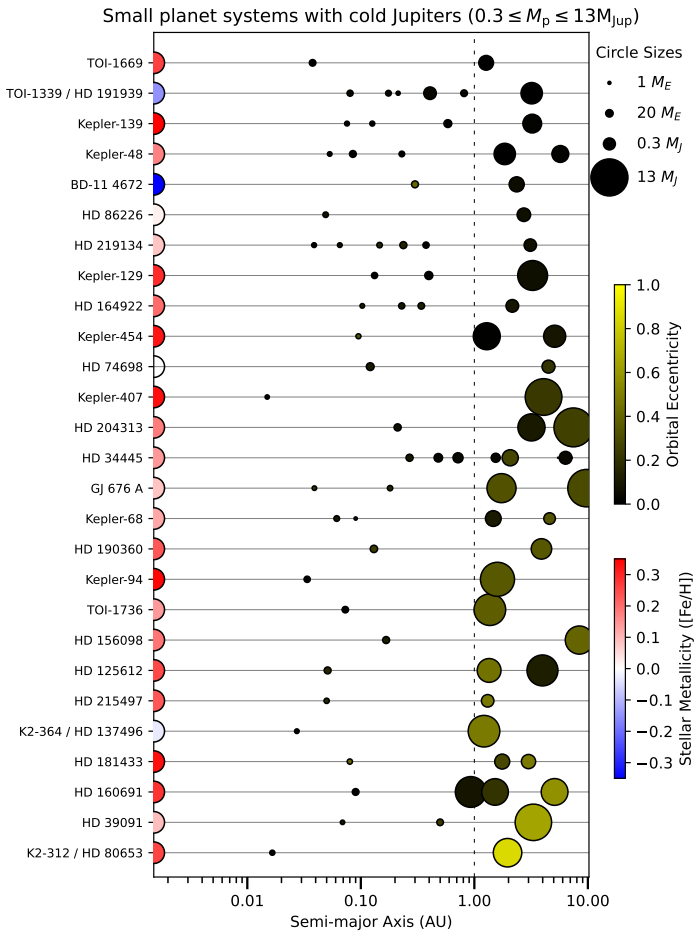


Fig. 3. The architectures of the 27 systems with both small planets and cold Jupiters in the mass range $0.3 \leq M_p \leq 13 M_{Jup}$, ordered according to increasing orbital eccentricity of the cold Jupiters (from top to bottom; in case of multiple cold Jupiters, the highest eccentricity was considered). The planet circles have sizes proportional to their mass (see legend in the top right corner), and colors depending on the orbital eccentricity (more eccentric planets are shown in yellow). The host stars are color coded as a function of stellar metallicity (metallicity increases from blue to red). All the systems with three or more inner small planets are accompanied by cold Jupiters with low eccentricities.

We could not unveil any SP-CJ trends with planet multiplicity and composition, which would further disfavor the anticorrelation models predicting a dearth of CJs in SP systems (Sect. 1). Nonetheless, it should be noted that (i) the limited sub-samples of SP systems with CJs (27 systems) inevitably result in large er-

ror bars on the CJ occurrence rates, making it difficult to reveal possible weak correlations or anticorrelations with planet properties; and (ii) the SP multiplicity considered in this work relies on the known (that is, detected) SPs and may be different from the true one, especially if non-transiting SPs with relatively long period ($P \sim 25 - 100$ d) and/or low mass went undetected by the RV follow up.

Our investigation of the architecture-composition relation in Sect. 4.5 must be considered with caution because it only concerned rocky planets. Yet, in principle it may also apply to rocky planets with tenuous H/He atmospheres, if some available gas was accreted by the super-Earths at the time of their formation, and was not later on stripped away by post-formation processes such as atmospheric photoevaporation (e.g., Lopez & Fortney 2014) or core-powered mass loss (e.g., Ginzburg et al. 2018). However, the well-known degeneracy in SP composition from the measurement of the bulk density alone does not allow us to distinguish whether or which non-rocky planets in the 10 transiting systems with CJs of our SP sample are actually dry (rocky worlds shrouded by thin H/He atmospheres, which formed within the water snowline) or icy (water worlds with possible H/He envelopes, which formed beyond the water snowline and then migrated inwards). This makes the investigation of the architecture-composition link challenging.

We showed that higher multiplicity SP systems are found in systems with CJs in low-eccentricity orbits, being immune to dynamical instabilities generated by highly eccentric CJs. In this sense, SPs are not indifferent to CJs, even in the great majority of cases where $f_{CJ|SP} \sim f_{CJ}$.

5.2. Caveats of our, BL24, and BL25 analyses

The occurrence rates derived in this work, BL24, and BL25 may be slightly underestimated mainly because of two reasons, which however should affect both the SP and comparison samples approximately in the same way, making the search for correlations in principle reliable. Firstly, the completenesses computed in our and BL24 works are optimistic because they only account for the formal RV uncertainties, and not for the uncorrelated jitter (as properly done by B23), which in some cases may be considerably higher than the former¹¹. Secondly, a few linear or quadratic RV trends, which might later result in CJ signals, were not taken into account in the computation of the occurrence rates, which relies on confirmed CJs only. Nevertheless, among the targets in the SP sample with relatively short temporal baselines, that is

¹¹ Nevertheless, proper Markov chain Monte Carlo analyses of the RV datasets of ~ 1350 systems considered here, similarly to B23, would require unrealistic computation times.

$1 \leq \Delta T \leq 4$ yr, we noticed only two targets with RV long-term trends still compatible with CJs (namely TOI-1279 and TOI-1778). Moreover, such trends are very often induced by brown dwarfs or low-mass stellar companions, or they correlate with activity indicators (see B23).

Conversely, occurrence rates might decrease if the minimum masses ($M_p \sin i$) of some of the considered CJs turned into true mass (M_p) measurements above the 20 (or 13) M_{Jup} upper limit, corresponding to brown dwarfs or low-mass stellar objects, due to low orbital inclinations (e.g., Xiao et al. 2023).

5.3. Perspectives

As more and more SP systems are characterized with high-precision RV follow up and monitored over the years, more precise and accurate determinations of $f_{CJ|SP}$ can be derived, by allowing to investigate more deeply the SP-CJ relation, even at the lower CJ mass range $0.3 - 13 M_{Jup}$. We plan to update our results over time by adding the increasing number of well-characterized SP systems.

Crucial help in this regard will come from the Gaia (e.g., Sozzetti 2024) and PLATO (Rauer et al. 2014, 2025) space missions. The Gaia mission, in particular with Data Release 4 foreseen in 2026, is expected to (i) give crucial information on the presence of CJs (e.g., Holl et al. 2023), especially around relatively bright stars; (ii) provide CJ true masses (note that about 30% of the CJs in the SP sample have already measured M_p thanks to the combination of RVs and Hipparcos-Gaia proper motion anomalies; see, e.g., Kervella et al. 2022; Errico et al. 2022; and Table E.1); and (iii) help us unveil the origin of some RV long-term trends (e.g., Bardalez Gagliuffi et al. 2021). PLATO is expected to detect $\gtrsim 8,000$ SP systems orbiting bright solar-type stars with $V \leq 11^{12}$, which are thus amenable to high-precision RV follow up. Moreover, PLATO will reveal new SPs in known TESS systems, thus allowing for more in depth studies of $f_{CJ|SP}$ as a function of SP multiplicity.

Acknowledgements. We are grateful to the anonymous referee for her/his valuable comments, which allowed us to considerably improve this work. We are thankful to Profs. A. Morbidelli and B. Bitsch for useful discussions about theoretical predictions on SP-CJ relations. We also thank Dr. K. Bazzzo for her suggestion to use the Hypatia catalog. We acknowledge financial contribution from the INAF Large Grant 2023 “EXODEMO” and from the European Union - Next Generation EU RRF M4C2 1.1 PRIN MUR 2022 project 20229R43BH. D.G. gratefully acknowledges the financial support from the grant for internationalization (GAND_GFI_23_01) granted by the University of Turin (Italy). This research has made use of the NASA Exoplanet Archive, which is operated by the California Institute of Technology, under contract with the National Aeronautics and Space Administration under the Exoplanet Exploration Program. The research shown here acknowledges use of the Hypatia Catalog Database, an online compilation of stellar abundance data, which was supported by NASA’s Nexus for Exoplanet System Science (NExSS) research coordination network and the Vanderbilt Initiative in Data-Intensive Astrophysics (VIDA).

References

- Ahrer, E., Queloz, D., Rajpaul, V. M., et al. 2021, MNRAS, 503, 1248
 Akana Murphy, J. M., Batalha, N. M., Scarsdale, N., et al. 2023, AJ, 166, 153
 Akana Murphy, J. M., Kosiarek, M. R., Batalha, N. M., et al. 2021, AJ, 162, 294
 Alonso, R., Moutou, C., Endl, M., et al. 2014, A&A, 567, A112
 Alqasim, A., Grieves, N., Rosário, N. M., et al. 2024, MNRAS, 533, 1
 Anderson, D. R., Collier Cameron, A., Delrez, L., et al. 2014, MNRAS, 445, 1114
 Astudillo-Defru, N., Cloutier, R., Wang, S. X., et al. 2020, A&A, 636, A58
 Astudillo-Defru, N., Forveille, T., Bonfils, X., et al. 2017, A&A, 602, A88
 Azevedo Silva, T., Demangeon, O. D. S., Barros, S. C. C., et al. 2022, A&A, 657, A68
 Barbato, D., Pinamonti, M., Sozzetti, A., et al. 2020, A&A, 641, A68
 Barbato, D., Sozzetti, A., Desidera, S., et al. 2018, A&A, 615, A175
 Bardalez Gagliuffi, D. C., Faherty, J. K., Li, Y., et al. 2021, ApJ, 922, L43
 Barnes, J. R., Standing, M. R., Haswell, C. A., et al. 2023, MNRAS, 524, 5196
 Barros, S. C. C., Demangeon, O. D. S., Alibert, Y., et al. 2022, A&A, 665, A154
 Barros, S. C. C., Demangeon, O. D. S., Armstrong, D. J., et al. 2023, A&A, 673, A4
 Baycroft, T. A., Badnell, H., Blacker, S., & Triaud, A. H. M. J. 2023, Research Notes of the American Astronomical Society, 7, 175
 Beard, C., Robertson, P., Dai, F., et al. 2024, AJ, 167, 70
 Benedict, G. F. & Harrison, T. E. 2017, AJ, 153, 258
 Benedict, G. F., McArthur, B. E., Nelan, E. P., et al. 2022, AJ, 163, 295
 Bitsch, B. & Izidoro, A. 2023, A&A, 674, A178
 Bonomo, A. S., Dumusque, X., Massa, A., et al. 2023, A&A, 677, A33
 Bonomo, A. S., Sozzetti, A., Lovis, C., et al. 2014, A&A, 572, A2
 Borgniet, S., Lagrange, A. M., Meunier, N., & Galland, F. 2017, A&A, 599, A57
 Borucki, W. J., Koch, D. G., Batalha, N., et al. 2012, ApJ, 745, 120
 Bourrier, V., Dumusque, X., Dorn, C., et al. 2018, A&A, 619, A1
 Brewer, J. M., Zhao, L. L., Fischer, D. A., et al. 2023, AJ, 166, 46
 Brinkman, C. L., Weiss, L. M., Dai, F., et al. 2023, AJ, 165, 88
 Bryan, M. L., Knutson, H. A., Lee, E. J., et al. 2019, AJ, 157, 52
 Bryan, M. L. & Lee, E. J. 2024, ApJ, 968, L25
 Bryan, M. L. & Lee, E. J. 2025, ApJ, 982, L7
 Burt, J., Feng, F., Holden, B., et al. 2021, AJ, 161, 10
 Butler, R. P., Wright, J. T., Marcy, G. W., et al. 2006, ApJ, 646, 505
 Cloutier, R., Rodriguez, J. E., Irwin, J., et al. 2020, AJ, 160, 22
 Cochran, W. D., Fabrycky, D. C., Torres, G., et al. 2011, ApJS, 197, 7
 Courcol, B., Bouchy, F., Pepe, F., et al. 2015, A&A, 581, A38
 Dai, F., Howard, A. W., Batalha, N. M., et al. 2021, AJ, 162, 62
 Dalal, S., Rescigno, F., Cretignier, M., et al. 2024, MNRAS, 531, 4464
 Damasso, M., Rodrigues, J., Castro-González, A., et al. 2023, A&A, 679, A33
 Dawson, R. I. & Johnson, J. A. 2018, ARA&A, 56, 175
 Deeg, H. J., Georgieva, I. Y., Nowak, G., et al. 2023, A&A, 677, A12
 Delrez, L., Ehrenreich, D., Alibert, Y., et al. 2021, Nature Astronomy, 5, 775
 Desai, A., Turtelboom, E. V., Harada, C. K., et al. 2024, AJ, 167, 194
 Díaz, R. F., Segransan, D., Udry, S., et al. 2016, A&A, 585, A134
 DiTomasso, V., Nava, C., López-Morales, M., et al. 2023, AJ, 165, 38
 Donati, J. F., Cristofari, P. I., Finocci, B., et al. 2023, MNRAS, 525, 455
 Dumusque, X., Turner, O., Dorn, C., et al. 2019, A&A, 627, A43
 Errico, A., Wittenmyer, R. A., Horner, J., et al. 2022, AJ, 163, 273
 Feng, F., Butler, R. P., Vogt, S. S., et al. 2022, ApJS, 262, 21
 Feng, F., Crane, J. D., Xuesong Wang, S., et al. 2019, ApJS, 242, 25
 Feng, F., Shectman, S. A., Clement, M. S., et al. 2020, ApJS, 250, 29
 Feng, F., Tuomi, M., & Jones, H. R. A. 2017, MNRAS, 470, 4794
 Fischer, D. A., Gaidos, E., Howard, A. W., et al. 2012, ApJ, 745, 21
 Fischer, D. A. & Valenti, J. 2005, ApJ, 622, 1102
 Frensch, Y. G. C., Lo Curto, G., Bouchy, F., et al. 2023, A&A, 675, A173
 Fulton, B. J. & Petigura, E. A. 2018, AJ, 156, 264
 Fulton, B. J., Rosenthal, L. J., Hirsch, L. A., et al. 2021, ApJS, 255, 14
 Gan, T., Bedell, M., Wang, S. X., et al. 2021, MNRAS, 507, 2220
 Ginzburg, S., Schlichting, H. E., & Sari, R. 2018, MNRAS, 476, 759
 Grunblatt, S. K., Saunders, N., Huber, D., et al. 2024, AJ, 168, 1
 Haghhighipour, N., Butler, R. P., Rivera, E. J., Henry, G. W., & Vogt, S. S. 2012, ApJ, 756, 91
 Hara, N. C., Bouchy, F., Stalport, M., et al. 2020, A&A, 636, L6
 Hatzes, A. P., Gandolfi, D., Korth, J., et al. 2022, AJ, 163, 223
 Hawthorn, F., Bayliss, D., Wilson, T. G., et al. 2023, MNRAS, 520, 3649
 Haywood, R. D., Collier Cameron, A., Queloz, D., et al. 2014, MNRAS, 443, 2517
 Hébrard, G., Udry, S., Lo Curto, G., et al. 2010, A&A, 512, A46
 Heidari, N., Boisse, I., Orell-Miquel, J., et al. 2022, A&A, 658, A176
 Hidalgo, D., Pallé, E., Alonso, R., et al. 2020, A&A, 636, A89
 Hinkel, N. R., Timmes, F. X., Young, P. A., Pagano, M. D., & Turnbull, M. C. 2014, AJ, 148, 54
 Hobson, M. J., Bouchy, F., Lavie, B., et al. 2024, A&A, 688, A216
 Hobson, M. J., Díaz, R. F., Delfosse, X., et al. 2018, A&A, 618, A103
 Holl, B., Sozzetti, A., Sahlmann, J., et al. 2023, A&A, 674, A10
 Horner, J., Wittenmyer, R. A., Wright, D. J., et al. 2019, AJ, 158, 100
 Hua, X., Wang, S. X., Teske, J. K., et al. 2023, AJ, 166, 32
 Huang, C. X., Petrovich, C., & Deibert, E. 2017, AJ, 153, 210
 Izidoro, A., Raymond, S. N., Morbidelli, A., Hersant, F., & Pierens, A. 2015, ApJ, 800, L22
 Jenkins, J. S., Jones, H. R. A., Tuomi, M., et al. 2017, MNRAS, 466, 443
 Jenkins, J. S., Jones, H. R. A., Tuomi, M., et al. 2013, ApJ, 766, 67
 Johnson, J. A., Aller, K. M., Howard, A. W., & Crepp, J. R. 2010, PASP, 122, 905
 Kane, S. R., Yalçınkaya, S., Osborn, H. P., et al. 2020, AJ, 160, 129

¹² This can be estimated from the planet detection rate in Matuszewski et al. 2023 after 2+2 yr mission and the *Kepler* transit multiplicity distribution in Zhu & Dong 2021.

- Kervella, P., Arenou, F., & Thévenin, F. 2022, A&A, 657, A7
- Kipping, D. M. 2013, MNRAS, 434, L51
- Korth, J., Chaturvedi, P., Parviainen, H., et al. 2024, ApJ, 971, L28
- Kunimoto, M., Vanderburg, A., Huang, C. X., et al. 2023, AJ, 166, 7
- Lam, K. W. F., Santerne, A., Sousa, S. G., et al. 2018, A&A, 620, A77
- Lambrechts, M., Morbidelli, A., Jacobson, S. A., et al. 2019, A&A, 627, A83
- Li, Z., Kane, S. R., Brandt, T. D., et al. 2024, AJ, 167, 155
- Lillo-Box, J., Faria, J. P., Suárez Mascareño, A., et al. 2021, A&A, 654, A60
- Lillo-Box, J., Lopez, T. A., Santerne, A., et al. 2020, A&A, 640, A48
- Lo Curto, G., Mayor, M., Benz, W., et al. 2013, A&A, 551, A59
- Lo Curto, G., Mayor, M., Benz, W., et al. 2010, A&A, 512, A48
- Lopez, E. D. & Fortney, J. J. 2014, ApJ, 792, 1
- Lovis, C., Ségransan, D., Mayor, M., et al. 2011, A&A, 528, A112
- Lubin, J., Van Zandt, J., Holcomb, R., et al. 2022, AJ, 163, 101
- Luhn, J. K., Bastien, F. A., Wright, J. T., et al. 2019, AJ, 157, 149
- Luque, R., Osborn, H. P., Leleu, A., et al. 2023, Nature, 623, 932
- MacDougall, M. G., Petigura, E. A., Fetherolf, T., et al. 2022, AJ, 164, 97
- MacDougall, M. G., Petigura, E. A., Gilbert, G. J., et al. 2023, AJ, 166, 33
- Mantovani, G., Malavolta, L., Desidera, S., et al. 2024, A&A, 682, A129
- Marcy, G. W., Isaacson, H., Howard, A. W., et al. 2014, ApJS, 210, 20
- Marmier, M., Ségransan, D., Udry, S., et al. 2013, A&A, 551, A90
- Martioli, E., Hébrard, G., de Almeida, L., et al. 2023, A&A, 680, A84
- Martioli, E., Hébrard, G., Fouqué, P., et al. 2022, A&A, 660, A86
- Matuszewski, K., Nettelmann, N., Cabrera, J., Börner, A., & Rauer, H. 2023, A&A, 677, A133
- Mayo, A. W., Dressing, C. D., Vanderburg, A., et al. 2023, AJ, 165, 235
- Mayor, M., Marmier, M., Lovis, C., et al. 2011, arXiv e-prints, arXiv:1109.2497
- McCarthy, C., Butler, R. P., Tinney, C. G., et al. 2004, ApJ, 617, 575
- Ment, K., Fischer, D. A., Bakos, G., Howard, A. W., & Isaacson, H. 2018, AJ, 156, 213
- Mortier, A., Faria, J. P., Santos, N. C., et al. 2016, A&A, 585, A135
- Mortier, A., Santos, N. C., Sousa, S., et al. 2013, A&A, 551, A112
- Moutou, C., Almenara, J. M., Díaz, R. F., et al. 2014, MNRAS, 444, 2783
- Moutou, C., Lo Curto, G., Mayor, M., et al. 2015, A&A, 576, A48
- Moutou, C., Mayor, M., Lo Curto, G., et al. 2009, A&A, 496, 513
- Naef, D., Mayor, M., Benz, W., et al. 2007, A&A, 470, 721
- Naef, D., Mayor, M., Lo Curto, G., et al. 2010, A&A, 523, A15
- Napoliello, L., Mancini, L., Damasso, M., et al. 2022, A&A, 667, A8
- Napoliello, L., Mancini, L., Sozzetti, A., et al. 2023, Nature, 622, 255
- Napoliello, L., et al. in prep., A&A
- Nardiello, D., Malavolta, L., Desidera, S., et al. 2022, A&A, 664, A163
- Nascimbeni, V., Borsato, L., Zingales, T., et al. 2023, A&A, 673, A42
- Orell-Miquel, J., Carleo, I., Murgas, F., et al. 2024, A&A, 684, A96
- Orell-Miquel, J., Nowak, G., Murgas, F., et al. 2023, A&A, 669, A40
- Osborn, A., Armstrong, D. J., Cale, B., et al. 2021, MNRAS, 507, 2782
- Osborn, H. P., Nowak, G., Hébrard, G., et al. 2023, MNRAS, 523, 3069
- Osborne, H. L. M., Van Eylen, V., Goffo, E., et al. 2024, MNRAS, 527, 11138
- Otor, O. J., Montet, B. T., Johnson, J. A., et al. 2016, AJ, 152, 165
- Paethorpe, L., John, A. A., Mortier, A., et al. 2024, MNRAS, 529, 3323
- Perger, M., Ribas, I., Damasso, M., et al. 2017, A&A, 608, A63
- Petigura, E. A., Benneke, B., Batygin, K., et al. 2018, AJ, 156, 89
- Petigura, E. A., Livingston, J., Batygin, K., et al. 2020, AJ, 159, 2
- Petigura, E. A., Rogers, J. G., Isaacson, H., et al. 2022, AJ, 163, 179
- Philipot, F., Lagrange, A. M., Kiefer, F., et al. 2023, A&A, 678, A107
- Pidhorodetska, D., Gilbert, E. A., Kane, S. R., et al. 2024, AJ, 168, 135
- Pinamonti, M., Sozzetti, A., Maldonado, J., et al. 2022, A&A, 664, A65
- Polanski, A. S., Lubin, J., Beard, C., et al. 2024, ApJS, 272, 32
- Psaridi, A., Osborn, H., Bouchy, F., et al. 2024, A&A, 685, A5
- Rauer, H., Aerts, C., Cabrera, J., et al. 2025, Exp. Astron., 59, 26
- Rauer, H., Catala, C., Aerts, C., et al. 2014, Exp. Astron., 38, 249
- Rescigno, F., Hébrard, G., Vanderburg, A., et al. 2024, MNRAS, 527, 5385
- Rickman, E. L., Ségransan, D., Marmier, M., et al. 2019, A&A, 625, A71
- Rosenthal, L. J., Fulton, B. J., Hirsch, L. A., et al. 2021, ApJS, 255, 8
- Rosenthal, L. J., Knutson, H. A., Chachan, Y., et al. 2022, ApJS, 262, 1
- Rubenzahl, R. A., Dai, F., Howard, A. W., et al. 2024, AJ, 167, 153
- Ruggieri, A., et al. in prep., A&A
- Santos, N. C., Santerne, A., Faria, J. P., et al. 2016, A&A, 592, A13
- Scarsdale, N., Murphy, J., Batalha, N., et al. 2021, AJ, 162, 215
- Schlecker, M., Mordasini, C., Emsenhuber, A., et al. 2021, A&A, 656, A71
- Serrano, L. M., Gandolfi, D., Mustill, A. J., et al. 2022, Nature Astronomy, 6, 736
- Sinukoff, E., Howard, A. W., Petigura, E. A., et al. 2017, AJ, 153, 271
- Sousa, S. G., Santos, N. C., Israeli, G., Mayor, M., & Udry, S. 2011, A&A, 533, A141
- Sozzetti, A. 2024, Comptes Rendus Physique, 24, 152
- Sozzetti, A., Damasso, M., Bonomo, A. S., et al. 2021, A&A, 648, A75
- Sozzetti, A., Damasso, M., Fernández Fernández, J., et al. 2024, MNRAS, 535, 531
- Sreenivas, K. R., Perdelwitz, V., Tal-Or, L., et al. 2022, A&A, 660, A124
- Stalport, M., Cretignier, M., Udry, S., et al. 2023, A&A, 678, A90
- Stassun, K. G., Collins, K. A., & Gaudi, B. S. 2017, AJ, 153, 136
- Suárez Mascareño, A., González Hernández, J. I., Rebolo, R., et al. 2018, A&A, 612, A41
- Suárez Mascareño, A., Passegger, V. M., González Hernández, J. I., et al. 2024, A&A, 685, A56
- Sulis, S., Crossfield, I. J. M., Santerne, A., et al. 2024, A&A, 688, A14
- Teske, J., Díaz, M. R., Luque, R., et al. 2020, AJ, 160, 96
- Trifonov, T., Tal-Or, L., Zechmeister, M., et al. 2020, A&A, 636, A74
- Tuomi, M., Jones, H. R. A., Barnes, J. R., Anglada-Escudé, G., & Jenkins, J. S. 2014, MNRAS, 441, 1545
- Turtelboom, E. V., Weiss, L. M., Dressing, C. D., et al. 2022, AJ, 163, 293
- Udry, S., Dumusque, X., Lovis, C., et al. 2019, A&A, 622, A37
- Unger, N., Ségransan, D., Queloz, D., et al. 2021, A&A, 654, A104
- Van Zandt, J., Petigura, E. A., MacDougall, M., et al. 2023, AJ, 165, 60
- Vanderburg, A., Becker, J. C., Buchhave, L. A., et al. 2017, AJ, 154, 237
- Vissapragada, S., Jontof-Hutter, D., Shporer, A., et al. 2020, AJ, 159, 108
- Vogt, S. S., Butler, R. P., Burt, J., et al. 2017, AJ, 154, 181
- Weiss, L. M., Isaacson, H., Howard, A. W., et al. 2024, ApJS, 270, 8
- Wittenmyer, R. A., Endl, M., Cochran, W. D., Levison, H. F., & Henry, G. W. 2009, ApJS, 182, 97
- Wittenmyer, R. A., Horner, J., Mengel, M. W., et al. 2017, AJ, 153, 167
- Wittenmyer, R. A., Tan, X., Lee, M. H., et al. 2014, ApJ, 780, 140
- Wittenmyer, R. A., Wang, S., Horner, J., et al. 2020, MNRAS, 492, 377
- Xiao, G.-Y., Liu, Y.-J., Teng, H.-Y., et al. 2023, Research in Astronomy and Astrophysics, 23, 055022
- Zechmeister, M., Kürster, M., & Endl, M. 2009, A&A, 505, 859–871
- Zeng, L., & Sasselov, D. 2013, PASP, 125, 227
- Zhang, J., Weiss, L. M., Huber, D., et al. 2021, AJ, 162, 89
- Zhu, W. 2024, Research in Astronomy and Astrophysics, 24, 045013
- Zhu, W. & Dong, S. 2021, ARA&A, 59, 291
- Zhu, W., Petrovich, C., Wu, Y., Dong, S., & Xie, J. 2018, ApJ, 860, 101
- Zhu, W. & Wu, Y. 2018, AJ, 156, 92

Appendix A: Sample of solar-type stars in the small planet sample

Table A.1. Stars of the small planet sample and their properties.

Target	M _* [M _⊕]	[Fe/H] [dex]	N _{pl}	Method	N _{obs}	Baseline [yrs]	CJ [0.3 – 13 M _{Jup}]	CJ [0.5 – 20 M _{Jup}]	Ref. for RVs and parameters (if different from RVs)
61-Vir	0.91 ± 0.04	0.03 ± 0.06	3	RV	602	15.20	No	No	96
BD-08-2823	0.74 ± 0.07	0.00 ± 0.02 ¹	2	RV	83	5.04	No	No	49
BD-11-4672	0.65 ± 0.03	-0.35 ± 0.15	2	RV	111	14.16	Yes	Yes	10
CoRoT-7	0.90 ± 0.12	0.06 ± 0.10	3	Transit	180	3.90	No	No	48
CoRoT-22	1.10 ± 0.05	0.17 ± 0.12	1	Transit	23	4.90	No	No	77
CoRoT-24	0.91 ± 0.09	0.30 ± 0.15	2	Transit	37	3.10	No	No	4
DMPP-4	1.25 ± 0.02	-0.01 ± 0.06	2	RV	71	4.27	No	No	11
GJ-96	0.60 ± 0.07	0.14 ± 0.08	1	RV	72	5.53	No	No	52
GJ-160.2	0.69 ± 0.10	-0.26 ± 0.10 ¹	1	RV	100	6.37	No	No	120,111
GJ-338-B	0.64 ± 0.07	-0.03 ± 0.16	1	RV	114	9.25	No	No	33
GJ-414-A	0.69 ± 0.01	0.24 ± 0.07	2	RV	420	6.48	No	No	96
GJ-676	0.73 ± 0.21	0.08 ± 0.10	4	RV	127	8.85	Yes	Yes	21,105
GJ-2030	0.96 ± 0.13	-0.44 ± 0.14 ¹	2	RV	48	8.93	No	No	110,39
GJ-2056	0.62 ± 0.08	-0.08 ± 0.10 ¹	1	RV	51	9.07	No	No	38
GJ-3138	0.68 ± 0.10	-0.30 ± 0.12	3	RV	199	8.03	No	No	7
GJ-3222	0.89 ± 0.11	0.08 ± 0.04 ¹	1	RV	60	4.02	No	No	110,39
GJ-3942	0.63 ± 0.07	-0.04 ± 0.09	1	RV	145	3.30	No	No	87
GJ-9404	0.62 ± 0.07	-0.08 ± 0.04 ¹	1	RV	54	3.92	No	No	92,14
HD-1461	1.03 ± 0.05	0.18 ± 0.06	2	RV	846	23.30	No	No	96
HD-4308	0.93 ± 0.10	-0.35 ± 0.10	1	RV	348	13.92	No	No	110,105
HD-7924	0.80 ± 0.03	-0.12 ± 0.06	3	RV	967	18.10	No	No	96
HD-12235	1.10 ± 0.13	0.32 ± 0.05 ¹	2	RV	44	24.10	No	No	39
HD-13808	0.77 ± 0.02	-0.21 ± 0.02	2	RV	246	11.10	No	No	1
HD-18143	0.85 ± 0.10	0.32 ± 0.06 ¹	2	RV	80	20.99	No	No	39
HD-20003	0.88 ± 0.10	0.04 ± 0.02	2	RV	203	13.73	No	No	110,113
HD-20781	0.70 ± 0.10	-0.11 ± 0.02	4	RV	237	13.74	No	No	110,113
HD-21693	0.80 ± 0.10	0.00 ± 0.10	2	RV	213	11.25	No	No	110,113
HD-22496	0.68 ± 0.01	-0.08 ± 0.02	1	RV	43	6.90	No	No	63
HD-24085	1.22 ± 0.07	0.17 ± 0.06 ¹	1	RV	25	8.66	No	No	37
HD-31527	0.96 ± 0.10	-0.17 ± 0.01	3	RV	268	13.84	No	No	110,113
HD-34445	1.11 ± 0.06	0.14 ± 0.06	6	RV	222	21.80	Yes	Yes	96
HD-39091	1.07 ± 0.04	0.09 ± 0.04	3	RV	402	2.20	Yes	Yes	46
HD-39194	0.67 ± 0.04	-0.61 ± 0.02	3	RV	273	13.69	No	No	114
HD-39855	0.87 ± 0.05	-0.43 ± 0.04 ¹	1	RV	25	6.22	No	No	37
HD-40307	0.77 ± 0.10	-0.31 ± 0.03	5	RV	226	10.44	No	No	32
HD-45184	1.02 ± 0.05	0.04 ± 0.06	2	RV	339	23.40	No	No	96
HD-48948	0.69 ± 0.02	-0.21 ± 0.03	3	RV	189	9.50	No	No	27
HD-51608	0.80 ± 0.10	-0.07 ± 0.01	2	RV	201	9.95	No	No	39,113
HD-69830	0.89 ± 0.04	0.01 ± 0.06	3	RV	529	13.24	No	No	96
HD-74698	1.04 ± 0.03	0.07 ± 0.02	2	RV	119	14.10	Yes	No	41
HD-77338	1.37 ± 0.32	0.32 ± 0.10	1	RV	32	7.22	No	No	56,105
HD-86226	1.02 ± 0.06	0.02 ± 0.05	2	RV	27	5.10	Yes	No	109
HD-90156	0.86 ± 0.04	-0.18 ± 0.06	1	RV	167	23.18	No	No	96
HD-93351	0.94 ± 0.12	-0.20 ± 0.02	2	RV	37	13.97	No	No	110,39
HD-93385	1.04 ± 0.01	0.02 ± 0.01	3	RV	241	13.23	No	No	114
HD-96700	0.89 ± 0.01	-0.18 ± 0.01	3	RV	254	14.40	No	No	114
HD-97658	0.77 ± 0.03	-0.23 ± 0.06	1	RV	577	22.83	No	No	96
HD-125612	1.11 ± 0.20	0.25 ± 0.04	3	RV	72	12.13	Yes	Yes	75
HD-134060	1.09 ± 0.10	0.14 ± 0.01	2	RV	339	13.21	No	No	110,113
HD-134606	1.05 ± 0.10	0.34 ± 0.08	5	RV	66	17.30	No	No	61
HD-136352	0.87 ± 0.04	-0.24 ± 0.05	3	RV	246	13.20	No	No	30,57
HD-141004	1.05 ± 0.05	0.03 ± 0.06	1	RV	873	6.64	No	No	96
HD-144899	1.16 ± 0.16	0.37 ± 0.12 ¹	1	RV	22	6.34	No	No	110,39
HD-153557	0.79 ± 0.09	-0.26 ± 0.09	3	RV	36	22.20	No	No	96
HD-154088	0.91 ± 0.02	0.28 ± 0.03	1	RV	187	11.35	No	No	114
HD-155918	1.03 ± 0.13	-0.65 ± 0.06 ¹	2	RV	73	13.43	No	No	39
HD-156098	1.29 ± 0.20	0.19 ± 0.10 ¹	2	RV	61	12.94	Yes	Yes	110,39
HD-156668	0.77 ± 0.02	0.05 ± 0.06	1	RV	619	16.67	No	No	96
HD-158259	1.08 ± 0.10	0.00 ± 0.12 ¹	5	RV	580	7.01	No	No	45
HD-160691	1.13 ± 0.02	0.28 ± 0.03	4	RV	180	17.31	Yes	Yes	16
HD-164595	0.99 ± 0.03	-0.04 ± 0.08	1	RV	75	2.33	No	No	25
HD-164922	0.92 ± 0.03	0.20 ± 0.06	4	RV	413	23.68	Yes	No	96
HD-168009	0.99 ± 0.04	0.02 ± 0.06	1	RV	450	5.74	No	No	96
HD-175607	0.71 ± 0.01	-0.62 ± 0.01	1	RV	110	9.29	No	No	76
HD-176986	0.79 ± 0.02	0.03 ± 0.05	2	RV	259	13.16	No	No	106
HD-177565	1.00 ± 0.10	0.08 ± 0.01 ¹	1	RV	68	4.61	No	No	36
HD-179079	1.14 ± 0.19	0.23 ± 0.10	1	RV	86	11.20	No	No	75
HD-181433	0.78 ± 0.10	0.33 ± 0.13	3	RV	200	13.78	Yes	Yes	54
HD-189567	0.83 ± 0.01	-0.24 ± 0.01	2	RV	256	13.20	No	No	114
HD-190007	0.77 ± 0.02	0.16 ± 0.05	1	RV	157	6.23	No	No	22,104

Notes. From left to right, the columns report the name of the system, the mass and metallicity of the host star, the planet multiplicity, the method by which the system was detected (either RV or transit), the number and baseline of observations of the best RV dataset used, the presence or absence of confirmed CJs in the $0.3 - 13 M_{\text{Jup}}$ and $0.5 - 20 M_{\text{Jup}}$ mass ranges (“Yes” appears in both columns if at least one CJ in the overlapping range $0.5 - 13 M_{\text{Jup}}$ is present), the reference for the RV dataset and stellar parameters. References are given after Table A.2.

Table A.2. Stars of the mixed systems and their properties.

Target	M_{\star} [M_{\odot}]	[Fe/H] [dex]	N_{pl}	Method	N_{obs}	Baseline [yrs]	CJ [$0.3 - 13 M_{\text{Jup}}$]	CJ [$0.5 - 20 M_{\text{Jup}}$]	Ref. for RVs and parameters (if different from RVs)
55-Cnc	0.98 ± 0.05	0.38 ± 0.06	5	RV	679	15.30	Yes	Yes	96
HD-10180	1.06 ± 0.05	0.08 ± 0.01	6	RV	190	6.70	No	No	66
HD-99492	0.85 ± 0.02	0.30 ± 0.03	2	RV	197	23.10	No	No	96,104
HD-104067	0.82 ± 0.03	0.09 ± 0.06	2	RV	53	14.90	No	No	96
HD-107148	1.11 ± 0.04	0.30 ± 0.06	2	RV	110	15.60	No	No	96
HD-109271	1.05 ± 0.02	0.10 ± 0.05	2	RV	106	9.50	No	No	64
HIP-57274	0.73 ± 0.05	0.09 ± 0.05	3	RV	110	5.50	Yes	Yes	40
K2-19	0.88 ± 0.03	0.06 ± 0.05	3	Transit	51	2.90	No	No	89
Kepler-56	1.67 ± 0.15	0.40 ± 0.04	3	Transit	28	10.10	Yes	Yes	118,90
Kepler-88/KOI-142	0.99 ± 0.02	0.27 ± 0.04	2	Transit	47	9.00	No	No	118,90
Kepler-89/KOI-94	1.21 ± 0.04	0.07 ± 0.06	4	Transit	71	12.70	No	No	118,90
Kepler-100	1.10 ± 0.03	0.10 ± 0.04	4	Transit	112	13.50	No	No	118,90
Kepler-101	1.17 ± 0.07	0.33 ± 0.07	2	Transit	50	6.10	No	No	17
rho-CrB	0.95 ± 0.01	-0.20 ± 0.01	4	RV	587	13.70	No	No	96,19
TOI-500	0.74 ± 0.02	0.12 ± 0.08	4	Transit	197	1.00	No	No	100
TOI-815	0.78 ± 0.04	-0.09 ± 0.05	2	Transit	28	1.70	No	No	94
TOI-1272	0.85 ± 0.05	0.17 ± 0.06	2	Transit	62	1.80	No	No	68
TOI-1408	1.31 ± 0.09	0.25 ± 0.06	2	Transit	60	3.10	No	No	58
TOI-1410	0.79 ± 0.02	0.33 ± 0.09	2	Transit	56	2.70	No	No	93
TOI-1726/HD-63433	0.99 ± 0.03	0.08 ± 0.05	3	Transit	23	1.70	No	No	93
TOI-2134	0.74 ± 0.03	0.12 ± 0.02	2	Transit	108	2.20	No	No	95
TOI-4010	0.89 ± 0.03	0.37 ± 0.07	4	Transit	128	2.60	Yes	Yes	59
TOI-5398	1.15 ± 0.01	0.09 ± 0.06	2	Transit	86	1.20	No	No	70
WASP-47	1.04 ± 0.03	0.38 ± 0.05	4	Transit	142	9.20	Yes	Yes	115
WASP-84	0.84 ± 0.04	0.00 ± 0.10	2	Transit	64	5.20	No	No	6

Notes. Same as Table A.1

References: (1) Ahren et al. (2021), (2) Akana Murphy et al. (2021), (3) Akana Murphy et al. (2023), (4) Alonso et al. (2014), (5) Alqasim et al. (2024), (6) Anderson et al. (2014), (7) Astudillo-Defru et al. (2017), (8) Astudillo-Defru et al. (2020), (9) Azevedo Silva et al. (2022), (10) Barbato et al. (2020), (11) Barnes et al. (2023), (12) Barros et al. (2022), (13) Barros et al. (2023), (14) Baycroft et al. (2023), (15) Beard et al. (2024), (16) Benedict et al. (2022), (17) Bonomo et al. (2014), (18) Bonomo et al. (2023), (19) Brewer et al. (2023), (20) Brinkman et al. (2023), (21) Bryan et al. (2019), (22) Burt et al. (2021), (23) Cloutier et al. (2020), (24) Cochran et al. (2011), (25) Courcol et al. (2015), (26) Dai et al. (2021), (27) Dalal et al. (2024), (28) Damasso et al. (2023), (29) Deeg et al. (2023), (30) Delrez et al. (2021), (31) Desai et al. (2024), (32) Díaz et al. (2016), (33) DiTomasso et al. (2023), (34) Donati et al. (2023), (35) Dumusque et al. (2019), (36) Feng et al. (2017), (37) Feng et al. (2019), (38) Feng et al. (2020), (39) Feng et al. (2022), (40) Fischer et al. (2012), (41) Frensch et al. (2023), (42) Fulton & Petigura (2018), (43) Gan et al. (2021), (44) Grunblatt et al. (2024), (45) Hara et al. (2020), (46) Hatzes et al. (2022), (47) Hawthorn et al. (2023), (48) Haywood et al. (2014), (49) Hébrard et al. (2010), (50) Heidari et al. (2022), (51) Hidalgo et al. (2020), (52) Hobson et al. (2018), (53) Hobson et al. (2024), (54) Horner et al. (2019), (55) Hua et al. (2023), (56) Jenkins et al. (2013), (57) Kane et al. (2020), (58) Korth et al. (2024), (59) Kunimoto et al. (2023), (60) Lam et al. (2018), (61) Li et al. (2024), (62) Lillo-Box et al. (2020), (63) Lillo-Box et al. (2021), (64) Lo Curto et al. (2013), (65) Lo Curto et al. (2010), (66) Lovis et al. (2011), (67) Luque et al. (2023), (68) MacDougall et al. (2022), (69) MacDougall et al. (2023), (70) Mantovani et al. (2024), (71) Marcy et al. (2014), (72) Martioli et al. (2022), (73) Martioli et al. (2023), (74) Mayo et al. (2023), (75) Ment et al. (2018), (76) Mortier et al. (2016), (77) Moutou et al. (2014), (78) Naponiello et al. (2022), (79) Naponiello, L., et al. (in prep.), (80) Nardiello et al. (2022), (81) Orell-Miquel et al. (2023), (82) Orell-Miquel et al. (2024), (83) Osborn et al. (2021), (84) Osborn et al. (2023), (85) Osborne et al. (2024), (86) Paletorope et al. (2024), (87) Perger et al. (2017), (88) Petigura et al. (2018), (89) Petigura et al. (2020), (90) Petigura et al. (2022), (91) Pidhorodetska et al. (2024), (92) Pinamonti et al. (2022), (93) Polanski et al. (2024), (94) Psaridi et al. (2024), (95) Rescigno et al. (2024), (96) Rosenthal et al. (2021), (97) Rubenzahl et al. (2024), (98) Santos et al. (2016), (99) Scarsdale et al. (2021), (100) Serrano et al. (2020), (101) Sinukoff et al. (2017), (102) Sozzetti et al. (2021), (103) Sozzetti et al. (2024), (104) Stalport et al. (2023), (105) Stassun et al. (2017), (106) Suárez Mascareño et al. (2018), (107) Suárez Mascareño et al. (2024), (108) Sulis et al. (2024), (109) Teske et al. (2020), (110) Trifonov et al. (2020), (111) Tuomi et al. (2014), (112) Turtelboom et al. (2022), (113) Udry et al. (2019), (114) Unger et al. (2021), (115) Vanderburg et al. (2017), (116) Van Zandt et al. (2023), (117) Vissapragada et al. (2020), (118) Weiss et al. (2024), (119) Xiao et al. (2023), (120) Zechmeister et al. (2009), (121) Zhang et al. (2021)

¹ Metallicity taken from the Hypatia catalog (Hinkel et al. 2014) as not provided in the reference paper.

Appendix B: Sample of solar-type stars in the AAT, CLS, and HARPS radial velocity surveys

Table B.1. Stars of the AAT, CLS, HARPS radial velocity surveys and their properties.

Target	M_{\star} [M_{\odot}]	[Fe/H] [dex]	CJ		Ref.
			[$0.3 - 13 M_{\text{Jup}}$]	[$0.5 - 20 M_{\text{Jup}}$]	
BD-103166	1.00	0.370 ± 0.060	No	No	CLS
GJ 10	1.19	-0.340 ± 0.100	No	No	HARPS
GJ 1021	1.08	-0.06 ± 0.10	No	No	HARPS
GJ 1043	1.30	-0.25 ± 0.10	No	No	HARPS
GJ 1079	0.80	-0.140 ± 0.080	No	No	HARPS
GJ 1085	1.02	-0.23 ± 0.80	No	No	HARPS
GJ 1126	0.71	-0.57 ± 0.10	No	No	HARPS
GJ 1137	0.84	0.080 ± 0.040	No	No	HARPS
GJ 115	1.07	-0.600 ± 0.040	No	No	HARPS
GJ 117	0.89	0.07 ± 0.20	No	No	HARPS
GJ 1239	0.72	-0.230 ± 0.070	No	No	HARPS

Table B.1 (continued)

Target	M_\star [M_\odot]	[Fe/H] [dex]	CJ [0.3 – 13 M_{Jup}]	CJ [0.5 – 20 M_{Jup}]	Ref.
GJ 1247	0.76	-0.110 ± 0.060	No	No	HARPS
GJ 128	1.14	0.21 ± 0.20	Yes	Yes	HARPS
GJ 1282	1.24	-0.040 ± 0.040	No	No	HARPS
GJ 132	1.06	-0.470 ± 0.040	No	No	HARPS
GJ 138	1.06	-0.25 ± 0.30	No	No	HARPS
GJ 143	0.73	-0.050 ± 0.040	No	No	HARPS
GJ 149	0.72	-0.140 ± 0.040	No	No	HARPS
GJ 159	1.20	0.06 ± 0.10	No	No	HARPS
GJ 17	1.09	-0.21 ± 0.30	No	No	HARPS
GJ 177	1.05	0.01 ± 0.20	No	No	HARPS
GJ 189.2	1.30	-0.29 ± 0.20	No	No	HARPS
GJ 2030	0.96	-0.48 ± 0.10	No	No	HARPS
GJ 2046	0.79	-0.33 ± 0.10	No	No	HARPS
GJ 214	0.96	0.26 ± 0.10	No	No	HARPS
GJ 225.1	1.02	-0.380 ± 0.040	No	No	HARPS
GJ 245.1	1.24	-0.260 ± 0.040	No	No	HARPS
GJ 253	0.93	-0.100 ± 0.040	No	No	HARPS
GJ 260	0.95	0.150 ± 0.040	No	No	HARPS
GJ 275	0.99	0.030 ± 0.040	No	No	HARPS
GJ 279	1.20	-0.17 ± 0.20	Yes	Yes	HARPS
GJ 288	1.08	-0.81 ± 0.20	No	No	HARPS
GJ 29	1.12	-0.280 ± 0.100	No	No	HARPS
GJ 294 A	1.10	-0.32 ± 0.10	No	No	HARPS
GJ 3	0.73	-0.690 ± 0.080	No	No	HARPS
GJ 302	0.93	-0.04 ± 0.10	No	No	HARPS
GJ 309	0.89	-0.41 ± 0.10	No	No	HARPS
GJ 312	1.11	0.130 ± 0.090	No	No	HARPS
GJ 3187	0.85	-0.460 ± 0.060	No	No	HARPS
GJ 3200	1.03	-0.153 ± 0.070	No	No	HARPS
GJ 3222	0.89	0.040 ± 0.040	No	No	HARPS
GJ 3436	1.02	-0.560 ± 0.080	No	No	HARPS
GJ 3446	1.05	-0.070 ± 0.040	No	No	HARPS
GJ 3449	1.08	-0.70 ± 0.20	No	No	HARPS
GJ 3519	1.30	0.090 ± 0.040	No	No	HARPS
GJ 3535	1.05	-0.260 ± 0.060	No	No	HARPS
GJ 355	0.84	0.330 ± 0.040	No	No	HARPS
GJ 3615	0.86	0.040 ± 0.080	No	No	HARPS
GJ 3677	1.21	-0.270 ± 0.040	No	No	HARPS
GJ 3752	0.94	-0.620 ± 0.060	No	No	HARPS
GJ 379.1	1.06	-0.17 ± 0.20	No	No	HARPS
GJ 3830	0.95	-0.130 ± 0.060	No	No	HARPS
GJ 3944	1.04	-0.270 ± 0.060	No	No	HARPS
GJ 3952	1.54	0.0600 ± 0.0100	No	No	HARPS
GJ 398.1	1.14	-0.23 ± 0.10	No	No	HARPS
GJ 423.1	0.93	-0.260 ± 0.080	No	No	HARPS
GJ 4291	0.79	-0.08 ± 0.10	No	No	HARPS
GJ 4340	1.06	0.30 ± 0.20	No	No	HARPS
GJ 4377	0.79	-0.020 ± 0.020	No	No	HARPS
GJ 442	1.01	-0.31 ± 0.40	No	No	HARPS
GJ 446	0.98	-0.290 ± 0.080	No	No	HARPS
GJ 449	1.13	0.13 ± 0.20	No	No	HARPS
GJ 472	0.86	-0.310 ± 0.060	No	No	HARPS
GJ 506	0.98	-0.02 ± 0.50	No	No	HARPS
GJ 530	1.01	-0.050 ± 0.080	No	No	HARPS
GJ 541.1	1.01	0.27 ± 0.20	No	No	HARPS
GJ 542	0.80	0.24 ± 0.20	No	No	HARPS
GJ 550	1.00	-0.100 ± 0.050	No	No	HARPS
GJ 558.1	1.24	-0.170 ± 0.040	No	No	HARPS
GJ 570.1	1.01	0.082 ± 0.080	No	No	HARPS
GJ 570 A	0.75	-0.07 ± 0.20	No	No	HARPS
GJ 579.2	0.82	-1.40 ± 0.20	No	No	HARPS
GJ 579.3	0.89	-0.620 ± 0.060	No	No	HARPS
GJ 58	0.97	-0.410 ± 0.080	No	No	HARPS
GJ 587	0.90	-0.560 ± 0.020	No	No	HARPS
GJ 604	0.72	-0.370 ± 0.100	No	No	HARPS
GJ 613.0	0.85	-0.430 ± 0.060	No	No	HARPS
GJ 615	0.83	-1.26 ± 0.10	No	No	HARPS
GJ 616	1.04	0.04 ± 0.10	No	No	HARPS
GJ 624	1.14	-0.080 ± 0.080	No	No	HARPS
GJ 634.1	1.01	-0.36 ± 0.10	No	No	HARPS
GJ 641	0.94	-0.05 ± 0.10	No	No	HARPS
GJ 656	0.80	-0.710 ± 0.050	No	No	HARPS
GJ 666	0.93	-0.340 ± 0.030	No	No	HARPS
GJ 691	1.03	0.28 ± 0.20	Yes	Yes	HARPS
GJ 695.1	0.99	0.140 ± 0.080	No	No	HARPS

Table B.1 (continued)

Target	M_\star [M_\odot]	[Fe/H] [dex]	CJ [0.3 – 13 M_{Jup}]	CJ [0.5 – 20 M_{Jup}]	Ref.
GJ 699.2	1.39	-0.110 ± 0.040	No	No	HARPS
GJ 724.2	1.10	0.030 ± 0.080	No	No	HARPS
GJ 744	1.00	0.08 ± 0.10	No	No	HARPS
GJ 755	1.04	-0.010 ± 0.080	No	No	HARPS
GJ 768.1	1.15	0.110 ± 0.100	No	No	HARPS
GJ 776	1.02	-0.26 ± 0.30	No	No	HARPS
GJ 780	0.99	0.33 ± 0.10	No	No	HARPS
GJ 781.2	0.74	-0.260 ± 0.030	No	No	HARPS
GJ 785	0.85	-0.01 ± 0.20	No	No	HARPS
GJ 787	0.70	-0.310 ± 0.050	No	No	HARPS
GJ 805	1.35	0.040 ± 0.040	No	No	HARPS
GJ 811	1.22	-0.090 ± 0.070	No	No	HARPS
GJ 812.1	1.04	-0.650 ± 0.060	No	No	HARPS
GJ 825.2	1.05	-0.002 ± 0.060	No	No	HARPS
GJ 827.1	0.79	-0.710 ± 0.070	No	No	HARPS
GJ 836.7	1.08	-0.07 ± 0.10	No	No	HARPS
GJ 838	1.08	-0.03 ± 0.10	No	No	HARPS
GJ 845	0.73	-0.13 ± 0.40	No	No	HARPS
GJ 848	1.36	-0.16 ± 0.10	No	No	HARPS
GJ 849.1	1.22	0.090 ± 0.070	No	No	HARPS
GJ 853	1.06	-0.24 ± 0.20	No	No	HARPS
GJ 9003	0.87	-0.550 ± 0.040	No	No	HARPS
GJ 9007	1.01	-0.300 ± 0.040	No	No	HARPS
GJ 9008	1.08	-0.030 ± 0.050	No	No	HARPS
GJ 902	0.76	-0.37 ± 0.20	No	No	HARPS
GJ 9029	1.12	-0.390 ± 0.060	No	No	HARPS
GJ 904	1.21	-0.12 ± 0.20	No	No	HARPS
GJ 9075	1.16	0.040 ± 0.040	No	No	HARPS
GJ 9121	1.07	-0.84 ± 0.20	No	No	HARPS
GJ 9156	1.02	-0.054 ± 0.040	No	No	HARPS
GJ 9178	0.90	-0.170 ± 0.040	No	No	HARPS
GJ 9191	0.88	-0.640 ± 0.080	No	No	HARPS
GJ 9222	1.25	0.090 ± 0.020	No	No	HARPS
GJ 9252	1.07	-0.190 ± 0.070	No	No	HARPS
GJ 9255	1.22	-0.060 ± 0.080	No	No	HARPS
GJ 9263	1.02	-0.081 ± 0.050	No	No	HARPS
GJ 9269	0.99	0.29 ± 0.10	No	No	HARPS
GJ 9273	1.05	0.13 ± 0.10	No	No	HARPS
GJ 9322	1.00	-0.650 ± 0.100	No	No	HARPS
GJ 9324	1.31	0.120 ± 0.040	No	No	HARPS
GJ 9332	1.16	-0.46 ± 0.30	No	No	HARPS
GJ 9338	1.33	0.070 ± 0.060	No	No	HARPS
GJ 9356	0.76	-0.090 ± 0.040	No	No	HARPS
GJ 9367	1.32	0.060 ± 0.080	No	No	HARPS
GJ 9396	1.01	0.110 ± 0.080	No	No	HARPS
GJ 9467	1.10	-0.150 ± 0.060	No	No	HARPS
GJ 9473	1.18	-0.06 ± 0.20	No	No	HARPS
GJ 9476	1.17	-0.710 ± 0.030	No	No	HARPS
GJ 9479	0.75	0.090 ± 0.020	No	No	HARPS
GJ 9527	1.01	0.036 ± 0.100	No	No	HARPS
GJ 9630	1.00	-0.05 ± 0.10	No	No	HARPS
GJ 9659	1.04	0.029 ± 0.090	No	No	HARPS
GJ 9663	1.27	0.050 ± 0.050	No	No	HARPS
GJ 97	1.07	-0.070 ± 0.100	No	No	HARPS
GJ 9765	0.86	-0.170 ± 0.040	No	No	HARPS
GJ 9787	0.98	-0.020 ± 0.040	No	No	HARPS
GJ 9790	0.98	-0.480 ± 0.060	No	No	HARPS
GJ 9797	0.95	-0.200 ± 0.040	No	No	HARPS
GJ 9801	1.22	-0.24 ± 0.20	No	No	HARPS
GJ 9803	1.00	-0.38 ± 0.30	No	No	HARPS
GJ 9829	1.10	-0.230 ± 0.080	No	No	HARPS
GJ 9833	0.90	-0.19 ± 0.20	No	No	HARPS
GL397	0.70	0.225 ± 0.070	No	No	CLS
HD 10002	0.93	0.251 ± 0.060	No	No	CLS
HD 10008	0.90	0.024 ± 0.060	No	No	CLS
HD 100180	1.06	0.009 ± 0.060	No	No	CLS
HD 100508	0.94	0.360 ± 0.030	No	No	HARPS
HD 100623	0.75	-0.38 ± 0.10	No	No	AAT+CLS*
HD 100777	0.97	0.250 ± 0.060	Yes	Yes	HARPS
HD 101339	1.02	-0.130 ± 0.020	No	No	HARPS
HD 10145	0.92	0.004 ± 0.060	No	No	CLS
HD 101501	0.92	-0.009 ± 0.060	No	No	CLS
HD 101581	0.74	-0.55 ± 0.10	No	No	AAT
HD 101612	1.24	-0.390 ± 0.070	No	No	HARPS
HD 101644	1.01	-0.590 ± 0.020	No	No	HARPS

Table B.1 (continued)

Target	M_{\star} [M_{\odot}]	[Fe/H] [dex]	CJ [0.3 – 13 M_{Jup}]	CJ [0.5 – 20 M_{Jup}]	Ref.
HD 101650	0.69	-0.480 ± 0.020	No	No	HARPS
HD 10180	1.07	0.050 ± 0.080	No	No	HARPS*+AAT
HD 101959	1.12	-0.1100 ± 0.0100	No	No	AAT
HD 102117	1.01	0.274 ± 0.090	No	No	HARPS*+AAT
HD 102195	0.90	0.050 ± 0.040	No	No	HARPS
HD 103095	0.63	-1.146 ± 0.060	No	No	CLS
HD 103197	0.90	0.190 ± 0.020	No	No	HARPS
HD 10360	0.83	-0.24 ± 0.10	No	No	AAT
HD 10361	0.86	-0.200 ± 0.020	No	No	AAT
HD 103720	0.83	-0.010 ± 0.060	No	No	HARPS
HD 103743	1.00	-0.010 ± 0.020	No	No	HARPS
HD 103774	1.37	0.140 ± 0.060	No	No	HARPS
HD 103891	1.10	-0.220 ± 0.080	Yes	Yes	HARPS
HD 103932	0.72	0.117 ± 0.070	No	No	CLS
HD 104006	0.85	-0.78 ± 0.30	No	No	HARPS
HD 104067	0.81	-0.010 ± 0.100	No	No	HARPS+CLS*
HD 104263	0.96	-0.010 ± 0.060	No	No	HARPS
HD 104304	1.03	0.294 ± 0.060	No	No	CLS
HD 10476	0.84	0.004 ± 0.060	No	No	CLS
HD 104800	1.06	-0.820 ± 0.070	No	No	HARPS
HD 104982	1.01	-0.220 ± 0.090	No	No	HARPS
HD 105	1.12	0.05 ± 0.10	No	No	HARPS
HD 105113	1.05	-0.120 ± 0.060	No	No	CLS
HD 105328	1.09	0.090 ± 0.060	No	No	AAT
HD 105631	0.98	0.203 ± 0.060	No	No	CLS
HD 105690	0.99	-0.030 ± 0.020	No	No	HARPS
HD 105779	1.04	-0.250 ± 0.020	Yes	Yes	HARPS
HD 105837	1.08	-0.540 ± 0.080	No	No	HARPS
HD 106275	0.85	-0.110 ± 0.060	No	No	HARPS
HD 106453	1.00	0.050 ± 0.060	No	No	AAT
HD 10647	1.17	-0.03 ± 0.10	Yes	Yes	HARPS*+AAT
HD 10697	1.16	0.160 ± 0.060	Yes	Yes	CLS
HD 10700	0.92	-0.52 ± 0.20	No	No	HARPS*+CLS+AAT
HD 107148	1.03	0.280 ± 0.070	No	No	HARPS+CLS*
HD 107692	1.06	0.14 ± 0.10	No	No	AAT
HD 10780	0.90	0.055 ± 0.060	No	No	CLS
HD 10790	1.02	0.375 ± 0.060	No	No	CLS
HD 108063	1.17	0.520 ± 0.020	No	No	HARPS
HD 108147	1.22	0.17 ± 0.20	No	No	HARPS*+AAT
HD 108309	1.04	0.09 ± 0.10	No	No	HARPS+AAT*
HD 108341	0.89	0.020 ± 0.020	Yes	Yes	HARPS
HD 10853	0.72	-0.045 ± 0.080	No	No	CLS
HD 108564	0.74	-1.000 ± 0.040	No	No	HARPS
HD 108874	1.00	0.221 ± 0.060	Yes	Yes	CLS
HD 109271	1.05	0.070 ± 0.040	No	No	HARPS
HD 109358	0.90	-0.199 ± 0.060	No	No	CLS
HD 109409	1.03	0.300 ± 0.060	No	No	HARPS
HD 109684	1.10	-0.370 ± 0.040	No	No	HARPS
HD 109988	0.88	0.130 ± 0.060	No	No	HARPS
HD 110315	0.72	0.068 ± 0.050	No	No	CLS
HD 110537	1.02	0.104 ± 0.060	No	No	HARPS+CLS*
HD 110557	0.90	-0.090 ± 0.020	No	No	HARPS
HD 110619	0.99	-0.410 ± 0.020	No	No	HARPS
HD 110810	0.83	0.070 ± 0.040	No	No	AAT
HD 110897	0.82	-0.460 ± 0.060	No	No	CLS
HD 111031	1.10	0.272 ± 0.060	No	No	CLS
HD 11112	1.07	0.180 ± 0.070	No	No	AAT
HD 111232	0.96	-0.450 ± 0.090	Yes	Yes	HARPS
HD 111395	1.01	0.119 ± 0.060	No	No	CLS
HD 111484 B	1.20	0.118 ± 0.060	No	No	CLS
HD 111564	1.11	0.040 ± 0.040	No	No	HARPS
HD 111631	0.68	0.324 ± 0.080	No	No	CLS
HD 111777	1.01	-0.71 ± 0.10	No	No	HARPS
HD 11195	1.02	-0.099 ± 0.040	No	No	HARPS
HD 112257	0.93	-0.011 ± 0.060	No	No	CLS
HD 11226	1.14	0.010 ± 0.060	No	No	HARPS
HD 112914	0.71	-0.254 ± 0.060	No	No	CLS
HD 11397	0.98	-0.570 ± 0.090	No	No	HARPS
HD 114076	0.88	-0.470 ± 0.020	No	No	HARPS
HD 114174	0.97	0.061 ± 0.060	No	No	CLS
HD 114613	1.00	0.16 ± 0.20	No	No	HARPS+CLS*+AAT
HD 114642	1.27	-0.120 ± 0.100	No	No	HARPS
HD 114729	1.05	-0.28 ± 0.20	Yes	Yes	HARPS*+CLS
HD 114747	0.87	0.210 ± 0.060	No	No	HARPS
HD 114762	0.83	-0.603 ± 0.060	No	No	CLS

Table B.1 (continued)

Target	M_\star [M_\odot]	[Fe/H] [dex]	CJ [0.3 – 13 M_{Jup}]	CJ [0.5 – 20 M_{Jup}]	Ref.
HD 114783	0.87	0.151 ± 0.060	Yes	Yes	CLS
HD 114853	1.02	-0.240 ± 0.070	No	No	HARPS*+AAT
HD 115031	1.08	-0.030 ± 0.030	No	No	HARPS
HD 11505	1.03	-0.23 ± 0.10	No	No	HARPS
HD 115169	1.03	-0.043 ± 0.040	No	No	HARPS
HD 115404 A	0.78	-0.113 ± 0.060	No	No	CLS
HD 115585	1.01	0.320 ± 0.060	No	No	HARPS+AAT*
HD 115589	0.92	0.247 ± 0.060	No	No	CLS
HD 115674	1.00	-0.200 ± 0.050	No	No	HARPS
HD 115773	1.21	-0.110 ± 0.080	No	No	HARPS
HD 11608	0.82	0.240 ± 0.100	No	No	HARPS
HD 116321	1.64	0.290 ± 0.060	No	No	CLS
HD 116442	0.76	-0.310 ± 0.060	No	No	CLS
HD 116443	0.74	-0.289 ± 0.060	No	No	CLS
HD 116956	0.96	0.172 ± 0.060	No	No	CLS
HD 117105	1.07	-0.320 ± 0.070	No	No	HARPS*+AAT
HD 117176	1.06	-0.040 ± 0.060	No	No	CLS
HD 117207	0.99	0.220 ± 0.080	Yes	Yes	HARPS*+CLS
HD 117359	0.90	-0.160 ± 0.020	No	No	HARPS
HD 117618	1.10	0.000 ± 0.080	No	No	HARPS*+AAT
HD 117936	0.79	0.088 ± 0.060	No	No	CLS
HD 117939	1.01	-0.220 ± 0.030	No	No	AAT
HD 118466	0.84	0.200 ± 0.020	No	No	HARPS
HD 118972	0.89	-0.020 ± 0.060	No	No	AAT
HD 119173	1.08	-0.630 ± 0.090	No	No	HARPS
HD 11938	0.71	0.030 ± 0.050	No	No	HARPS
HD 119638	1.14	-0.180 ± 0.040	No	No	HARPS
HD 11964	0.91	0.080 ± 0.100	Yes	Yes	HARPS
HD 119949	1.22	-0.440 ± 0.020	No	No	HARPS
HD 120066	1.10	0.101 ± 0.060	No	No	CLS
HD 120136	1.40	0.272 ± 0.060	No	No	CLS
HD 120237 A	1.15	-0.0200 ± 0.0100	No	No	AAT
HD 120344	1.00	-0.190 ± 0.020	No	No	HARPS
HD 12039	1.01	-0.020 ± 0.020	No	No	HARPS
HD 120467	0.73	0.242 ± 0.070	No	No	CLS
HD 12051	0.97	0.230 ± 0.060	No	No	CLS
HD 121004	1.01	-0.71 ± 0.10	No	No	HARPS
HD 121504	1.12	0.13 ± 0.20	No	No	HARPS
HD 122064	0.80	0.147 ± 0.080	No	No	CLS
HD 122120	0.74	0.185 ± 0.070	No	No	CLS
HD 122194	1.06	0.060 ± 0.030	No	No	HARPS
HD 12264	1.04	-0.01 ± 0.10	No	No	HARPS
HD 122652	1.14	0.019 ± 0.060	No	No	CLS
HD 123265	0.92	0.160 ± 0.080	No	No	HARPS
HD 123319	1.03	-0.550 ± 0.020	No	No	HARPS
HD 12345	0.94	-0.210 ± 0.100	No	No	HARPS
HD 123651	1.10	-0.510 ± 0.040	No	No	HARPS
HD 12387	1.02	-0.270 ± 0.060	No	No	HARPS
HD 124523	1.03	-0.026 ± 0.030	No	No	HARPS
HD 124584	1.08	-0.060 ± 0.040	No	No	AAT
HD 124642	0.76	0.104 ± 0.080	No	No	CLS
HD 125455	0.81	-0.088 ± 0.060	No	No	CLS
HD 125881	1.12	0.030 ± 0.080	No	No	HARPS*+AAT
HD 126053	0.84	-0.282 ± 0.060	No	No	CLS
HD 12661	1.09	0.338 ± 0.060	Yes	Yes	CLS
HD 126614	1.02	0.408 ± 0.050	Yes	No	CLS
HD 126793	1.05	-0.740 ± 0.100	No	No	HARPS
HD 126803	0.96	-0.640 ± 0.060	No	No	HARPS
HD 127124	0.83	-0.030 ± 0.020	No	No	HARPS
HD 127334	1.05	0.229 ± 0.060	No	No	CLS
HD 128165	0.77	0.015 ± 0.060	No	No	CLS
HD 128311	0.84	0.134 ± 0.060	Yes	Yes	CLS
HD 128356	0.79	0.06 ± 0.40	No	No	HARPS
HD 12846	0.87	-0.195 ± 0.060	No	No	CLS
HD 128571	1.18	-0.400 ± 0.020	No	No	HARPS
HD 128620	1.11	0.2000 ± 0.0100	No	No	AAT
HD 128621	0.90	0.2400 ± 0.0100	No	No	AAT
HD 128674	0.98	-0.380 ± 0.060	No	No	HARPS*+AAT
HD 129060	1.16	0.070 ± 0.040	No	No	AAT
HD 129191	1.03	0.210 ± 0.050	No	No	HARPS
HD 129814	1.06	-0.026 ± 0.040	No	No	HARPS
HD 130004	0.75	-0.208 ± 0.050	No	No	CLS
HD 130307	0.78	-0.131 ± 0.060	No	No	CLS
HD 130322	0.93	0.01 ± 0.10	No	No	HARPS
HD 13043	1.09	0.092 ± 0.060	No	No	CLS

Table B.1 (continued)

Target	M_{\star} [M_{\odot}]	[Fe/H] [dex]	CJ [0.3 – 13 M_{Jup}]	CJ [0.5 – 20 M_{Jup}]	Ref.
HD 13060	0.90	0.020 ± 0.060	No	No	HARPS
HD 130930	0.83	-0.010 ± 0.020	No	No	HARPS
HD 130992	0.76	-0.030 ± 0.060	No	No	CLS
HD 131653	0.92	-0.660 ± 0.020	No	No	HARPS
HD 131664	1.06	0.280 ± 0.040	No	No	HARPS
HD 132142	0.76	-0.294 ± 0.060	No	No	CLS
HD 132569	0.84	-0.260 ± 0.020	No	No	HARPS
HD 132648	0.95	-0.370 ± 0.060	No	No	HARPS
HD 13350	0.97	0.42 ± 0.20	No	No	HARPS
HD 133600	1.04	0.020 ± 0.030	No	No	HARPS
HD 133633	1.00	-0.480 ± 0.020	No	No	HARPS
HD 134060	1.09	0.110 ± 0.060	No	No	HARPS*+AAT
HD 134088	1.01	-0.780 ± 0.060	No	No	HARPS
HD 134113	1.03	-0.77 ± 0.10	No	No	HARPS
HD 134330	0.99	0.120 ± 0.080	No	No	AAT
HD 134331	1.09	0.000 ± 0.080	No	No	AAT
HD 13445	0.88	-0.23 ± 0.10	No	No	AAT
HD 134606	1.00	0.260 ± 0.100	No	No	HARPS*+AAT
HD 134664	1.05	0.070 ± 0.060	No	No	HARPS
HD 134987	1.02	0.26 ± 0.20	Yes	Yes	HARPS+CLS*+AAT
HD 135101 A	1.01	0.078 ± 0.060	No	No	CLS
HD 135468	1.25	-0.050 ± 0.020	No	No	HARPS
HD 135625	1.12	0.090 ± 0.020	Yes	Yes	HARPS
HD 13612B	0.99	0.107 ± 0.060	No	No	CLS
HD 136352	1.03	-0.34 ± 0.20	No	No	HARPS*+CLS+AAT
HD 136713	0.85	0.222 ± 0.060	No	No	CLS
HD 136894	0.94	-0.110 ± 0.020	No	No	HARPS
HD 136925	0.88	-0.217 ± 0.060	Yes	Yes	CLS
HD 13724	1.05	0.200 ± 0.020	No	No	HARPS
HD 137388	0.88	0.180 ± 0.070	No	No	HARPS
HD 137778	0.90	0.236 ± 0.060	No	No	CLS
HD 13808	0.85	-0.210 ± 0.060	No	No	HARPS
HD 138549	0.98	-0.030 ± 0.030	No	No	HARPS*+CLS
HD 138573	1.02	-0.02 ± 0.10	No	No	HARPS
HD 138763	1.14	0.040 ± 0.040	No	No	HARPS
HD 138799	0.89	-0.010 ± 0.020	No	No	HARPS
HD 139189	0.84	0.010 ± 0.020	No	No	HARPS
HD 139211	1.24	-0.24 ± 0.10	No	No	HARPS
HD 13931	1.02	0.041 ± 0.060	Yes	Yes	CLS
HD 139323	0.91	0.349 ± 0.060	No	No	CLS
HD 139477	0.74	0.030 ± 0.080	No	No	CLS
HD 139590	1.17	0.100 ± 0.040	No	No	HARPS
HD 139879	1.21	0.270 ± 0.020	No	No	HARPS
HD 140785	1.03	-0.05 ± 0.10	No	No	AAT
HD 140901	0.99	0.090 ± 0.080	No	No	AAT
HD 141004	1.05	0.025 ± 0.060	No	No	CLS
HD 141272	0.90	0.033 ± 0.060	No	No	CLS
HD 141399	1.09	0.366 ± 0.060	Yes	Yes	CLS
HD 141624	1.06	-0.410 ± 0.030	No	No	HARPS
HD 142267	0.83	-0.381 ± 0.060	No	No	CLS
HD 142331	1.01	0.017 ± 0.040	No	No	HARPS
HD 142 A	1.21	0.07 ± 0.20	Yes	Yes	HARPS*+AAT
HD 143114	1.05	-0.440 ± 0.070	No	No	HARPS*+AAT
HD 143291	0.76	-0.344 ± 0.060	No	No	CLS
HD 143361	0.97	0.250 ± 0.080	Yes	Yes	HARPS
HD 143638	1.09	-0.300 ± 0.020	No	No	HARPS
HD 143761	0.91	-0.194 ± 0.060	No	No	CLS
HD 143790	1.34	-0.090 ± 0.020	No	No	HARPS
HD 144009	0.99	0.060 ± 0.040	No	No	AAT
HD 14412	0.77	-0.405 ± 0.060	No	No	CLS
HD 144287	0.87	-0.007 ± 0.060	No	No	CLS
HD 144411	0.79	-0.320 ± 0.050	No	No	HARPS
HD 144550	1.02	0.25 ± 0.10	No	No	HARPS
HD 144579	0.73	-0.529 ± 0.050	No	No	CLS
HD 144585	1.04	0.300 ± 0.100	No	No	HARPS*+CLS
HD 144589	1.24	-0.080 ± 0.020	No	No	HARPS
HD 144899	1.16	0.32 ± 0.10	No	No	HARPS
HD 145377	1.10	0.090 ± 0.040	No	No	HARPS
HD 145598	0.95	-0.790 ± 0.040	No	No	HARPS
HD 145675	0.97	0.405 ± 0.050	Yes	Yes	CLS
HD 145927	1.04	-0.041 ± 0.100	No	No	HARPS
HD 145958 A	0.91	0.052 ± 0.060	No	No	CLS
HD 145958 B	0.90	0.058 ± 0.060	No	No	CLS
HD 1461	1.03	0.180 ± 0.070	No	No	HARPS+CLS*
HD 146481	1.02	-0.460 ± 0.020	No	No	AAT

Table B.1 (continued)

Target	M_\star [M_\odot]	[Fe/H] [dex]	CJ [0.3 – 13 M_{Jup}]	CJ [0.5 – 20 M_{Jup}]	Ref.
HD 146775	0.96	-0.055 ± 0.060	No	No	CLS
HD 147231	0.92	0.018 ± 0.060	No	No	CLS
HD 14745	1.21	-0.170 ± 0.040	No	No	HARPS
HD 14747	0.98	-0.390 ± 0.040	No	No	HARPS
HD 147512	0.97	-0.090 ± 0.030	No	No	HARPS
HD 147518	1.00	-0.660 ± 0.070	No	No	HARPS
HD 147722	1.10	0.090 ± 0.080	No	No	AAT
HD 147723	1.12	0.130 ± 0.040	No	No	AAT
HD 147873	1.18	0.08 ± 0.30	Yes	Yes	HARPS
HD 148156	1.18	0.220 ± 0.030	Yes	Yes	HARPS
HD 148211	1.08	-0.650 ± 0.080	No	No	HARPS
HD 148467	0.68	0.012 ± 0.070	No	No	CLS
HD 148577	1.01	-0.120 ± 0.020	No	No	HARPS
HD 148816	1.06	-0.74 ± 0.20	No	No	HARPS
HD 149143	1.06	0.25 ± 0.10	No	No	HARPS
HD 149189	1.08	0.25 ± 0.10	No	No	HARPS
HD 149396	1.01	0.190 ± 0.040	No	No	HARPS
HD 149612	1.02	-0.440 ± 0.040	No	No	AAT
HD 149661	0.89	0.074 ± 0.060	No	No	CLS
HD 149806	0.95	0.238 ± 0.060	No	No	CLS
HD 150177	1.16	-0.58 ± 0.10	No	No	HARPS
HD 150437	1.05	0.270 ± 0.050	No	No	HARPS
HD 150474	0.95	0.000 ± 0.060	No	No	AAT
HD 151288	0.65	0.056 ± 0.080	No	No	CLS
HD 151337	1.37	0.020 ± 0.040	No	No	AAT
HD 151504	0.95	0.060 ± 0.060	No	No	HARPS
HD 151541	0.83	-0.114 ± 0.060	No	No	CLS
HD 152555	1.10	0.090 ± 0.060	No	No	HARPS
HD 153075	1.05	-0.540 ± 0.060	No	No	AAT
HD 15337	0.88	0.030 ± 0.100	No	No	HARPS
HD 153525	0.77	-0.030 ± 0.060	No	No	CLS
HD 153950	1.11	-0.040 ± 0.030	Yes	Yes	HARPS
HD 154088	0.94	0.28 ± 0.10	No	No	HARPS+CLS*
HD 154221	1.09	0.120 ± 0.080	No	No	HARPS
HD 154345	0.89	-0.070 ± 0.060	Yes	Yes	CLS
HD 154363	0.64	-0.234 ± 0.070	No	No	CLS
HD 154672	1.03	0.250 ± 0.090	No	No	HARPS
HD 154857	0.99	-0.220 ± 0.040	Yes	Yes	AAT
HD 154962	1.04	0.290 ± 0.050	No	No	HARPS
HD 155712	0.78	-0.048 ± 0.050	No	No	CLS
HD 155918	1.03	-0.690 ± 0.060	No	No	AAT
HD 155974	1.23	-0.210 ± 0.060	No	No	AAT
HD 156079	1.07	0.250 ± 0.060	No	No	HARPS
HD 156098	1.29	0.150 ± 0.100	Yes	Yes	HARPS
HD 15612	0.90	-0.110 ± 0.020	No	No	HARPS
HD 156274 B	0.60	-0.460 ± 0.060	No	No	AAT
HD 156279	0.96	0.192 ± 0.060	Yes	Yes	CLS
HD 156365	1.35	0.289 ± 0.060	No	No	CLS
HD 156411	1.07	-0.110 ± 0.100	Yes	Yes	HARPS
HD 156423	0.88	-0.450 ± 0.020	No	No	HARPS
HD 156668	0.79	0.049 ± 0.060	No	No	CLS
HD 156985	0.75	-0.082 ± 0.060	No	No	CLS
HD 157172	0.95	0.110 ± 0.040	No	No	HARPS
HD 157214	0.85	-0.296 ± 0.060	No	No	CLS
HD 157338	1.09	-0.090 ± 0.060	No	No	HARPS+CLS*
HD 157347	1.02	0.030 ± 0.080	No	No	HARPS+CLS*
HD 157830	0.98	-0.250 ± 0.050	No	No	HARPS
HD 158633	0.76	-0.356 ± 0.060	No	No	CLS
HD 159062	0.79	-0.272 ± 0.060	No	No	CLS
HD 159063	1.36	0.254 ± 0.060	No	No	CLS
HD 159222	1.10	0.166 ± 0.060	No	No	CLS
HD 159868	0.97	-0.07 ± 0.10	Yes	Yes	AAT
HD 16008	1.03	-0.090 ± 0.040	No	No	HARPS
HD 160693	0.83	-0.435 ± 0.060	No	No	CLS
HD 160836	0.77	-0.150 ± 0.020	No	No	HARPS
HD 161050	1.10	-0.100 ± 0.050	No	No	AAT
HD 161098	0.99	-0.270 ± 0.080	No	No	HARPS
HD 161256	1.01	0.130 ± 0.040	No	No	HARPS
HD 16141	1.03	0.13 ± 0.20	No	No	HARPS+CLS*
HD 161566	1.17	-0.310 ± 0.020	No	No	HARPS
HD 16160	0.75	-0.036 ± 0.070	No	No	CLS
HD 161797	1.16	0.318 ± 0.060	No	No	CLS
HD 162396	1.15	-0.35 ± 0.10	No	No	HARPS
HD 16280	0.77	-0.180 ± 0.020	No	No	HARPS
HD 163153	1.21	0.376 ± 0.060	No	No	CLS

Table B.1 (continued)

Target	M_\star [M_\odot]	[Fe/H] [dex]	CJ [0.3 – 13 M_{Jup}]	CJ [0.5 – 20 M_{Jup}]	Ref.
HD 163272	1.13	0.2200 ± 0.0100	No	No	AAT
HD 163441	1.04	0.020 ± 0.050	No	No	HARPS
HD 16417	1.05	0.120 ± 0.100	No	No	HARPS*+AAT
HD 164427	1.07	0.060 ± 0.080	No	No	AAT
HD 164509	1.06	0.210 ± 0.040	No	No	HARPS
HD 164595	0.91	-0.061 ± 0.060	No	No	CLS
HD 164922	0.92	0.197 ± 0.060	Yes	No	CLS
HD 165131	1.06	0.030 ± 0.020	No	Yes	HARPS
HD 165155	0.94	0.210 ± 0.080	Yes	Yes	HARPS
HD 165269	1.14	0.270 ± 0.030	No	No	AAT
HD 165401	0.87	-0.322 ± 0.060	No	No	CLS
HD 16548	1.02	0.12 ± 0.10	No	No	HARPS
HD 165920	0.92	0.290 ± 0.050	No	No	HARPS
HD 166	0.98	0.139 ± 0.060	No	No	CLS
HD 166553	1.09	-0.020 ± 0.060	No	No	AAT
HD 166620	0.78	-0.112 ± 0.060	No	No	CLS
HD 166724	0.86	-0.090 ± 0.050	Yes	Yes	HARPS
HD 167060	1.05	-0.015 ± 0.040	No	No	HARPS
HD 16714	0.97	-0.200 ± 0.040	No	No	HARPS
HD 167215	1.05	-0.306 ± 0.060	No	No	CLS
HD 167300	1.05	-0.480 ± 0.080	No	No	HARPS
HD 167665	1.06	-0.141 ± 0.060	No	No	CLS
HD 167677	0.96	-0.320 ± 0.100	Yes	Yes	HARPS
HD 168009	0.99	0.018 ± 0.060	No	No	CLS
HD 168060	0.98	0.280 ± 0.040	No	No	AAT
HD 168443	1.04	0.076 ± 0.060	Yes	Yes	CLS
HD 168746	0.98	-0.10 ± 0.20	No	No	HARPS
HD 168769	0.91	-0.010 ± 0.040	No	No	HARPS
HD 168863	0.80	0.180 ± 0.020	No	No	HARPS
HD 168871	1.10	-0.120 ± 0.080	No	No	HARPS*+AAT
HD 16905	0.79	0.170 ± 0.080	Yes	Yes	HARPS
HD 169830	1.17	0.17 ± 0.20	Yes	Yes	HARPS+CLS*
HD 170469	1.14	0.311 ± 0.060	Yes	Yes	CLS
HD 170493	0.79	0.206 ± 0.080	No	No	CLS
HD 17051	1.17	0.16 ± 0.20	No	No	AAT
HD 170657	0.79	-0.126 ± 0.060	No	No	CLS
HD 171028	1.01	-0.480 ± 0.100	Yes	Yes	HARPS
HD 171067	0.95	-0.012 ± 0.060	No	No	CLS
HD 171587	0.95	-0.640 ± 0.020	No	No	HARPS
HD 171834	1.46	-0.100 ± 0.040	No	No	HARPS
HD 17190	0.84	-0.026 ± 0.060	No	No	CLS
HD 172051	1.00	-0.207 ± 0.060	No	No	CLS*+AAT
HD 17230	0.71	0.166 ± 0.070	No	No	CLS
HD 172513	0.97	-0.050 ± 0.080	No	No	HARPS+CLS*
HD 172568	1.02	-0.390 ± 0.020	No	No	HARPS
HD 173701	1.00	0.353 ± 0.060	No	No	CLS
HD 17382	0.91	0.103 ± 0.050	No	No	CLS
HD 174080	0.76	0.112 ± 0.080	No	No	CLS
HD 17439	1.04	0.050 ± 0.020	No	No	HARPS
HD 174545	0.88	0.190 ± 0.080	No	No	HARPS
HD 17548	1.11	-0.560 ± 0.070	No	No	HARPS
HD 175607	0.94	-0.620 ± 0.060	No	No	HARPS
HD 176377	0.91	-0.229 ± 0.060	No	No	CLS
HD 176986	0.82	0.050 ± 0.060	No	No	HARPS
HD 177153	1.04	-0.049 ± 0.060	No	No	CLS
HD 177409	1.07	-0.070 ± 0.040	No	No	HARPS
HD 177758	1.07	-0.610 ± 0.080	No	No	HARPS
HD 178911 B	1.03	0.260 ± 0.060	No	No	CLS
HD 179346	1.16	-0.060 ± 0.050	No	No	HARPS
HD 179949	1.17	0.19 ± 0.20	No	No	HARPS+CLS+AAT*
HD 179957	0.94	0.009 ± 0.060	No	No	CLS
HD 179958	0.97	0.039 ± 0.060	No	No	CLS
HD 180161	0.97	0.184 ± 0.060	No	No	CLS
HD 180409	1.11	-0.200 ± 0.040	No	No	HARPS
HD 181327	1.32	-0.17 ± 0.10	No	No	HARPS
HD 181428	1.13	0.03 ± 0.10	No	No	AAT
HD 18143	0.83	0.168 ± 0.060	No	No	CLS
HD 181433	0.81	0.38 ± 0.10	Yes	Yes	HARPS
HD 181720	1.04	-0.560 ± 0.030	Yes	No	HARPS
HD 182488	0.95	0.199 ± 0.060	No	No	CLS
HD 182572	1.10	0.370 ± 0.060	No	No	CLS
HD 183263	1.17	0.278 ± 0.060	Yes	Yes	CLS
HD 183414	1.02	-0.020 ± 0.040	No	No	HARPS
HD 183579	1.04	-0.036 ± 0.030	No	No	HARPS
HD 183650	1.14	0.309 ± 0.060	No	No	CLS

Table B.1 (continued)

Target	M_\star [M_\odot]	[Fe/H] [dex]	CJ [0.3 – 13 M_{Jup}]	CJ [0.5 – 20 M_{Jup}]	Ref.
HD 183870	0.82	0.019 ± 0.060	No	No	CLS
HD 183877	0.99	-0.200 ± 0.060	No	No	AAT
HD 185144	0.81	-0.172 ± 0.060	No	No	CLS
HD 185283	0.79	-0.070 ± 0.060	Yes	Yes	HARPS
HD 185414	0.95	-0.095 ± 0.060	No	No	CLS
HD 185615	0.98	0.080 ± 0.030	No	No	HARPS
HD 186194	1.03	0.190 ± 0.080	No	No	HARPS
HD 18632	0.89	0.230 ± 0.060	No	No	CLS
HD 186408	1.02	0.089 ± 0.060	No	No	CLS
HD 186427	0.98	0.074 ± 0.060	Yes	Yes	CLS
HD 187085	1.15	0.090 ± 0.100	Yes	Yes	AAT
HD 187123	1.02	0.106 ± 0.060	Yes	Yes	CLS
HD 187237	1.04	0.065 ± 0.060	No	No	CLS
HD 187532	1.48	-0.140 ± 0.040	No	No	HARPS
HD 187897	1.11	0.129 ± 0.060	No	No	CLS
HD 187923	0.98	-0.087 ± 0.060	No	No	CLS
HD 188015	1.04	0.253 ± 0.060	Yes	Yes	CLS
HD 18803	0.98	0.128 ± 0.060	No	No	CLS
HD 188748	1.00	-0.120 ± 0.040	No	No	HARPS
HD 188815	1.21	-0.56 ± 0.10	No	No	HARPS
HD 189625	1.06	0.178 ± 0.030	No	No	HARPS+CLS*
HD 189733	0.83	0.041 ± 0.060	No	No	CLS
HD 190007	0.76	0.209 ± 0.070	No	No	CLS
HD 190067	0.79	-0.288 ± 0.060	No	No	CLS
HD 190125	1.03	0.170 ± 0.080	No	No	HARPS
HD 19034	0.80	-0.354 ± 0.060	No	No	CLS
HD 190360	0.99	0.230 ± 0.060	Yes	Yes	CLS
HD 190404	0.70	-0.476 ± 0.050	No	No	CLS
HD 190406	1.07	0.051 ± 0.060	No	No	CLS
HD 190647	1.00	0.230 ± 0.100	Yes	Yes	HARPS
HD 190954	0.95	-0.410 ± 0.020	No	No	HARPS
HD 190984	1.10	-0.520 ± 0.020	Yes	Yes	HARPS
HD 191408	0.84	-0.522 ± 0.060	No	No	CLS+AAT*
HD 191785	0.81	-0.044 ± 0.050	No	No	CLS
HD 192020	0.85	0.016 ± 0.060	No	No	CLS
HD 192031	0.89	-0.870 ± 0.050	No	No	HARPS
HD 192263	0.82	0.03 ± 0.10	No	No	HARPS+CLS*
HD 19308	1.06	0.150 ± 0.060	No	No	CLS
HD 193202	0.70	0.235 ± 0.070	No	No	CLS
HD 193307	1.12	-0.290 ± 0.080	No	No	AAT
HD 19373	1.14	0.116 ± 0.060	No	No	CLS
HD 194490	1.06	0.070 ± 0.080	No	No	HARPS
HD 194640	0.98	-0.040 ± 0.020	No	No	AAT
HD 195019	1.05	0.050 ± 0.060	No	No	CLS
HD 195145	1.05	0.170 ± 0.060	No	No	HARPS
HD 19518	1.04	-0.11 ± 0.10	No	No	HARPS
HD 195564	1.12	0.089 ± 0.060	No	No	CLS
HD 196050	1.07	0.22 ± 0.20	Yes	Yes	HARPS+AAT*
HD 196068	1.08	0.200 ± 0.080	No	No	AAT
HD 19632	1.03	0.12 ± 0.20	No	No	AAT
HD 196378	1.13	-0.43 ± 0.20	No	No	HARPS+AAT*
HD 196390	1.07	0.057 ± 0.060	No	No	HARPS
HD 19641	1.06	-0.040 ± 0.020	No	No	HARPS
HD 19668	0.95	-0.040 ± 0.040	No	No	HARPS
HD 196761	0.96	-0.197 ± 0.060	No	No	CLS*+AAT
HD 196800	1.10	0.160 ± 0.060	No	No	HARPS*+AAT
HD 196850	0.92	-0.094 ± 0.060	No	No	CLS
HD 196892	1.08	-1.05 ± 0.30	No	No	HARPS
HD 197027	1.02	-0.016 ± 0.030	No	No	HARPS
HD 197076	0.98	-0.065 ± 0.060	No	No	CLS
HD 197083	1.03	-0.480 ± 0.050	No	No	HARPS
HD 197197	1.04	-0.490 ± 0.020	No	No	HARPS
HD 197536	1.13	-0.440 ± 0.060	No	No	HARPS
HD 197823	0.93	0.110 ± 0.080	No	No	HARPS
HD 1979	1.00	-0.090 ± 0.020	No	No	HARPS
HD 198075	1.05	-0.270 ± 0.060	No	No	HARPS
HD 198390	1.28	-0.32 ± 0.10	No	No	HARPS
HD 198425	0.79	-0.039 ± 0.060	No	No	CLS
HD 198802	1.24	0.009 ± 0.060	No	No	CLS
HD 199190	1.08	0.140 ± 0.070	No	No	HARPS+AAT*
HD 199289	1.06	-1.04 ± 0.10	No	No	HARPS
HD 199476	0.80	-0.311 ± 0.060	No	No	CLS
HD 199509	1.04	-0.310 ± 0.050	No	No	AAT
HD 199604	1.05	-0.650 ± 0.060	No	No	HARPS
HD 199847	1.03	-0.570 ± 0.020	No	No	HARPS

Table B.1 (continued)

Target	M _★ [M _⊙]	[Fe/H] [dex]	CJ [0.3 – 13 M _{Jup}]	CJ [0.5 – 20 M _{Jup}]	Ref.
HD 199960	1.07	0.25 ± 0.20	No	No	HARPS+CLS*
HD 20003	0.96	0.040 ± 0.060	No	No	HARPS
HD 200083	0.78	-0.120 ± 0.020	No	No	HARPS
HD 200143	0.86	0.010 ± 0.020	No	No	HARPS
HD 20029	1.17	0.120 ± 0.060	No	No	AAT
HD 200349	0.78	-0.290 ± 0.020	No	No	HARPS
HD 200538	1.11	0.098 ± 0.020	No	No	HARPS
HD 200565	1.06	0.049 ± 0.060	No	No	CLS
HD 200633	1.05	0.040 ± 0.040	No	No	HARPS
HD 200968	0.87	0.096 ± 0.060	No	No	CLS
HD 201092	0.62	-0.395 ± 0.050	No	No	CLS
HD 20165	0.84	0.023 ± 0.060	No	No	CLS
HD 20201	1.10	0.080 ± 0.060	No	No	AAT
HD 202206	1.03	0.29 ± 0.20	No	Yes	HARPS
HD 202575	0.74	-0.074 ± 0.060	No	No	CLS
HD 202751	0.75	-0.024 ± 0.070	No	No	CLS
HD 202871	1.11	-0.120 ± 0.040	No	No	HARPS
HD 203384	0.98	0.230 ± 0.050	No	No	HARPS
HD 203432	0.99	0.278 ± 0.060	No	No	HARPS
HD 2039	1.09	0.31 ± 0.20	Yes	Yes	AAT
HD 204287	1.05	-0.070 ± 0.020	No	No	AAT
HD 204313	1.03	0.160 ± 0.040	Yes	Yes	HARPS
HD 204385	1.12	0.040 ± 0.090	No	No	HARPS*+AAT
HD 204587	0.67	0.071 ± 0.070	No	No	CLS
HD 204941	0.83	-0.200 ± 0.050	No	No	HARPS
HD 205294	1.23	-0.280 ± 0.060	No	No	HARPS
HD 205390	0.84	-0.170 ± 0.040	No	No	AAT
HD 205536	0.95	-0.050 ± 0.030	No	No	HARPS
HD 205591	1.32	-0.110 ± 0.020	No	No	HARPS
HD 205739	1.24	0.180 ± 0.040	No	No	HARPS
HD 206172	0.99	-0.240 ± 0.040	No	No	HARPS
HD 20619	0.91	-0.172 ± 0.060	No	No	CLS
HD 206387	1.15	0.226 ± 0.060	No	No	CLS
HD 206395	1.20	0.200 ± 0.040	No	No	AAT
HD 206683	1.14	0.290 ± 0.080	No	No	HARPS
HD 20675	1.54	0.162 ± 0.060	No	No	CLS
HD 206998	1.05	-0.720 ± 0.080	No	No	HARPS
HD 2071	1.02	-0.090 ± 0.040	No	No	HARPS
HD 207190	1.18	-0.450 ± 0.050	No	No	HARPS
HD 20766	1.03	-0.23 ± 0.20	No	No	AAT
HD 207700	1.01	0.030 ± 0.040	No	No	HARPS*+AAT
HD 20781	0.90	-0.110 ± 0.040	No	No	HARPS
HD 20782	1.04	-0.060 ± 0.080	Yes	Yes	HARPS*+AAT
HD 207832	1.02	0.130 ± 0.040	Yes	Yes	HARPS
HD 207869	0.98	-0.450 ± 0.020	No	No	HARPS
HD 20794	0.94	-0.40 ± 0.20	No	No	AAT
HD 208	1.08	-0.340 ± 0.030	No	No	HARPS
HD 208038	0.81	-0.028 ± 0.060	No	No	CLS
HD 208272	0.89	-0.070 ± 0.060	No	No	HARPS
HD 208313	0.82	0.010 ± 0.060	No	No	CLS
HD 208487	1.17	0.050 ± 0.090	No	No	HARPS*+AAT
HD 20852	1.45	-0.380 ± 0.020	No	No	HARPS
HD 20868	0.78	0.070 ± 0.020	No	No	HARPS
HD 208704	1.05	-0.096 ± 0.050	No	No	HARPS
HD 208998	1.08	-0.330 ± 0.100	No	No	AAT
HD 209268	1.13	-0.080 ± 0.040	No	No	AAT
HD 209458	1.07	-0.006 ± 0.060	No	No	CLS
HD 209653	1.10	-0.140 ± 0.040	No	No	AAT
HD 209875	1.13	-0.087 ± 0.060	No	No	CLS
HD 210277	0.96	0.20 ± 0.10	Yes	Yes	HARPS+CLS*
HD 210312	1.07	0.253 ± 0.060	No	No	CLS
HD 210918	1.16	-0.110 ± 0.070	No	No	AAT
HD 210975	0.76	-0.460 ± 0.060	No	No	HARPS
HD 211080	1.26	0.330 ± 0.060	No	No	CLS
HD 211188	0.84	-0.150 ± 0.030	No	No	HARPS
HD 211317	1.09	0.240 ± 0.100	No	No	AAT
HD 21132	1.25	-0.400 ± 0.040	No	No	HARPS
HD 211976	1.34	-0.110 ± 0.040	No	No	HARPS
HD 211998	1.45	-1.51 ± 0.20	No	No	AAT
HD 212036	1.04	-0.010 ± 0.020	No	No	HARPS
HD 21209 A	0.74	-0.440 ± 0.040	No	No	HARPS
HD 212168	1.08	-0.010 ± 0.040	No	No	AAT
HD 212291	0.90	-0.119 ± 0.060	No	No	CLS
HD 212330	1.01	-0.06 ± 0.20	No	No	AAT
HD 212708	1.01	0.255 ± 0.090	No	No	HARPS+AAT*

Table B.1 (continued)

Target	M_\star [M_\odot]	[Fe/H] [dex]	CJ [0.3 – 13 M_{Jup}]	CJ [0.5 – 20 M_{Jup}]	Ref.
HD 212918	0.84	-0.240 ± 0.020	No	No	HARPS
HD 213042	0.79	0.199 ± 0.080	No	No	CLS
HD 213240	1.10	0.14 ± 0.20	Yes	Yes	AAT
HD 213472	1.05	0.125 ± 0.060	No	No	CLS
HD 213575	1.01	-0.17 ± 0.20	No	No	HARPS
HD 214094	1.19	-0.040 ± 0.060	No	No	HARPS
HD 214385	1.01	-0.370 ± 0.060	No	No	HARPS
HD 214683	0.71	-0.262 ± 0.060	No	No	CLS
HD 214749	0.72	0.088 ± 0.070	No	No	CLS
HD 214953 A	1.15	-0.050 ± 0.050	No	No	AAT
HD 2151	1.33	-0.12 ± 0.20	No	No	AAT
HD 215257	1.06	-0.64 ± 0.10	No	No	HARPS
HD 215497	0.86	0.170 ± 0.020	Yes	No	HARPS
HD 215641	0.97	0.020 ± 0.040	No	No	HARPS
HD 215906	1.21	-0.310 ± 0.020	No	No	HARPS
HD 216259	0.68	-0.556 ± 0.040	No	No	CLS
HD 216435	1.10	0.21 ± 0.20	Yes	Yes	HARPS+AAT*
HD 216437	1.06	0.22 ± 0.20	Yes	Yes	HARPS+AAT*
HD 216520	0.79	-0.124 ± 0.060	No	No	CLS
HD 216770	0.94	0.240 ± 0.100	No	No	HARPS
HD 21693	0.95	-0.030 ± 0.050	No	No	HARPS
HD 217004	1.04	-0.030 ± 0.060	No	No	CLS
HD 217014	1.07	0.206 ± 0.060	No	No	CLS
HD 217107	1.06	0.340 ± 0.060	Yes	Yes	CLS
HD 217165	1.07	0.044 ± 0.060	No	No	CLS
HD 217343	1.03	0.00 ± 0.10	No	No	HARPS
HD 217357	0.63	0.025 ± 0.070	No	No	CLS
HD 217786	1.14	-0.170 ± 0.030	No	Yes	HARPS
HD 217877	1.00	-0.089 ± 0.060	No	No	CLS
HD 217958	1.08	0.25 ± 0.10	No	No	AAT
HD 218209	0.81	-0.376 ± 0.060	No	No	CLS
HD 218249	0.82	-0.430 ± 0.060	No	No	HARPS
HD 218379	1.10	0.120 ± 0.020	No	No	HARPS
HD 218504	1.09	-0.580 ± 0.080	No	No	HARPS
HD 218544	1.04	-0.017 ± 0.040	No	No	HARPS
HD 218566	0.80	0.28 ± 0.10	No	No	HARPS+CLS*
HD 218860	0.98	0.110 ± 0.020	No	No	HARPS
HD 218868	1.00	0.231 ± 0.060	No	No	CLS
HD 219057	1.05	-0.063 ± 0.040	No	No	HARPS
HD 219077	0.92	-0.16 ± 0.10	Yes	Yes	HARPS+AAT*
HD 219134	0.79	0.083 ± 0.060	Yes	No	CLS
HD 219249	0.96	-0.400 ± 0.060	No	No	HARPS
HD 21938	1.04	-0.480 ± 0.040	No	No	HARPS
HD 219538	0.83	0.008 ± 0.060	No	No	CLS
HD 219542	1.04	0.165 ± 0.060	No	No	CLS
HD 219828	1.04	0.15 ± 0.10	No	Yes	HARPS
HD 219834 B	0.90	0.224 ± 0.060	No	No	CLS
HD 220221	0.81	0.161 ± 0.060	No	No	CLS
HD 220339	0.75	-0.213 ± 0.060	No	No	CLS
HD 220367	1.16	-0.240 ± 0.020	No	No	HARPS
HD 220449	0.85	-0.09 ± 0.50	Yes	Yes	HARPS+CLS*
HD 220507	1.01	0.000 ± 0.060	No	No	HARPS
HD 22104	1.04	0.320 ± 0.100	No	No	AAT
HD 221146	1.07	0.080 ± 0.040	No	No	HARPS
HD 221287	1.27	0.01 ± 0.10	Yes	Yes	HARPS
HD 221354	0.86	0.099 ± 0.060	No	No	CLS
HD 221575	0.85	-0.060 ± 0.080	No	No	HARPS
HD 221851	0.84	-0.025 ± 0.060	No	No	CLS
HD 222480	1.05	0.150 ± 0.020	No	No	HARPS+AAT*
HD 222582	1.04	-0.01 ± 0.20	Yes	Yes	HARPS+CLS*
HD 222595	1.00	0.010 ± 0.040	No	No	HARPS
HD 222669	1.07	0.030 ± 0.050	No	No	HARPS
HD 223121	0.85	0.060 ± 0.040	No	No	HARPS
HD 223171	1.05	0.110 ± 0.090	No	No	HARPS+AAT
HD 223238	1.06	0.024 ± 0.060	No	No	HARPS+CLS*
HD 223282	0.92	-0.430 ± 0.040	No	No	HARPS
HD 223498	0.97	0.184 ± 0.060	No	No	CLS
HD 223691	1.06	-0.169 ± 0.060	No	No	CLS
HD 223854	1.14	-0.570 ± 0.080	No	No	HARPS
HD 224383	1.04	-0.036 ± 0.080	No	No	HARPS
HD 224393	1.04	-0.410 ± 0.030	No	No	HARPS
HD 224538	1.23	0.28 ± 0.10	Yes	Yes	HARPS
HD 224619	0.96	-0.220 ± 0.080	No	No	HARPS+CLS
HD 224685	0.97	-0.400 ± 0.030	No	No	HARPS
HD 224693	1.07	0.250 ± 0.070	No	No	HARPS

Table B.1 (continued)

Target	M _★ [M _⊙]	[Fe/H] [dex]	CJ [0.3 – 13 M _{Jup}]	CJ [0.5 – 20 M _{Jup}]	Ref.
HD 224789	0.88	-0.040 ± 0.040	No	No	HARPS
HD 224817	1.07	-0.560 ± 0.060	No	No	HARPS
HD 224983	0.88	0.147 ± 0.060	No	No	CLS
HD 225261	0.77	-0.323 ± 0.060	No	No	CLS
HD 23079	1.10	-0.14 ± 0.10	Yes	Yes	HARPS+AAT*
HD 23127	1.05	0.34 ± 0.20	Yes	Yes	AAT
HD 231701	1.15	-0.010 ± 0.080	No	No	HARPS
HD 23249	1.22	0.12 ± 0.60	No	No	AAT
HD 23356	0.82	-0.10 ± 0.20	No	No	HARPS+CLS*
HD 23439	0.68	-0.733 ± 0.040	No	No	CLS
HD 23456	1.18	-0.350 ± 0.080	No	No	HARPS
HD 23901	0.91	-0.400 ± 0.020	No	No	HARPS
HD 24040	1.10	0.197 ± 0.060	Yes	Yes	CLS
HD 24062	1.12	0.250 ± 0.070	No	No	HARPS
HD 24112	1.16	0.130 ± 0.040	No	No	HARPS
HD 24238	0.72	-0.357 ± 0.040	No	No	CLS
HD 24496	0.93	0.030 ± 0.060	No	No	CLS
HD 245409	0.62	0.066 ± 0.080	No	No	CLS
HD 24558	0.92	-0.490 ± 0.040	No	No	HARPS
HD 24712	1.63	-5.100 ± 0.040	No	No	HARPS
HD 24892	0.95	-0.271 ± 0.060	No	No	CLS
HD 24916	0.69	-0.140 ± 0.100	No	No	HARPS
HD 25061	0.91	0.070 ± 0.070	No	No	HARPS
HD 25171	1.20	-0.140 ± 0.040	Yes	Yes	HARPS
HD 25665	0.81	0.021 ± 0.060	No	No	CLS
HD 2567	1.14	0.190 ± 0.020	No	No	HARPS
HD 25673	0.87	-0.510 ± 0.080	No	No	HARPS
HD 25912	1.08	0.090 ± 0.040	No	No	HARPS
HD 26151	0.98	0.308 ± 0.060	No	No	CLS
HD 26161	1.13	-0.009 ± 0.060	No	No	CLS
HD 2638	0.88	0.120 ± 0.060	No	No	HARPS
HD 26736	1.10	0.194 ± 0.060	No	No	CLS
HD 26887	1.11	-0.380 ± 0.030	No	No	HARPS
HD 26923	1.08	-0.030 ± 0.040	No	No	HARPS
HD 26965	0.85	-0.34 ± 0.20	No	No	HARPS*+CLS+AAT
HD 27063	1.04	0.05 ± 0.10	No	No	HARPS
HD 27274	0.71	-0.15	No	No	AAT
HD 27442 A	1.21	0.39 ± 0.20	Yes	Yes	AAT
HD 2768	0.98	-0.060 ± 0.020	No	No	HARPS
HD 27894	0.81	0.26 ± 0.20	Yes	Yes	HARPS
HD 28005	1.13	0.313 ± 0.060	No	No	CLS
HD 28185	1.02	0.227 ± 0.060	Yes	Yes	CLS
HD 28254	1.00	0.330 ± 0.020	Yes	Yes	HARPS
HD 28255 A	1.07	0.050 ± 0.040	No	No	AAT
HD 28255b	1.00	0.090 ± 0.040	No	No	AAT
HD 28343	0.70	0.375 ± 0.070	No	No	CLS
HD 28635	1.15	0.100 ± 0.020	No	No	HARPS
HD 28701	1.02	-0.320 ± 0.060	No	No	HARPS
HD 28821	1.01	-0.120 ± 0.050	No	No	HARPS
HD 28946	0.85	-0.101 ± 0.060	No	No	CLS
HD 290038	0.83	0.030 ± 0.020	No	No	HARPS
HD 290327	0.97	-0.170 ± 0.020	Yes	Yes	HARPS
HD 29137	1.03	0.270 ± 0.020	No	No	HARPS
HD 297396	0.76	0.080 ± 0.040	No	No	HARPS
HD 29883	0.78	-0.094 ± 0.050	No	No	CLS
HD 30053	1.19	-0.250 ± 0.060	No	No	HARPS
HD 30177	0.98	0.37 ± 0.20	Yes	Yes	AAT
HD 30295	0.94	0.300 ± 0.090	No	No	AAT
HD 30306	0.98	0.173 ± 0.060	No	No	HARPS
HD 30669	0.94	0.130 ± 0.040	Yes	No	HARPS
HD 3074 A	1.14	0.056 ± 0.060	No	No	CLS
HD 30876	0.84	-0.060 ± 0.040	No	No	AAT
HD 31103	1.14	0.060 ± 0.020	No	No	HARPS
HD 31253	1.33	0.140 ± 0.060	Yes	No	CLS
HD 31527	1.07	-0.200 ± 0.070	No	No	HARPS*+AAT
HD 31532	1.07	-0.110 ± 0.020	No	No	HARPS
HD 31560	0.77	0.130 ± 0.080	No	No	CLS
HD 31822	1.13	-0.220 ± 0.040	No	No	HARPS
HD 31827	0.98	0.44 ± 0.10	No	No	AAT
HD 32147	0.80	0.186 ± 0.080	No	No	CLS
HD 32564	0.98	-0.010 ± 0.030	No	No	HARPS
HD 32724	1.05	-0.200 ± 0.060	No	No	HARPS
HD 32923	1.00	-0.140 ± 0.060	No	No	CLS
HD 32963	0.98	0.075 ± 0.060	Yes	Yes	CLS
HD 33473	1.03	-0.13 ± 0.10	No	No	HARPS

Table B.1 (continued)

Target	M_\star [M_\odot]	[Fe/H] [dex]	CJ [0.3 – 13 M_{Jup}]	CJ [0.5 – 20 M_{Jup}]	Ref.
HD 33636	1.02	-0.071 ± 0.060	No	No	CLS
HD 34411	1.03	0.074 ± 0.060	No	No	CLS
HD 34445	1.11	0.138 ± 0.060	Yes	Yes	CLS
HD 34721	1.05	-0.046 ± 0.060	No	No	CLS
HD 36003	0.74	0.155 ± 0.070	No	No	CLS
HD 36108	1.08	-0.240 ± 0.060	No	No	AAT
HD 36152	1.03	0.057 ± 0.060	No	No	HARPS
HD 36379	1.12	-0.170 ± 0.040	No	No	HARPS
HD 36395	0.62	0.397 ± 0.060	No	No	CLS
HD 3651	0.89	0.168 ± 0.060	No	No	CLS
HD 37008	0.73	-0.322 ± 0.060	No	No	CLS
HD 37124	0.81	-0.326 ± 0.060	Yes	Yes	CLS
HD 37213	0.93	-0.419 ± 0.060	No	No	CLS
HD 37226	1.18	-0.150 ± 0.020	No	No	HARPS
HD 37394	0.92	0.159 ± 0.060	No	No	CLS
HD 37572	0.86	-0.110 ± 0.040	No	No	HARPS
HD 3765	0.85	0.172 ± 0.060	No	No	CLS
HD 377	1.11	0.138 ± 0.060	No	No	CLS
HD 3795	0.86	-0.513 ± 0.060	No	No	CLS
HD 37990	1.18	-0.030 ± 0.050	No	No	HARPS
HD 3821	1.06	-0.060 ± 0.040	No	No	HARPS
HD 38230	0.83	-0.006 ± 0.050	No	No	CLS
HD 38283	1.10	-0.250 ± 0.100	Yes	No	HARPS+AAT*
HD 38382	1.12	0.000 ± 0.100	No	No	AAT
HD 38459	0.90	0.210 ± 0.080	No	No	HARPS
HD 38677	1.17	0.180 ± 0.040	No	No	HARPS
HD 38973	1.11	0.030 ± 0.090	No	No	AAT
HD 38B	0.62	0.054 ± 0.080	No	No	CLS
HD 39091	1.10	0.07 ± 0.10	Yes	Yes	HARPS*+AAT
HD 39427	1.01	-0.180 ± 0.020	No	No	HARPS
HD 3964	1.04	0.050 ± 0.020	No	No	HARPS
HD 39881	0.92	-0.091 ± 0.060	No	No	CLS
HD 40397	0.88	-0.042 ± 0.060	No	No	CLS
HD 40979	1.24	0.203 ± 0.060	No	No	CLS
HD 41248	1.04	-0.400 ± 0.020	No	No	HARPS
HD 41593	0.91	0.087 ± 0.060	No	No	CLS
HD 4203	1.14	0.380 ± 0.060	Yes	Yes	CLS
HD 4208	0.85	-0.220 ± 0.060	Yes	Yes	CLS
HD 42250	0.88	0.047 ± 0.060	No	No	CLS
HD 4256	0.85	0.256 ± 0.060	No	No	CLS
HD 42618	1.03	-0.09 ± 0.10	No	No	HARPS+CLS*
HD 42936	0.86	0.19 ± 0.20	No	No	HARPS
HD 4307	1.02	-0.199 ± 0.060	No	No	CLS
HD 4308	1.01	-0.340 ± 0.090	No	No	HARPS*+AAT
HD 43197	0.96	0.360 ± 0.040	Yes	Yes	HARPS
HD 43834	0.99	0.10 ± 0.10	No	No	AAT
HD 43947	0.92	-0.255 ± 0.060	No	No	CLS
HD 44219	1.03	0.020 ± 0.020	Yes	Yes	HARPS
HD 44420	1.03	0.265 ± 0.070	No	No	HARPS
HD 44447	1.11	-0.25 ± 0.10	No	No	HARPS*+AAT
HD 4457	0.80	-0.380 ± 0.020	No	No	HARPS
HD 44573	0.84	-0.060 ± 0.040	No	No	HARPS
HD 44594	1.05	0.130 ± 0.070	No	No	HARPS*+AAT
HD 44627	0.84	-0.120 ± 0.090	No	No	HARPS
HD 44665	1.02	-0.004 ± 0.050	No	No	HARPS
HD 44804	0.93	0.030 ± 0.020	No	No	HARPS
HD 45021	1.01	0.007 ± 0.050	No	No	HARPS
HD 45067	1.17	-0.049 ± 0.060	No	No	CLS
HD 45184	1.06	0.040 ± 0.060	No	No	HARPS*+CLS
HD 45270	1.08	-0.030 ± 0.040	No	No	HARPS
HD 45289	1.02	-0.050 ± 0.060	No	No	HARPS*+AAT
HD 45346	1.02	-0.057 ± 0.050	No	No	HARPS
HD 45350	1.05	0.292 ± 0.060	Yes	Yes	CLS
HD 45364	0.95	-0.200 ± 0.040	No	No	HARPS
HD 457	1.15	0.310 ± 0.060	No	No	HARPS
HD 45701	1.05	0.20 ± 0.10	No	No	AAT
HD 4614	0.91	-0.241 ± 0.060	No	No	CLS
HD 4628	0.74	-0.235 ± 0.060	No	No	CLS
HD 46375	0.93	0.271 ± 0.060	No	No	CLS
HD 47157	1.09	0.351 ± 0.060	No	No	CLS
HD 47186	1.00	0.216 ± 0.080	Yes	No	HARPS
HD 4747	0.83	-0.166 ± 0.060	No	No	CLS
HD 47752	0.73	-0.049 ± 0.080	No	No	CLS
HD 48115	1.07	-0.220 ± 0.020	No	No	HARPS
HD 48265	1.04	0.35 ± 0.20	Yes	Yes	HARPS

Table B.1 (continued)

Target	M _★ [M _⊙]	[Fe/H] [dex]	CJ [0.3 – 13 M _{Jup}]	CJ [0.5 – 20 M _{Jup}]	Ref.
HD 48682	1.12	0.083 ± 0.060	No	No	CLS
HD 48938	0.86	-0.404 ± 0.060	No	No	CLS
HD 49035	1.00	0.240 ± 0.040	No	No	HARPS
HD 4915	1.01	-0.240 ± 0.100	No	No	HARPS+CLS*
HD 49674	1.06	0.300 ± 0.060	No	No	CLS
HD 49933 A	1.38	-0.43 ± 0.10	No	No	HARPS
HD 50281	0.74	0.017 ± 0.080	No	No	CLS
HD 50499	1.25	0.305 ± 0.060	Yes	Yes	CLS
HD 50554	1.04	-0.021 ± 0.060	Yes	Yes	CLS
HD 50590	0.79	-0.250 ± 0.060	No	No	HARPS
HD 50652	1.02	0.290 ± 0.100	No	No	HARPS
HD 50692	0.91	-0.179 ± 0.060	No	No	CLS
HD 50806	1.04	0.063 ± 0.060	No	No	CLS
HD 51419	0.84	-0.308 ± 0.060	No	No	CLS
HD 51754	1.03	-0.580 ± 0.100	No	No	HARPS
HD 51866	0.81	0.088 ± 0.060	No	No	CLS
HD 52265	1.11	0.20 ± 0.20	No	No	HARPS+CLS*
HD 52711	0.93	-0.119 ± 0.060	No	No	CLS
HD 52919	0.74	0.073 ± 0.080	No	No	CLS
HD 53705	1.04	-0.24 ± 0.30	No	No	AAT
HD 53706	0.91	-0.29 ± 0.20	No	No	AAT
HD 5372	1.14	0.238 ± 0.060	No	No	CLS
HD 5388	1.21	-0.310 ± 0.060	No	No	HARPS
HD 54351	1.05	-0.110 ± 0.100	No	No	HARPS
HD 55575	0.87	-0.309 ± 0.060	No	No	CLS
HD 55693	1.07	0.26 ± 0.20	No	No	HARPS*+AAT
HD 55720	0.96	-0.350 ± 0.060	No	No	AAT
HD 56380	0.92	-0.440 ± 0.040	No	No	HARPS
HD 564	1.11	-0.230 ± 0.020	Yes	No	HARPS
HD 58489	0.77	0.120 ± 0.030	No	No	HARPS
HD 59711 A	1.02	-0.13 ± 0.10	No	No	HARPS
HD 60491	0.79	-0.152 ± 0.050	No	No	CLS
HD 61005	0.97	0.030 ± 0.040	No	No	HARPS
HD 6101	0.79	-0.018 ± 0.050	No	No	CLS
HD 61051	0.94	-0.100 ± 0.080	No	No	HARPS
HD 61383	1.02	-0.520 ± 0.050	No	No	HARPS
HD 61606	0.81	0.033 ± 0.060	No	No	CLS
HD 61902	1.15	-0.650 ± 0.080	No	No	HARPS
HD 61986	1.03	-0.340 ± 0.030	No	No	HARPS
HD 6204	1.05	0.02 ± 0.10	No	No	HARPS
HD 62128	1.04	0.330 ± 0.030	No	No	HARPS
HD 62364	1.19	-0.140 ± 0.030	No	Yes	HARPS
HD 62613	0.89	-0.063 ± 0.060	No	No	CLS
HD 63454	0.78	0.130 ± 0.080	No	No	HARPS
HD 6348	0.85	-0.590 ± 0.060	No	No	HARPS
HD 63487	1.05	0.059 ± 0.040	No	No	HARPS
HD 63608	0.92	0.100 ± 0.020	No	No	HARPS
HD 63754	1.45	0.175 ± 0.060	No	No	CLS
HD 63765	0.95	-0.190 ± 0.040	No	No	HARPS
HD 6434	1.04	-0.54 ± 0.20	No	No	HARPS
HD 65277	0.74	-0.059 ± 0.070	No	No	CLS
HD 65430	0.82	-0.039 ± 0.050	No	No	CLS
HD 65562	0.84	-0.130 ± 0.030	No	No	HARPS
HD 6558	1.29	0.240 ± 0.060	No	No	CLS
HD 65583	0.73	-0.541 ± 0.050	No	No	CLS
HD 66040	0.89	0.320 ± 0.020	No	No	HARPS
HD 66221	0.99	0.152 ± 0.020	No	No	HARPS
HD 66340	0.91	0.030 ± 0.020	No	No	HARPS
HD 66428	1.01	0.250 ± 0.090	Yes	Yes	HARPS+CLS*
HD 66653	1.06	0.100 ± 0.100	No	No	HARPS
HD 67	1.03	0.00 ± 0.80	No	No	HARPS
HD 6718	1.02	-0.07 ± 0.10	Yes	Yes	HARPS
HD 67199	0.87	0.030 ± 0.020	No	No	AAT
HD 67200	1.18	0.290 ± 0.020	No	No	HARPS
HD 6735	1.14	-0.090 ± 0.040	No	No	HARPS
HD 67556	1.21	0.190 ± 0.040	No	No	AAT
HD 6790	1.17	0.010 ± 0.080	No	No	HARPS
HD 68017	0.82	-0.324 ± 0.060	No	No	CLS
HD 68168	1.02	0.12 ± 0.10	No	No	HARPS
HD 68284	1.08	-0.530 ± 0.100	No	No	HARPS
HD 68607	0.88	0.040 ± 0.040	No	No	HARPS
HD 68978	1.09	0.010 ± 0.040	No	No	HARPS
HD 68988	1.17	0.305 ± 0.060	No	No	CLS
HD 69611	1.04	-0.580 ± 0.100	No	No	HARPS
HD 69655	1.09	-0.210 ± 0.070	No	No	HARPS*+AAT

Table B.1 (continued)

Target	M_\star [M_\odot]	[Fe/H] [dex]	CJ [0.3 – 13 M_{Jup}]	CJ [0.5 – 20 M_{Jup}]	Ref.
HD 70642	1.01	0.170 ± 0.080	Yes	Yes	HARPS+AAT*
HD 70889	1.11	0.086 ± 0.040	No	No	HARPS+AAT*
HD 7134	1.09	-0.320 ± 0.070	No	No	HARPS
HD 71479	1.08	0.21 ± 0.10	No	No	HARPS
HD 71685	1.12	-0.400 ± 0.020	No	No	HARPS
HD 71835	0.95	-0.040 ± 0.040	No	No	HARPS
HD 7199	0.93	0.270 ± 0.070	No	No	HARPS
HD 72579	0.95	0.170 ± 0.050	No	No	HARPS
HD 72659	1.09	-0.020 ± 0.080	Yes	Yes	HARPS+CLS*
HD 73121	1.12	0.060 ± 0.080	No	No	HARPS+AAT
HD 73256	0.97	0.230 ± 0.060	No	Yes	HARPS
HD 73267	0.93	0.050 ± 0.030	Yes	Yes	HARPS
HD 73344	1.18	0.131 ± 0.060	No	No	CLS
HD 73526	0.98	0.25 ± 0.20	Yes	Yes	AAT
HD 73667	0.71	-0.409 ± 0.040	No	No	CLS
HD 74000	1.19	-2.01 ± 0.10	No	No	HARPS
HD 74014	0.98	0.200 ± 0.060	No	No	HARPS
HD 74156	1.15	0.079 ± 0.060	Yes	Yes	CLS
HD 7449	1.12	-0.140 ± 0.040	Yes	Yes	HARPS
HD 74698	1.05	0.060 ± 0.040	Yes	No	HARPS
HD 74868	1.19	0.240 ± 0.040	No	No	AAT
HD 74957	1.07	-0.210 ± 0.040	No	No	HARPS
HD 75289	1.12	0.28 ± 0.20	No	No	HARPS+AAT*
HD 75302	1.01	0.08 ± 0.10	Yes	Yes	HARPS
HD 75530	0.92	-0.570 ± 0.100	No	No	HARPS
HD 7570	1.15	0.15 ± 0.10	No	No	AAT
HD 75732	0.98	0.383 ± 0.060	Yes	Yes	CLS
HD 75881	1.17	0.040 ± 0.040	No	No	HARPS
HD 76188	1.11	-0.470 ± 0.020	No	No	HARPS
HD 7661	0.95	0.020 ± 0.030	No	No	HARPS
HD 76700	1.00	0.350 ± 0.060	No	No	HARPS+AAT*
HD 76849	0.90	-0.26 ± 0.20	No	No	HARPS
HD 76909	1.09	0.341 ± 0.060	No	No	CLS
HD 77110	1.02	-0.520 ± 0.020	No	No	HARPS
HD 77338	0.93	0.33 ± 0.10	No	No	HARPS
HD 78286	1.05	0.230 ± 0.080	No	No	HARPS
HD 78429	1.03	0.078 ± 0.070	No	No	HARPS+AAT
HD 78534	1.04	0.038 ± 0.040	No	No	HARPS
HD 78558	1.06	-0.440 ± 0.090	No	No	HARPS
HD 78660	1.02	-0.012 ± 0.050	No	No	HARPS
HD 78747	1.03	-0.70 ± 0.20	No	No	HARPS
HD 7924	0.80	-0.123 ± 0.060	No	No	CLS
HD 79601	1.04	-0.620 ± 0.080	No	No	HARPS
HD 80606	1.05	0.348 ± 0.060	No	No	CLS
HD 80913	1.11	-0.6900 ± 0.0100	No	No	AAT
HD 81639	0.97	-0.200 ± 0.050	No	No	HARPS
HD 81700	1.08	0.120 ± 0.020	No	No	HARPS
HD 81767	0.82	0.070 ± 0.100	No	No	HARPS
HD 82516	0.85	0.020 ± 0.040	No	No	HARPS
HD 82783	0.92	0.180 ± 0.020	No	No	HARPS
HD 82943	1.08	0.25 ± 0.20	Yes	Yes	HARPS*+CLS
HD 83443	0.95	0.34 ± 0.20	Yes	Yes	HARPS*+CLS
HD 83529	1.07	-0.250 ± 0.060	No	No	HARPS
HD 8389	0.95	0.406 ± 0.050	No	No	CLS
HD 84035	0.77	0.269 ± 0.070	No	No	CLS
HD 8406	1.02	-0.10 ± 0.10	No	No	HARPS
HD 84117	1.16	-0.035 ± 0.060	No	No	CLS*+AAT
HD 84737	1.19	0.136 ± 0.060	No	No	CLS
HD 85119	0.94	-0.230 ± 0.070	No	No	HARPS
HD 8535	1.18	0.010 ± 0.020	Yes	Yes	HARPS
HD 85390	0.87	-0.090 ± 0.030	No	No	HARPS
HD 85512	0.69	-0.280 ± 0.080	No	No	HARPS*+AAT
HD 85683	1.17	0.040 ± 0.020	No	No	AAT
HD 85725	1.09	0.120 ± 0.080	No	No	HARPS
HD 8574	1.09	-0.010 ± 0.060	No	No	CLS
HD 86065	0.81	-0.030 ± 0.090	No	No	HARPS
HD 86140	0.79	-0.280 ± 0.050	No	No	HARPS
HD 8648	1.08	0.188 ± 0.060	No	No	CLS
HD 86728	1.07	0.226 ± 0.060	No	No	CLS
HD 86819	1.10	-0.080 ± 0.020	No	No	AAT
HD 87359	0.98	0.070 ± 0.060	No	No	CLS
HD 8765	1.03	0.223 ± 0.060	No	No	CLS
HD 87836	1.18	0.329 ± 0.060	No	No	CLS
HD 87838	1.15	-0.430 ± 0.060	No	No	HARPS
HD 87883	0.83	0.104 ± 0.060	Yes	Yes	CLS

Table B.1 (continued)

Target	M _★ [M _⊙]	[Fe/H] [dex]	CJ [0.3 – 13 M _{Jup}]	CJ [0.5 – 20 M _{Jup}]	Ref.
HD 88072	1.04	0.02 ± 0.10	No	No	HARPS
HD 88084	1.03	-0.100 ± 0.050	No	No	HARPS
HD 88230	0.63	-0.040 ± 0.070	No	No	CLS
HD 8828	0.93	-0.160 ± 0.040	No	No	HARPS
HD 8859	0.97	-0.100 ± 0.040	No	No	HARPS
HD 88742	1.10	-0.050 ± 0.060	No	No	AAT
HD 88986	1.10	0.078 ± 0.060	No	No	CLS
HD 89269	0.87	-0.138 ± 0.060	No	No	CLS
HD 89454	1.02	0.110 ± 0.050	No	No	HARPS
HD 89839	1.24	0.010 ± 0.040	Yes	Yes	HARPS
HD 89920	0.78	-0.060 ± 0.020	No	No	HARPS
HD 89965	0.84	-0.110 ± 0.020	No	No	HARPS
HD 90156	1.00	-0.240 ± 0.050	No	No	HARPS+CLS*
HD 90422	1.13	-0.650 ± 0.060	No	No	HARPS
HD 90520	1.12	0.200 ± 0.100	No	No	HARPS
HD 90711	1.00	0.311 ± 0.060	No	No	CLS
HD 90812	0.87	-0.380 ± 0.040	No	No	HARPS
HD 90875	0.77	0.309 ± 0.070	No	No	CLS
HD 90905	1.14	0.070 ± 0.040	No	No	HARPS
HD 91204	1.16	0.211 ± 0.060	No	No	CLS
HD 91379	1.17	-0.320 ± 0.020	No	No	HARPS
HD 92719	1.04	-0.130 ± 0.080	No	No	HARPS*+CLS
HD 92788	1.08	0.277 ± 0.060	Yes	Yes	CLS
HD 9280	1.01	0.32 ± 0.10	No	No	AAT
HD 92987	1.04	-0.010 ± 0.070	No	No	AAT
HD 93351	0.94	-0.260 ± 0.020	No	No	HARPS
HD 93372	1.28	0.090 ± 0.040	No	No	HARPS
HD 93385	1.10	-0.010 ± 0.080	No	No	HARPS*+AAT
HD 93745	1.22	0.113 ± 0.060	No	No	CLS
HD 9407	0.93	0.029 ± 0.060	No	No	CLS
HD 94151	0.99	0.040 ± 0.060	No	No	HARPS
HD 94771	1.00	0.190 ± 0.020	Yes	Yes	HARPS
HD 95128	1.01	0.026 ± 0.060	Yes	Yes	CLS
HD 95456	1.23	0.130 ± 0.060	No	No	HARPS
HD 95521	1.03	-0.180 ± 0.060	No	No	HARPS
HD 95542	1.14	-0.060 ± 0.020	No	No	HARPS
HD 9562	1.33	0.222 ± 0.060	No	No	CLS
HD 9578	1.13	0.080 ± 0.040	No	No	HARPS
HD 96116	1.05	-0.010 ± 0.050	No	No	HARPS
HD 96423	1.02	0.100 ± 0.070	No	No	HARPS*+AAT
HD 967	0.99	-0.680 ± 0.040	No	No	HARPS
HD 96700	1.06	-0.210 ± 0.060	No	No	HARPS
HD 97037	1.06	-0.100 ± 0.080	No	No	HARPS
HD 97101	0.70	0.243 ± 0.070	No	No	CLS
HD 97320	1.12	-1.17 ± 0.20	No	No	HARPS
HD 97343	0.88	0.020 ± 0.060	No	No	CLS
HD 97658	0.77	-0.228 ± 0.060	No	No	CLS
HD 9782	1.11	0.060 ± 0.030	No	No	HARPS
HD 9796	0.87	-0.250 ± 0.040	No	No	HARPS
HD 97998	1.02	-0.450 ± 0.060	No	No	HARPS
HD 9826	1.29	0.122 ± 0.060	Yes	Yes	CLS
HD 98284	1.12	-0.870 ± 0.020	No	No	HARPS
HD 984	1.30	0.090 ± 0.080	No	No	HARPS
HD 99109	0.97	0.384 ± 0.060	Yes	No	CLS
HD 99491	1.02	0.331 ± 0.060	No	No	CLS
HD 99492	0.85	0.32 ± 0.10	No	No	HARPS+CLS*
HD 9986	1.04	0.083 ± 0.100	No	No	HARPS+CLS*
HIP 100233	1.10	-0.080 ± 0.080	No	No	HARPS
HIP 100396	1.18	0.100 ± 0.100	No	No	HARPS
HIP 105388	0.98	0.02 ± 0.20	No	No	HARPS
HIP 106931	0.98	-0.200 ± 0.060	No	No	HARPS
HIP 108065	0.97	0.050 ± 0.040	No	No	HARPS
HIP 108095	1.11	-0.410 ± 0.060	No	No	HARPS
HIP 108950	1.04	0.380 ± 0.020	No	No	HARPS
HIP 109149	0.82	-0.130 ± 0.020	No	No	HARPS
HIP 110156	0.77	0.050 ± 0.020	No	No	HARPS
HIP 11048	0.60	0.220 ± 0.080	No	No	CLS
HIP 111978	0.95	0.170 ± 0.040	No	No	HARPS
HIP 112414	1.04	-0.12 ± 0.20	No	No	HARPS
HIP 115381	0.87	-0.130 ± 0.040	No	No	HARPS
HIP 115803	1.20	-0.010 ± 0.050	No	No	HARPS
HIP 18918	0.72	-0.230 ± 0.020	No	No	HARPS
HIP 19165	0.66	-0.071 ± 0.070	No	No	CLS
HIP 2247	0.74	-0.020 ± 0.020	Yes	Yes	HARPS
HIP 29788	1.12	0.090 ± 0.080	No	No	HARPS

Table B.1 (continued)

Target	M_\star [M_\odot]	[Fe/H] [dex]	CJ [0.3 – 13 M_{Jup}]	CJ [0.5 – 20 M_{Jup}]	Ref.
HIP 30112	0.70	0.139 ± 0.070	No	No	CLS
HIP 32127	0.91	-0.670 ± 0.020	No	No	HARPS
HIP 32812	0.82	-0.010 ± 0.020	No	No	HARPS
HIP 39470	0.72	-0.370 ± 0.050	No	No	HARPS
HIP 40774	0.79	-0.220 ± 0.060	No	No	HARPS
HIP 41659	0.88	-0.550 ± 0.030	No	No	HARPS
HIP 42220	0.64	0.136 ± 0.070	No	No	CLS
HIP 45301	0.77	-0.140 ± 0.020	No	No	HARPS
HIP 49067	0.78	-0.040 ± 0.020	No	No	HARPS
HIP 5114	0.79	-0.670 ± 0.080	No	No	HARPS
HIP 52776	0.73	-0.150 ± 0.020	No	No	HARPS
HIP 54597	0.78	-0.250 ± 0.020	Yes	Yes	HARPS
HIP 58289	0.78	-0.130 ± 0.020	No	No	HARPS
HIP 60051	0.98	-0.510 ± 0.020	No	No	HARPS
HIP 60633	0.76	0.288 ± 0.070	No	No	CLS
HIP 6276	0.92	-0.020 ± 0.040	No	No	HARPS
HIP 63719	1.42	-0.240 ± 0.020	No	No	HARPS
HIP 69570	0.99	-0.300 ± 0.040	No	No	HARPS
HIP 70681	0.98	-1.17 ± 0.20	No	No	HARPS
HIP 72779	1.01	0.060 ± 0.040	No	No	HARPS
HIP 78408	0.98	0.330 ± 0.080	No	No	HARPS
HIP 79578	1.04	0.048 ± 0.060	No	No	HARPS
HIP 80683	0.80	-0.060 ± 0.040	No	No	HARPS
HIP 8361	0.77	0.040 ± 0.040	No	No	HARPS
HIP 90194	0.92	-0.320 ± 0.020	No	No	HARPS
HIP 93745	1.16	-0.400 ± 0.020	No	No	HARPS
HIP 98106	0.78	-0.010 ± 0.070	No	No	HARPS
HIP 99695	0.85	-0.090 ± 0.020	No	No	HARPS
TYC6296-1176-1	1.11	0.000 ± 0.040	No	No	HARPS
TYC6296-478-1	1.02	0.060 ± 0.040	No	No	HARPS
TYC9111-1423-1	1.15	-0.68 ± 0.20	No	No	HARPS

Notes. From left to right, the columns report the name of the star, its mass and metallicity as taken from the Hypatia catalog (Hinkel et al. 2014), the presence or absence of confirmed CJs in the $0.3 - 13 M_{\text{Jup}}$ and $0.5 - 20 M_{\text{Jup}}$ mass ranges (“Yes” appears in both columns if at least one CJ in the overlapping range $0.5 - 13 M_{\text{Jup}}$ is present), and the name of the radial velocity survey (AAT and/or CLS and/or HARPS). In case the star was observed by more than one survey, the asterisk indicates the survey with the best RV dataset in terms of baseline and/or RV precision that was used in this work.

Appendix C: Comparison of the stellar properties of the small planet and merged RV samples

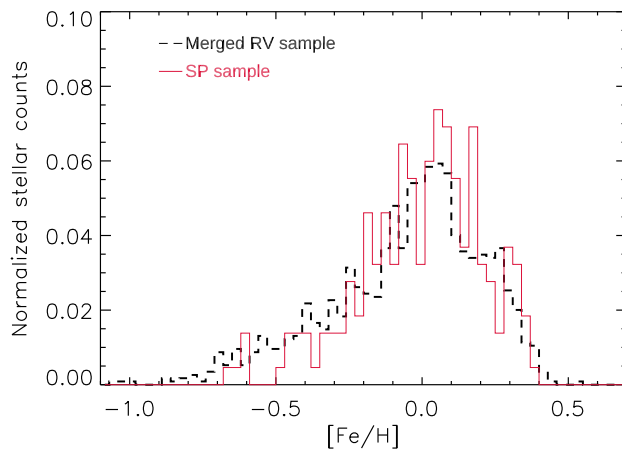


Fig. C.1. Stellar metallicity distributions in the small planet sample (red solid line) and merged (AAT+CLS+HARPS) radial velocity comparison sample (black dashed line). Note that the relative stellar counts of the SP and RV merged samples cannot be directly compared as they were normalized from different distributions.

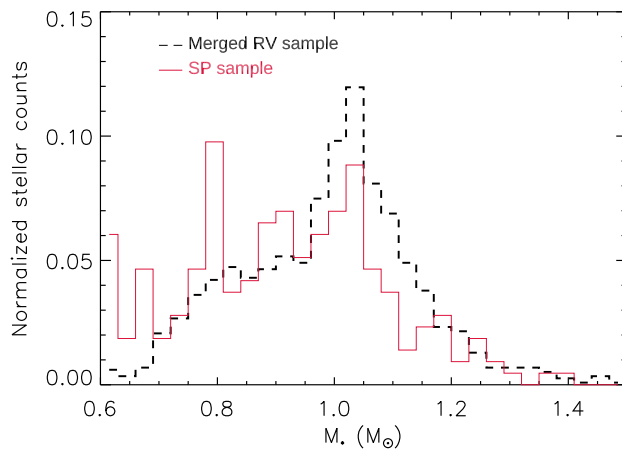


Fig. C.2. Stellar mass distributions in the small planet sample (red solid line) and merged (AAT+CLS+HARPS) radial velocity comparison sample (black dashed line). Note that the relative stellar counts of the SP and RV merged samples cannot be directly compared as they were normalized from different distributions.

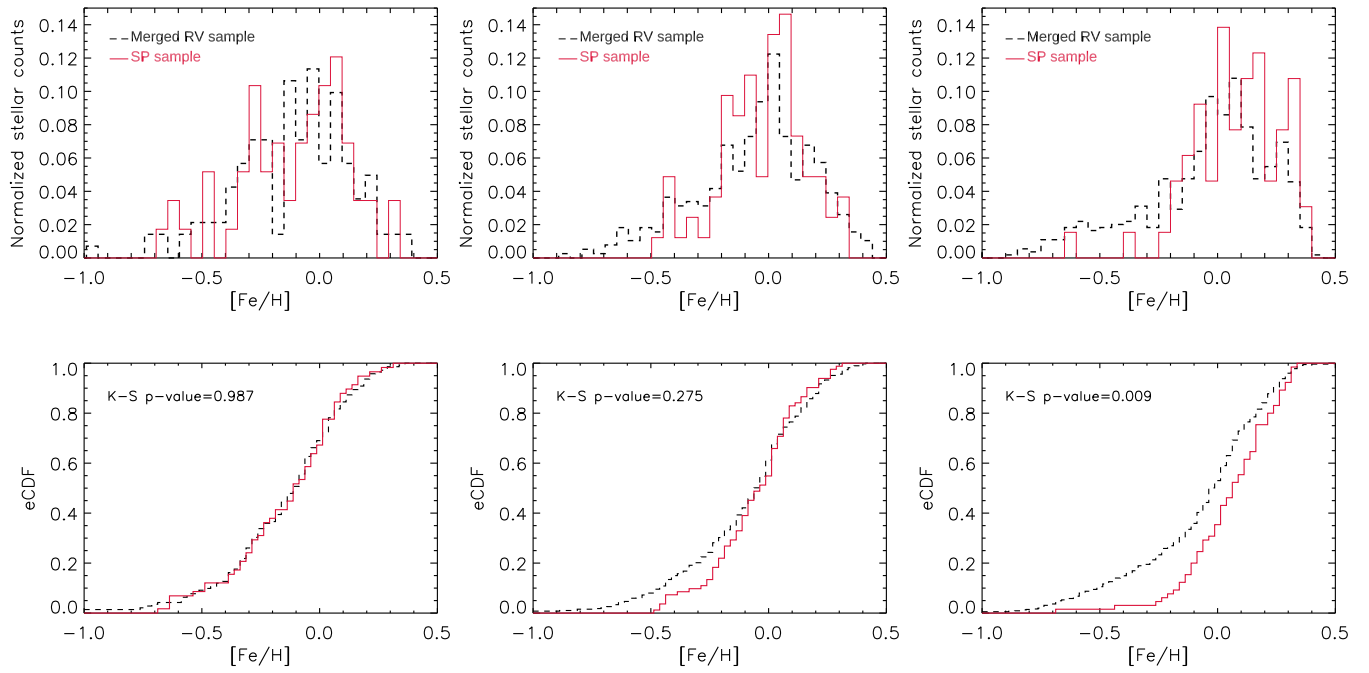


Fig. C.3. *Upper panels:* same as Fig. C.1 for the three different bins of stellar mass $0.6 - 0.8 M_{\odot}$ (left), $0.8 - 1.0 M_{\odot}$ (center), and $1.0 - 1.2 M_{\odot}$ (right). Note that the relative stellar counts of the SP and RV merged samples cannot be directly compared as they were normalized from different distributions. *Lower panels:* empirical cumulative distribution functions for the same bins of stellar mass as above. The p-values of the Kolmogorov-Smirnov test are also reported.

Appendix D: Completenesses of the considered samples

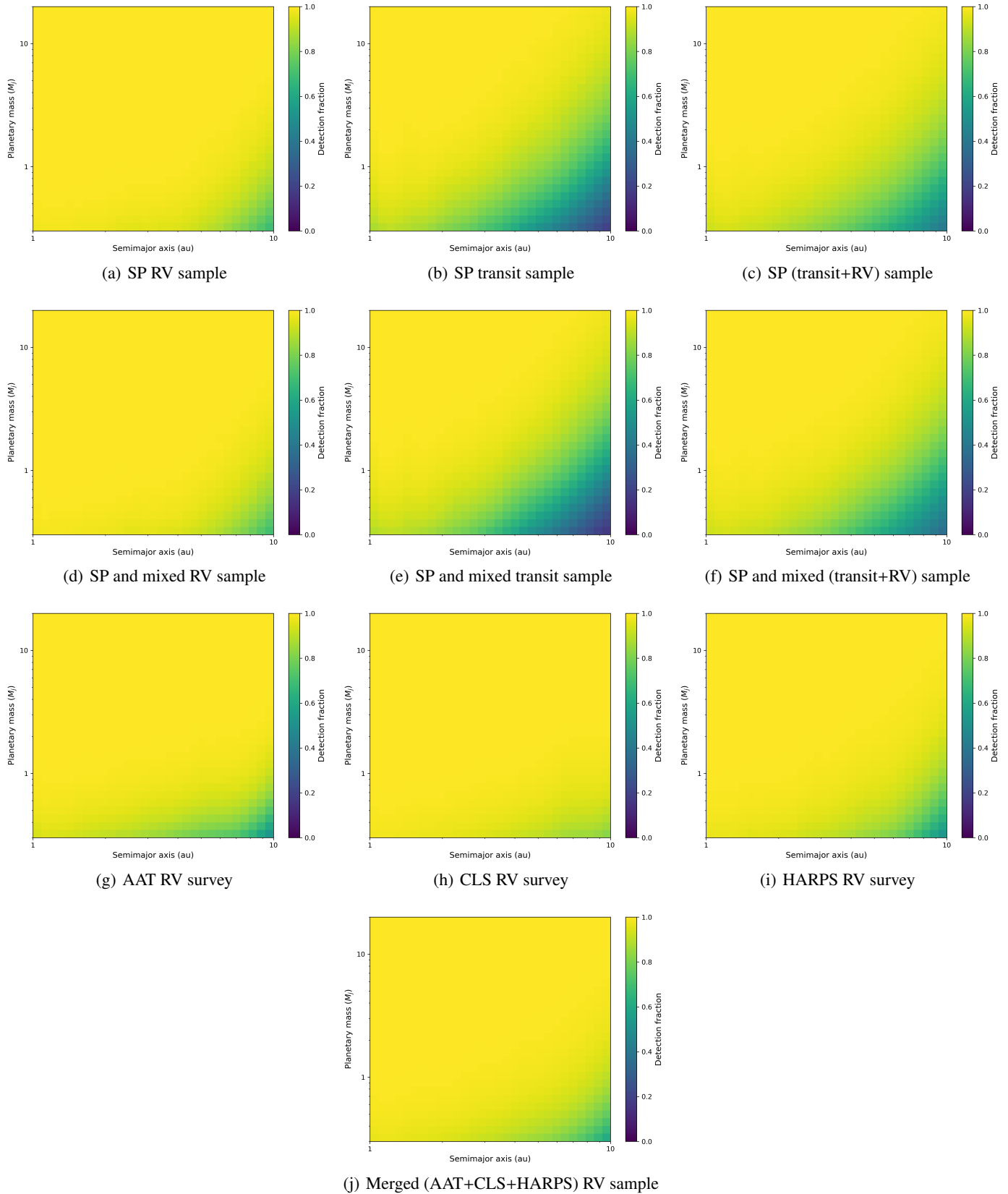


Fig. D.1. Average completenesses of all the samples considered in this work. As indicated in the color bars, the detection rate/sensitivity increases from dark blue (0%) to green (~ 50 – 80%) and yellow (100%).

Appendix E: Cold Jupiters and their occurrence rates in the small planet and radial velocity comparison samples

Table E.1. Cold Jupiters in the small planet sample.

Target	$M_p \sin(i)$ or M_p [M_{Jup}]	a [AU]	M_\star [M_\odot]	[Fe/H] [dex]	Ref.
BD-11 4672 b	$0.65^{+0.05}_{-0.06}$	2.360 ± 0.040	0.650 ± 0.030	-0.35 ± 0.20	Barbato et al. (2020)
GJ 676A b	$5.790^{+0.500}_{-0.477} *$	$1.735^{+0.056}_{-0.060}$	0.73 ± 0.20	0.080	Feng et al. (2022)
GJ 676A c	$13.500^{+1.000}_{-0.927} *$	$9.726^{+0.629}_{-0.793}$	0.73 ± 0.20	0.080	Feng et al. (2022)
HD 125612 b	$2.974^{+0.225}_{-0.258}$	$1.349^{+0.034}_{-0.036}$	1.11 ± 0.20	0.250 ± 0.040	Feng et al. (2022)
HD 125612 d	$7.180^{+0.900}_{-0.445} *$	$3.982^{+0.189}_{-0.174}$	1.11 ± 0.20	0.250 ± 0.040	Feng et al. (2022)
HD 156098 c	$5.228^{+0.338}_{-1.287} *$	$8.41^{+0.396}_{-0.629}$	1.29 ± 0.20	0.190 ± 0.100	Feng et al. (2022)
HD 160691 b	1.67 ± 0.11	1.50 ± 0.02	1.130 ± 0.020	0.280 ± 0.030	McCarthy et al. (2004)
HD 160691 c	3.10 ± 0.71	4.17 ± 0.07	1.130 ± 0.020	0.280 ± 0.030	McCarthy et al. (2004)
HD 164922 b	0.344 ± 0.013	2.149 ± 0.025	0.920 ± 0.030	0.200 ± 0.060	Rosenthal et al. (2021)
HD 181433 c	0.674 ± 0.003	1.819 ± 0.001	0.780	0.33 ± 0.10	Horner et al. (2019)
HD 181433 d	0.612 ± 0.004	6.60 ± 0.22	0.780	0.33 ± 0.10	Horner et al. (2019)
HD 190360 b	1.492 ± 0.043	$3.955^{+0.051}_{-0.053}$	0.990 ± 0.040	0.230 ± 0.060	Rosenthal et al. (2021)
HD 204313 b	$4.96^{+1.70}_{-0.45} *$	$3.208^{+0.034}_{-0.035}$	1.045 ± 0.030	0.180 ± 0.020	Xiao et al. (2023)
HD 204313 e	$15.300^{+4.900}_{-5.183} *$	$7.457^{+0.399}_{-0.427}$	1.045 ± 0.030	0.180 ± 0.020	Feng et al. (2022)
HD 215497 c	$0.35 \pm 0.02 *$	1.310 ± 0.020	0.920 ± 0.050	0.230 ± 0.070	Philipot et al. (2023)
HD 219134 h	0.308 ± 0.014	2.968 ± 0.037	0.790 ± 0.030	0.080 ± 0.060	Rosenthal et al. (2021)
HD 219828 c	$16.10^{+3.50}_{-1.27} *$	$5.657^{+0.228}_{-0.242}$	1.18 ± 0.20	0.180	Feng et al. (2022)
HD 34445 b	$0.658^{+0.041}_{-0.040}$	$2.105^{+0.038}_{-0.039}$	1.110 ± 0.060	0.140 ± 0.060	Rosenthal et al. (2021)
HD 34445 g	0.38 ± 0.13	6.36 ± 1.02	1.110 ± 0.060	0.140 ± 0.060	Vogt et al. (2017)
HD 39091 b/ π Men b	$12.300^{+1.200}_{-1.384} *$	$3.311^{+0.134}_{-0.148}$	1.070 ± 0.040	0.090 ± 0.040	Feng et al. (2022)
HD 74698 c	0.40 ± 0.06	4.5 ± 0.2	1.040 ± 0.025	0.07 ± 0.02	Frensch et al. (2023)
HD 86226 b	$0.45^{+0.04}_{-0.05} *$	2.730 ± 0.060	1.020 ± 0.060	0.020 ± 0.050	Teske et al. (2020)
Kepler-48 e	2.163 ± 0.062	1.898	0.880 ± 0.060	0.170 ± 0.070	Weiss et al. (2024)
Kepler-48 f	0.939 ± 0.292	5.719	0.880 ± 0.060	0.170 ± 0.070	Weiss et al. (2024)
Kepler-68 d	0.749 ± 0.017	1.469 ± 0.010	1.080 ± 0.050	0.120 ± 0.070	Bonomo et al. (2023)
Kepler-94 c	8.885 ± 0.117	1.597	0.810 ± 0.060	0.340 ± 0.070	Weiss et al. (2024)
Kepler-129 d	$8.30^{+1.10}_{-0.70}$	4.00 ± 0.10	1.178 ± 0.030	0.290 ± 0.100	Zhang et al. (2021)
Kepler-139 e	1.341 ± 0.134	3.236	1.078 ± 0.030	0.350 ± 0.040	Weiss et al. (2024)
Kepler-407 c	11.089 ± 0.049	3.27	1.000 ± 0.060	0.330 ± 0.070	Weiss et al. (2024)
Kepler-454 c	4.51 ± 0.12	1.287 ± 0.017	1.030 ± 0.040	0.320 ± 0.080	Bonomo et al. (2023)
Kepler-454 d	$2.31^{+0.27}_{-0.16}$	$5.10^{+0.34}_{-0.19}$	1.030 ± 0.040	0.320 ± 0.080	Bonomo et al. (2023)
K2-312 c/HD 80653 c	$5.41^{+0.52}_{-0.44}$	1.961 ± 0.027	1.180 ± 0.040	0.255 ± 0.070	Bonomo et al. (2023)
K2-364 c/HD 137496 c	7.66 ± 0.11	1.2163 ± 0.0087	1.040 ± 0.020	-0.030 ± 0.040	Azevedo Silva et al. (2022)
TOI-1669 c	$0.601^{+0.079}_{-0.076}$	1.27 ± 0.03	1.00 ± 0.05	0.26 ± 0.06	Polanski et al. (2024)
TOI-1736 c	$8.70^{+1.50}_{-0.60} *$	1.381 ± 0.017	1.080 ± 0.040	0.138 ± 0.010	Martioli et al. (2023)
TOI-1339 f/HD 191939 f	6.50 ± 4.515	4.80 ± 2.20	0.810 ± 0.040	-0.150 ± 0.060	Lubin et al. (2022)

Notes. From left to right, the columns report the name of the cold Jupiter, its mass and semi-major axis, the mass and metallicity of the host star, and the reference for the cold-Jupiter mass determination. Asterisks denote true masses instead of minimum masses thanks to the combination of radial velocities and measurements of Hipparcos-Gaia proper motion anomalies (e.g., Kervella et al. 2022).

Table E.2. Cold Jupiters in the mixed system sample.

Target	$M_p \sin(i)$ or M_p [M_{Jup}]	a [AU]	M_\star [M_\odot]	[Fe/H] [dex]	Ref.
55 Cnc d	3.12 ± 0.10	5.96 ± 0.07	0.975 ± 0.045	0.383 ± 0.055	Bourrier et al. (2018)
HIP 57274 d	0.53 ± 0.03	1.01	0.73 ± 0.05	0.09 ± 0.05	Fischer et al. (2012)
Kepler-56 d	5.61 ± 0.38	2.16 ± 0.08	1.67 ± 0.15	0.40 ± 0.04	Otor et al. (2016)
Kepler-88 d/KOI-142 d	3.15 ± 0.17	2.47	0.985 ± 0.021	0.27 ± 0.04	Weiss et al. (2024)
TOI-4010 e	$2.18^{+0.21}_{-0.20}$	$1.57^{+0.12}_{-0.13}$	0.89 ± 0.03	0.37 ± 0.07	Kunimoto et al. (2023)
WASP-47 c	$1.41^{+0.06}_{-0.07}$	1.393 ± 0.014	1.04 ± 0.03	0.38 ± 0.05	Nascimbeni et al. (2023)

Notes. Same as Table E.1 but for cold Jupiters within mixed systems.

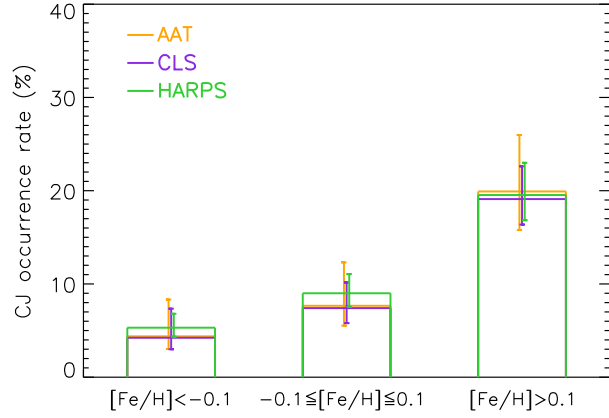


Fig. E.1. Similarly to Fig. 1, occurrence rates of cold Jupiters with $M_p = 0.5 - 20 M_{\text{Jup}}$ in the AAT (orange), CLS (violet), and HARPS (green) radial velocity surveys, at sub-solar ($[\text{Fe}/\text{H}] < -0.1$), solar ($-0.1 \leq [\text{Fe}/\text{H}] \leq 0.1$), and super-solar ($[\text{Fe}/\text{H}] > 0.1$) metallicity. Almost identical occurrence rates are obtained for $M_p = 0.3 - 13 M_{\text{Jup}}$. See also Table B.1.

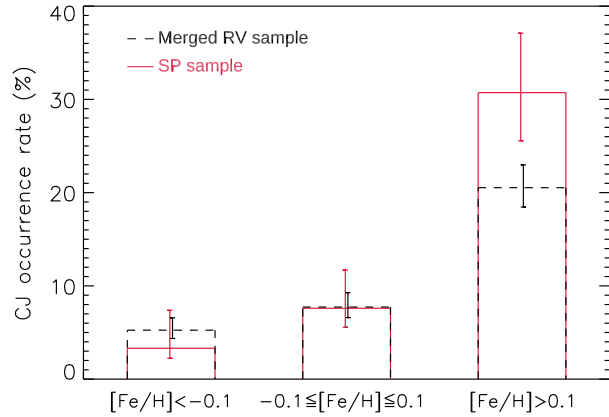


Fig. E.2. Same as Fig. 1 for $M_p = 0.3 - 13 M_{\text{Jup}}$. See also Table F.1.

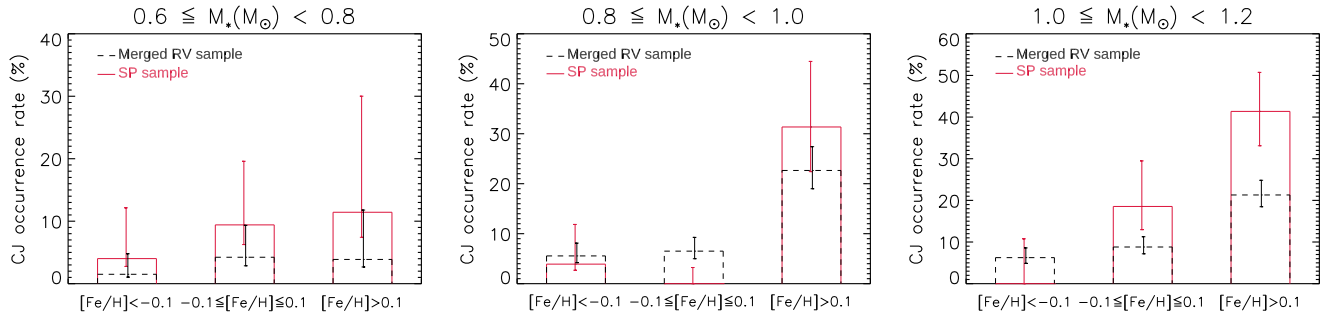


Fig. E.3. Same as Fig. 2 for $M_p = 0.3 - 13 M_{\text{Jup}}$. See also Table F.2.

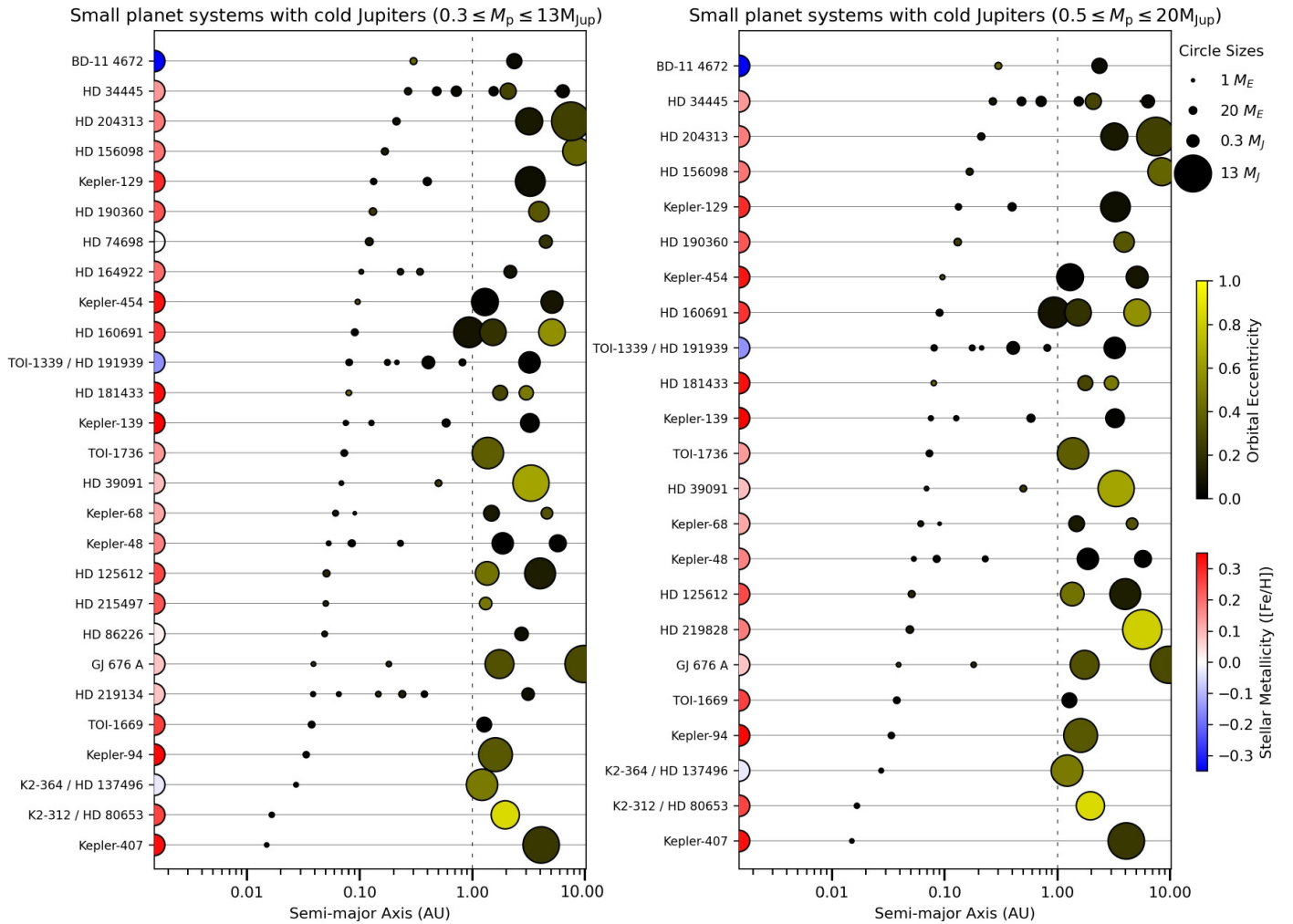


Fig. E.4. The architectures of the systems with both small planets and cold Jupiters considered in this work and ordered according to increasing semi-major axis of the innermost planet (from bottom to top). The cold Jupiters in the left (27 systems) and right (23 systems) panels have masses $0.3 \leq M_p \leq 13 M_{J_{\text{up}}}$ and $0.5 \leq M_p \leq 20 M_{J_{\text{up}}}$, respectively, with a large overlap for cold Jupiters with $0.5 \leq M_p \leq 13 M_{J_{\text{up}}}$. The planet circles have sizes proportional to their mass (see legend in the top right corner), and colors depending on the orbital eccentricity (more eccentric planets are shown in yellow). The host stars are color coded as a function of stellar metallicity (metallicity increases from blue to red).

Table E.3 (continued)

Target	CJ name	$M_p \sin(i)$ or M_p [M _{Jup}]	a [AU]	M_\star [M _⊕]	[Fe/H] [dex]	Ref.
"	47 UMa c	$0.497^{+0.032}_{-0.030}$	$3.404^{+0.054}_{-0.056}$	1.01	0.026 ± 0.060	Rosenthal et al. (2021)
HD 9826	ups And d	4.100 ± 0.100	$2.517^{+0.026}_{-0.027}$	1.29	0.122 ± 0.060	Rosenthal et al. (2021)
HD 99109	HD 99109 b	0.474 ± 0.035	1.122 ± 0.017	0.97	0.384 ± 0.060	Rosenthal et al. (2021)
HIP 2247	BD-17 63 b	2.85 ± 1.16	1.340 ± 0.020	0.74	-0.020 ± 0.020	Stassun et al. (2017)
HIP 54597	HIP 54597 b	2.010 ± 0.030	3.810 ± 0.020	0.78	-0.250 ± 0.020	Frensch et al. (2023)

Notes. From left to right, the columns report the HD or HIP identifier of the host star, the name of the cold Jupiter, its mass and semi-major axis, the stellar mass and metallicity, and the reference for the cold-Jupiter mass determination. Asterisks denote true masses instead of minimum masses thanks to the combination of radial velocities and measurements of Hipparcos-Gaia proper motion anomalies (e.g., Kervella et al. 2022).

Appendix F: Occurrence rates of cold Jupiters in the small planet and in the large RV comparison sample as a function of stellar metallicity and/or mass.

Table F.1. Occurrence rates of cold Jupiters in the small planet sample and in the large RV comparison one as a function of stellar metallicity.

[Fe/H]	$M_p = 0.3 - 13 M_{\text{Jup}}$			$M_p = 0.5 - 20 M_{\text{Jup}}$		
	$N_\star d$	C	$f_{\text{CJ}} [\%]$	$N_\star d$	C	$f_{\text{CJ}} [\%]$
Small planet (transit+radial velocity) sample						
[Fe/H] = -0.011 ± 0.005	217 27	0.928	$13.4^{+2.8}_{-2.0}$	217 23	0.958	$11.1^{+2.5}_{-1.8}$
[Fe/H] < -0.1	64 2	0.943	$3.3^{+4.1}_{-1.1}$	64 2	0.969	$3.2^{+4.0}_{-1.0}$
$-0.1 \leq [\text{Fe/H}] \leq +0.1$	86 6	0.918	$7.6^{+4.1}_{-2.0}$	86 3	0.952	$3.7^{+3.3}_{-1.1}$
[Fe/H] > $+0.1$	67 19	0.923	$30.7^{+6.4}_{-5.2}$	67 18	0.954	$28.2^{+6.2}_{-4.9}$
[Fe/H] ≤ 0	102 3	0.932	$3.2^{+2.9}_{-1.0}$	102 3	0.961	$3.1^{+2.8}_{-0.9}$
[Fe/H] > 0	115 24	0.923	$22.6^{+4.5}_{-3.5}$	115 20	0.954	$18.2^{+4.2}_{-3.1}$
Merged (AAT+CLS+HARPS) radial velocity comparison sample						
[Fe/H] = -0.072 ± 0.009	1167 118	0.974	$10.4^{+1.0}_{-0.8}$	1167 113	0.988	$9.8^{+0.9}_{-0.8}$
[Fe/H] < -0.1	430 22	0.974	$5.2^{+1.3}_{-0.9}$	430 21	0.988	$4.9^{+1.3}_{-0.8}$
$-0.1 \leq [\text{Fe/H}] \leq +0.1$	413 31	0.971	$7.7^{+1.5}_{-1.1}$	413 31	0.986	$7.6^{+1.5}_{-1.1}$
[Fe/H] > $+0.1$	324 65	0.977	$20.5^{+2.4}_{-2.1}$	324 61	0.990	$19.0^{+2.4}_{-2.0}$
[Fe/H] ≤ 0	624 33	0.973	$5.4^{+1.1}_{-0.8}$	624 32	0.988	$5.2^{+1.0}_{-0.7}$
[Fe/H] > 0	543 85	0.974	$16.1^{+1.7}_{-1.5}$	543 81	0.988	$15.1^{+1.7}_{-1.4}$

Notes. From left to right, the columns report the stellar metallicity ([Fe/H]), the total number of stars (N_\star) and the number of stars with confirmed CJs (d), the average completeness (C), and the occurrence rate of CJs (f_{CJ}), for the small planet (top) and RV comparison sample (bottom) and their sub-samples at sub-solar, solar, and super-solar metallicity, by considering two ranges for the CJ mass: $0.3 - 13 M_{\text{Jup}}$ (columns 2-4) and $0.5 - 20 M_{\text{Jup}}$ (columns 5-7). We note that f_{CJ} for the small planet sample is equivalent to $f_{\text{CJ,SP}}$.

Table F.2. Occurrence rates of cold Jupiters in the small planet and in the large RV comparison sample as a function of stellar metallicity in three intervals of stellar mass.

[Fe/H]	$M_p = 0.3 - 13 M_{Jup}$			$M_p = 0.5 - 20 M_{Jup}$		
	$N_\star d$	C	$f_{CJ} [\%]$	$N_\star d$	C	$f_{CJ} [\%]$
$0.6 \leq M_\star < 0.8 M_\odot$						
Small planet (transit+radial velocity) sample						
[Fe/H] = -0.114 ± 0.011	58 4	0.947	$7.3^{+5.1}_{-2.1}$	58 3	0.971	$5.3^{+4.7}_{-1.6}$
[Fe/H] < -0.1	26 1	0.959	$4.0^{+8.1}_{-1.2}$	26 1	0.979	$3.9^{+8.0}_{-1.2}$
$-0.1 \leq [Fe/H] \leq +0.1$	23 2	0.924	$9.4^{+10.2}_{-3.1}$	23 1	0.955	$4.5^{+9.1}_{-1.4}$
[Fe/H] > $+0.1$	9 1	0.972	$11.4^{+18.6}_{-4.0}$	9 1	0.986	$11.3^{+18.4}_{-3.9}$
Merged (AAT+CLS+HARPS) radial velocity comparison sample						
[Fe/H] = -0.121 ± 0.014	142 4	0.983	$2.9^{+2.2}_{-0.8}$	142 4	0.993	$2.8^{+2.1}_{-0.9}$
[Fe/H] < -0.1	68 1	0.980	$1.5^{+3.3}_{-0.4}$	68 1	0.991	$1.5^{+3.2}_{-0.4}$
$-0.1 \leq [Fe/H] \leq +0.1$	48 2	0.984	$4.2^{+5.1}_{-1.4}$	48 2	0.993	$4.2^{+5.1}_{-1.4}$
[Fe/H] > $+0.1$	26 1	0.991	$3.9^{+7.9}_{-1.2}$	26 1	0.997	$3.9^{+7.8}_{-1.2}$
$0.8 \leq M_\star < 1.0 M_\odot$						
Small planet (transit+radial velocity) sample						
[Fe/H] = -0.030 ± 0.007	82 6	0.923	$7.9^{+4.3}_{-2.1}$	82 4	0.954	$5.1^{+3.7}_{-1.5}$
[Fe/H] < -0.1	27 1	0.948	$3.9^{+7.9}_{-1.2}$	27 1	0.971	$3.8^{+7.8}_{-1.2}$
$-0.1 \leq [Fe/H] \leq +0.1$	37 0	0.922	< 3.2	37 0	0.955	< 3.1
[Fe/H] > $+0.1$	18 5	0.886	$31.3^{+13.1}_{-8.9}$	18 3	0.926	$18.0^{+12.7}_{-5.8}$
Merged (AAT+CLS+HARPS) radial velocity comparison sample						
[Fe/H] = -0.073 ± 0.016	387 39	0.981	$10.3^{+1.8}_{-1.3}$	387 36	0.992	$9.4^{+1.7}_{-1.3}$
[Fe/H] < -0.1	147 8	0.981	$5.5^{+2.6}_{-1.3}$	147 8	0.992	$5.5^{+2.5}_{-1.3}$
$-0.1 \leq [Fe/H] \leq +0.1$	141 9	0.981	$6.5^{+2.7}_{-1.5}$	141 9	0.991	$6.4^{+2.7}_{-1.5}$
[Fe/H] > $+0.1$	99 22	0.981	$22.6^{+4.8}_{-3.7}$	99 19	0.992	$19.3^{+4.6}_{-1.3}$
$1.0 \leq M_\star < 1.2 M_\odot$						
Small planet (transit+radial velocity) sample						
[Fe/H] = 0.077 ± 0.008	65 16	0.915	$26.9^{+6.4}_{-4.9}$	65 15	0.951	$24.3^{+6.2}_{-4.6}$
[Fe/H] < -0.1	10 0	0.903	< 10.8	10 0	0.950	< 10.3
$-0.1 \leq [Fe/H] \leq +0.1$	24 4	0.899	$18.5^{+10.9}_{-5.6}$	24 2	0.941	$8.9^{+9.7}_{-3.0}$
[Fe/H] > $+0.1$	31 12	0.936	$41.4^{+9.4}_{-8.2}$	31 13	0.959	$43.7^{+9.2}_{-8.4}$
Merged (AAT+CLS+HARPS) radial velocity comparison sample						
[Fe/H] = -0.056 ± 0.014	549 63	0.972	$11.8^{+1.5}_{-1.3}$	549 62	0.988	$11.4^{+1.5}_{-1.2}$
[Fe/H] < -0.1	181 11	0.973	$6.2^{+2.3}_{-1.4}$	181 10	0.988	$5.6^{+2.2}_{-1.3}$
$-0.1 \leq [Fe/H] \leq +0.1$	200 17	0.966	$8.8^{+2.5}_{-1.6}$	200 17	0.984	$8.6^{+2.4}_{-1.6}$
[Fe/H] > $+0.1$	168 35	0.978	$21.3^{+3.5}_{-2.8}$	168 35	0.991	$21.0^{+3.5}_{-2.8}$

Notes. Same columns as Table F.1.

Appendix G: Occurrence rates of cold Jupiters in the small planet transit, RV, and transit+RV samples, without and with mixed systems, as a function of stellar metallicity.

Table G.1. Occurrence rates of cold Jupiters in the small planet transit, RV, and transit+RV samples, without and with the inclusion of mixed systems, as a function of stellar metallicity.

[Fe/H]	$M_p = 0.3 - 13 M_{Jup}$			$M_p = 0.5 - 20 M_{Jup}$		
	$N_\star d$	C	$f_{CJ} [\%]$	$N_\star d$	C	$f_{CJ} [\%]$
Small planet transit sample						
[Fe/H] = $+0.002 \pm 0.006$	134 12	0.894	$10.0^{+3.4}_{-2.1}$	134 12	0.938	$9.5^{+3.3}_{-2.0}$
[Fe/H] < -0.1	36 1	0.910	$3.0^{+6.4}_{-0.9}$	36 1	0.949	$2.9^{+6.1}_{-0.9}$
$-0.1 \leq [Fe/H] \leq +0.1$	56 1	0.884	$2.0^{+4.3}_{-0.6}$	56 1	0.931	$1.9^{+4.1}_{-0.6}$
[Fe/H] > $+0.1$	42 10	0.889	$26.8^{+8.3}_{-5.9}$	42 10	0.932	$25.5^{+8.0}_{-5.6}$
[Fe/H] ≤ 0	62 2	0.900	$3.6^{+4.4}_{-1.1}$	62 2	0.942	$3.4^{+4.2}_{-1.1}$
[Fe/H] > 0	72 10	0.886	$15.7^{+5.6}_{-3.5}$	72 10	0.931	$14.9^{+5.4}_{-3.3}$
Small planet radial velocity sample						
[Fe/H] = -0.033 ± 0.008	83 15	0.982	$18.4^{+5.0}_{-3.5}$	83 11	0.992	$13.4^{+4.6}_{-2.9}$
[Fe/H] < -0.1	28 1	0.985	$3.6^{+7.4}_{-1.1}$	28 1	0.994	$3.6^{+7.4}_{-1.1}$
$-0.1 \leq [Fe/H] \leq +0.1$	30 5	0.979	$17.0^{+9.0}_{-4.8}$	30 2	0.990	$6.7^{+7.7}_{-2.2}$
[Fe/H] > $+0.1$	25 9	0.982	$36.7^{+10.3}_{-8.3}$	25 8	0.992	$32.3^{+10.4}_{-7.7}$
[Fe/H] ≤ 0	40 1	0.981	$2.5^{+5.4}_{-0.8}$	40 1	0.991	$2.5^{+5.3}_{-0.8}$
[Fe/H] > 0	43 14	0.983	$33.1^{+7.8}_{-6.3}$	43 10	0.992	$23.4^{+7.6}_{-5.2}$
Small planet (transit+radial velocity) sample						
[Fe/H] = -0.011 ± 0.005	217 27	0.928	$13.4^{+2.8}_{-2.0}$	217 23	0.958	$11.1^{+2.5}_{-1.8}$
[Fe/H] < -0.1	64 2	0.943	$3.3^{+4.1}_{-1.1}$	64 2	0.969	$3.2^{+4.0}_{-1.0}$
$-0.1 \leq [Fe/H] \leq +0.1$	86 6	0.918	$7.6^{+4.1}_{-2.0}$	86 3	0.952	$3.7^{+3.3}_{-1.1}$
[Fe/H] > $+0.1$	67 19	0.923	$30.7^{+6.4}_{-5.2}$	67 18	0.954	$28.2^{+6.2}_{-4.9}$
[Fe/H] ≤ 0	102 3	0.932	$3.2^{+2.9}_{-1.0}$	102 3	0.961	$3.1^{+2.8}_{-0.9}$
[Fe/H] > 0	115 24	0.923	$22.6^{+4.5}_{-3.5}$	115 20	0.954	$18.2^{+4.2}_{-3.1}$
Small planet and mixed transit sample						
[Fe/H] = $+0.022 \pm 0.006$	151 16	0.891	$11.9^{+3.4}_{-2.2}$	151 16	0.935	$11.3^{+3.2}_{-2.1}$
[Fe/H] < -0.1	36 1	0.910	$3.0^{+6.4}_{-0.9}$	36 1	0.949	$2.9^{+6.1}_{-0.9}$
$-0.1 \leq [Fe/H] \leq +0.1$	63 1	0.881	$1.8^{+3.9}_{-0.5}$	63 1	0.929	$1.7^{+3.7}_{-0.5}$
[Fe/H] > $+0.1$	52 14	0.883	$30.5^{+7.5}_{-5.8}$	52 14	0.928	$29.0^{+7.2}_{-5.6}$
[Fe/H] ≤ 0	64 2	0.899	$3.5^{+4.2}_{-1.1}$	64 2	0.942	$3.3^{+4.1}_{-1.1}$
[Fe/H] > 0	87 14	0.881	$18.3^{+5.2}_{-3.6}$	87 14	0.927	$17.4^{+5.0}_{-3.4}$
Small planet and mixed radial velocity sample						
[Fe/H] = -0.018 ± 0.007	91 17	0.983	$19.0^{+4.8}_{-3.4}$	91 13	0.992	$14.4^{+4.5}_{-2.9}$
[Fe/H] < -0.1	29 1	0.985	$3.5^{+7.2}_{-1.1}$	29 1	0.993	$3.5^{+7.2}_{-1.1}$
$-0.1 \leq [Fe/H] \leq +0.1$	34 6	0.979	$18.0^{+8.4}_{-4.8}$	34 3	0.990	$8.9^{+7.4}_{-2.8}$
[Fe/H] > $+0.1$	28 10	0.983	$36.3^{+9.8}_{-7.9}$	28 9	0.993	$32.4^{+9.8}_{-7.4}$
[Fe/H] ≤ 0	41 1	0.981	$2.5^{+5.3}_{-0.8}$	41 1	0.991	$2.5^{+5.2}_{-0.7}$
[Fe/H] > 0	50 16	0.983	$32.5^{+7.2}_{-5.9}$	50 12	0.993	$24.2^{+7.0}_{-5.0}$
Small planet and mixed (transit+radial velocity) sample						
[Fe/H] = 0.007 ± 0.004	242 33	0.926	$14.7^{+2.7}_{-2.1}$	242 29	0.957	$12.5^{+2.5}_{-1.8}$
[Fe/H] < -0.1	65 2	0.944	$3.3^{+4.0}_{-1.0}$	65 2	0.969	$3.2^{+3.9}_{-1.0}$
$-0.1 \leq [Fe/H] \leq +0.1$	97 7	0.915	$7.9^{+3.8}_{-2.0}$	97 4	0.950	$4.3^{+3.2}_{-1.3}$
[Fe/H] > $+0.1$	80 24	0.918	$32.7^{+5.8}_{-4.9}$	80 23	0.951	$30.2^{+5.7}_{-4.7}$
[Fe/H] ≤ 0	105 3	0.931	$3.1^{+2.8}_{-0.9}$	105 3	0.961	$3.0^{+2.7}_{-0.9}$
[Fe/H] > 0	137 30	0.918	$23.8^{+4.2}_{-3.4}$	137 26	0.951	$20.0^{+3.9}_{-3.0}$

Notes. Same columns as Table F.1.

Appendix H: Occurrence rates of cold Jupiters in the AAT, CLS, and HARPS RV surveys

Table H.1. Occurrence rates of cold Jupiters in the CLS survey by using the selection criteria in BL24 (top) and this work (bottom).

[Fe/H]	$M_p = 0.3 - 13 M_{Jup}$			$M_p = 0.5 - 20 M_{Jup}$		
	$N_\star d$	C	$f_{CJ} [\%]$	$N_\star d$	C	$f_{CJ} [\%]$
CLS radial velocity sample (BL24)						
$[\text{Fe}/\text{H}] = +0.008 \pm 0.004$	562 51	0.981	$9.2^{+1.9}_{-1.1}$	562 46	0.993	$8.2^{+1.3}_{-1.0}$
$[\text{Fe}/\text{H}] < -0.1$	135 4	0.980	$3.0^{+2.3}_{-0.9}$	135 4	0.993	$3.0^{+2.3}_{-0.9}$
$-0.1 \leq [\text{Fe}/\text{H}] \leq +0.1$	201 12	0.985	$6.1^{+2.2}_{-1.3}$	201 11	0.994	$5.5^{+2.1}_{-1.2}$
$[\text{Fe}/\text{H}] > +0.1$	226 35	0.979	$15.8^{+2.8}_{-2.1}$	226 31	0.992	$13.8^{+2.6}_{-2.0}$
CLS radial velocity sample (this work)						
$[\text{Fe}/\text{H}] = +0.025 \pm 0.004$	402 50	0.987	$12.6^{+1.8}_{-1.5}$	402 45	0.995	$11.2^{+1.8}_{-1.4}$
$[\text{Fe}/\text{H}] < -0.1$	95 4	0.990	$4.2^{+3.1}_{-1.2}$	95 4	0.996	$4.2^{+3.1}_{-1.2}$
$-0.1 \leq [\text{Fe}/\text{H}] \leq +0.1$	149 12	0.989	$8.1^{+2.8}_{-1.7}$	149 11	0.996	$7.4^{+2.7}_{-1.6}$
$[\text{Fe}/\text{H}] > +0.1$	158 34	0.985	$21.8^{+3.6}_{-2.9}$	158 30	0.994	$19.1^{+3.5}_{-2.7}$

Notes. Same columns as Table F.1.

Table H.2. Occurrence rates of cold Jupiters in the AAT (top), CLS (middle), and HARPS (bottom) surveys.

[Fe/H]	$M_p = 0.3 - 13 M_{Jup}$			$M_p = 0.5 - 20 M_{Jup}$		
	$N_\star d$	C	$f_{CJ} [\%]$	$N_\star d$	C	$f_{CJ} [\%]$
AAT radial velocity survey						
$[\text{Fe}/\text{H}] = -0.045 \pm 0.018$	196 20	0.971	$10.5^{+2.6}_{-1.8}$	196 20	0.989	$10.3^{+2.6}_{-1.8}$
$[\text{Fe}/\text{H}] < -0.1$	69 3	0.977	$4.4^{+4.0}_{-1.4}$	69 3	0.992	$4.4^{+3.9}_{-1.3}$
$-0.1 \leq [\text{Fe}/\text{H}] \leq +0.1$	66 5	0.969	$7.8^{+4.7}_{-2.2}$	66 5	0.989	$7.7^{+4.6}_{-2.1}$
$[\text{Fe}/\text{H}] > +0.1$	61 12	0.966	$20.4^{+6.2}_{-4.2}$	61 12	0.988	$19.9^{+6.1}_{-4.1}$
CLS radial velocity survey						
$[\text{Fe}/\text{H}] = +0.025 \pm 0.004$	402 50	0.987	$12.6^{+1.8}_{-1.5}$	402 45	0.995	$11.2^{+1.8}_{-1.4}$
$[\text{Fe}/\text{H}] < -0.1$	95 4	0.990	$4.2^{+3.1}_{-1.2}$	95 4	0.996	$4.2^{+3.1}_{-1.2}$
$-0.1 \leq [\text{Fe}/\text{H}] \leq +0.1$	149 12	0.989	$8.1^{+2.8}_{-1.7}$	149 11	0.996	$7.4^{+2.7}_{-1.6}$
$[\text{Fe}/\text{H}] > +0.1$	158 34	0.985	$21.8^{+3.6}_{-2.9}$	158 30	0.994	$19.1^{+3.5}_{-2.7}$
HARPS radial velocity survey						
$[\text{Fe}/\text{H}] = -0.122 \pm 0.011$	782 75	0.968	$9.9^{+1.2}_{-1.0}$	782 74	0.984	$9.6^{+1.2}_{-1.0}$
$[\text{Fe}/\text{H}] < -0.1$	344 19	0.970	$5.7^{+1.5}_{-1.0}$	344 18	0.986	$5.3^{+1.5}_{-1.0}$
$-0.1 \leq [\text{Fe}/\text{H}] \leq +0.1$	272 24	0.963	$9.2^{+2.1}_{-1.5}$	272 24	0.981	$9.0^{+2.1}_{-1.5}$
$[\text{Fe}/\text{H}] > +0.1$	166 32	0.972	$19.8^{+3.5}_{-2.8}$	166 32	0.986	$19.5^{+3.4}_{-2.7}$

Notes. Same columns as Table F.1.